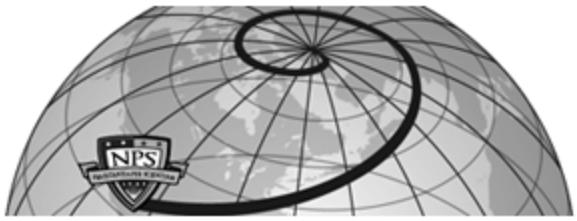

A METHOD FOR THREE-DIMENSIONAL FLOW ANALYSIS IN A ROTOR USING A HIGH SPEED DIGITAL COMPUTER

DONALD L. FELT

A METHOD FOR THREE - DIMENSIONAL FLOW ANALYSIS IN A ROTOR USING A HIGH SPEED DIGITAL COMPUTER

* * * * *

Donald L. Felt

A METHOD FOR THREE - DIMENSIONAL FLOW ANALYSIS IN A ROTOR USING A HIGH SPEED DIGITAL COMPUTER

by

Donald L. Felt
//
Lieutenant Commander, United States Navy

Submitted in partial fulfillment of
the requirements for the degree of

AERONAUTICAL ENGINEER

United States Naval Postgraduate School
Monterey, California

1 9 6 3

A METHOD FOR THREE - DIMENSIONAL FLOW ANALYSIS IN A ROTOR USING A HIGH SPEED DIGITAL COMPUTER

by

Donald L. Felt

This work is accepted as fulfilling
the thesis requirements for the degree of
AERONAUTICAL ENGINEER

from the
United States Naval Postgraduate School

ABSTRACT

Theoretical analyses of flow with rotating passages or turbo-machinery have become necessary for the proper design of turbo-pump elements in liquid fuel boosters and power conversion units. One such theory is presented, and a numerical solution derived. This theory develops a method for the analysis of steady, inviscid, adiabatic flow through arbitrary rotors. A detailed analysis in a meridional plane is given, assuming axial symmetry. A simplified approach to the blade to blade solution is also presented. The merits of these theories are compared with other proposed methods. The inverse, or design, approach is considered, and found to be unnecessary.

A numerical solution for incompressible flow is derived and applied to the flow solution in the impeller of a mixed flow compressor with backwards-bent blades of arbitrary shape. Meridional streamlines and relative velocity distributions are progressively calculated on a CDC 1604 computer, using FORTRAN program language. Data are measured from a detailed presentation of the blade shape in a meridional plane. Blade to blade relative velocity distributions are calculated from the meridional plane analysis.

It is concluded that the results completely define the flow and are sufficiently accurate for engineering applications. Validation is based upon the reliability of the theory, and upon comparisons with results of other methods. Extensions of the scope of this approach are recommended, which include the compressible solution and the solution of flows in unbladed passages.

The writer wished to express his appreciation for the assistance and encouragement given him by Professor M. H. Vavra of the U. S. Naval Postgraduate School. His guidance in the development of this solution was invaluable.

TABLE OF CONTENTS

TABLE OF CONTENTS (Continued)

LIST OF ILLUSTRATIONS

LIST OF SYMBOLS

Symbol	Definition	Units
A	Area	sq. in.
a	Coefficient	
B	Blade thickness factor	
b	Coefficient	
C	Characteristic number	
c	Coefficient	
D	Grouping of terms	
E(x)	Product of function on a characteristic	
$\vec{F}$	Blade force	lb./slug
F(L)	Leading edge function	
$\vec{f}$	Friction force	lb./slug
H	Total enthalpy	ft.lb./slug
h	Static enthalpy	ft.lb./slug
K	Separation parameter	
K(n)	Entrance function	
k	Curvature	$in.^{-1}$
L	leading edge distance	in.
l	Θ = constant curve distance	in.
M	Streamline number	
$\vec{M}$	Moment about axis	lb./ft.
m	Streamline distance	in.
N	Number of blades	
dN, ΔN, δN, dN*	Incremental distances along streamline	in.
n	Normal distance	in.

LIST OF SYMBOLS (Continued)

Symbol	Definition	Units
P	Arbitrary point	
P*	Point on Characteristic	
p	Static pressure	lb./sq. in.
Q	Volumetric flow rate	cu. ft./sec.
R	Radius	in.
R_e	Reynold's Number	
s	Entropy	ft.lb./ (slug-^oR)
T	Temperature	deg. R
t	Time	sec.
Δt	Blade thickness	in.
$\Delta t'$	Equivalent blade thickness	in.
V	Absolute velocity	ft./sec.
W	Relative velocity	ft./sec.
X	Coefficient	
x	Distance along characteristic	in.
Z	Axial distance	in.
$\hat{u},\hat{m},\hat{n}$	Unit vectors in axisymmetric coordinate system	
α	Slope of leading edge	
β	Blade or flow angle	deg.
γ	Angular inclination of characteristic from normal	deg.
δ	Angular inclination of Θ = constant curve from normal	deg.

LIST OF SYMBOLS (Continued)

Symbol	Definition	Units
ϵ	Angular deviation of blade from radial direction	deg.
Θ	Circumferential reference angle	deg.
λ	Slope of streamline	deg.
ν	Kinematic viscosity	sq. ft./sec.
ρ	Density	slugs/cu. ft.
ω	Angular velocity	per sec.

Subscripts

B	Blade
e	Entrance
H	Hub
i	Point on streamline
j	Point on normal
k	Point on characteristic
L	Leading edge
l	Θ =constant curve
m	Stream direction
n	Normal
p	Pressure side of blade
R	Relative
s	Suction side of blade
T	Tip
u	Circumferential direction
x	Characteristic direction
0,1,2,3	Sequential indices

A METHOD FOR THREE - DIMENSIONAL FLOW ANALYSIS IN A ROTOR USING A HIGH SPEED DIGITAL COMPUTER

INTRODUCTION

There is an increasing demand for compact, high speed, high power output turbomachines for use in liquid fuel rocket engines and power conversion units. These units are being designed to work with such media as cryogenics and liquid metals. The proper design of such machinery largely depends upon the accuracy of the theoretical analysis, used prior to fabrication. The method used should reasonably predict aerodynamic forces and tendencies toward flow separation and cavitation.

The more simplified approaches, using conditions ahead of and after the rotor, ignore conditions within the rotor passage itself, and therefore, are unsatisfactory. Potential flow analyses are useful for stationary cascades, but cannot be accurately applied to flows in rotating passages. The need for more precise methods, required for the proper analysis of modern rotor designs, was anticipated. Several three-dimensional theories have been postulated. In general, these theories are quite complex and are difficult to apply.

One such theory was developed by the NACA's Lewis Laboratory in the early 1950's. The three dimensional problem was reduced to an iterative process between two-

dimensional solutions on hub to tip, and blade to blade stream surfaces. Ref. 1 presents an analysis on a meridional, or hub to tip, surface. A similar approach is developed in Ref. 2. A blade to blade analysis is described in Ref. 3. These treatments were combined into a general theory in Ref. 4. Subsequent efforts were directed towards applications of this theory to specific examples. The complex nature of the theory required the introduction of certain simplifying assumptions. The development of the high speed digital computer made solutions more practical, as demonstrated in Refs. 5 through 7.

Prior to the NACA's work, a method of solution in a meridional plane, similar to that of Ref. 1, was developed by Meyer in Ref. 8. This method uses an iterative, graphical process to solve two simultaneous, linear differential equations along the characteristics of the equations. The equations are derived from the Eulerian equations of motion, and the characteristics are defined by the geometry of the flow channel. In Ref. 9, Vavra reorganized Meyer's scheme into a more general theory, reducing the equations of motion to one non-linear equation which is also solved along characteristics. In addition, a simplified blade-to-blade analysis was developed.

The purpose of this thesis is to transform the theoretical development of Ref. 9 into a method of solution for arbitrary rotors, using the CDC 1604 digital computer. A completely contained computer solution was presumed to

be quite long. It was anticipated that the amount of input data, required for acceptable accuracy, would exceed computer capacity and that long preparation and computer run time would be required. It was decided to use a series of short computations, which could be repeated as often, or at such intervals, as required to obtain the desired accuracy.

The theoretical development may be applied to both the design and inverse problems. The major portion of this thesis is devoted to the latter application; the analysis of flow in a given rotor. A design attempt is made to provide a physical model for the evaluation of the analytical methods. This attempt is not completed because of time considerations, and an actual rotor is used for the model. This impeller is a part of a compressor test rig located at the U. S. Naval Postgraduate School. Details of this machine are enumerated in Ref. 10. The rotor is of the mixed flow type, with non-radial blades. The blades have a constant thickness, and are of the deloaded type, with a reversal in curvature over the rear section. This configuration presents an arbitrary design which does not conform to standard impeller types.

The methods developed in this thesis are applied to this model, using simplified initial conditions, which do not reflect actual operating conditions, but are within the compressor's operating range. No correlation is made between theoretical and test results, however theoretical

results are presented for validation. Both the theory and the results of this analysis are compared with those of Refs. 1 through 7, to substantiate the applicability of this method.

II. THEORY

A complete derivation of the theory is presented in Ref. 9. This section contains those equations and developments that are considered necessary for clarity and continuity, in following the subsequent transformation from theory to numerical methods.

A. Meridional Plane Analysis

1. The following assumptions are made to establish a model for the hub to tip analysis. A more thorough treatment of these assumptions is conducted in Section IV.

   a. The rotor cascade contains an infinite number of infinitely thin blades. Thus, stream surfaces and fluid motion are axisymmetric.

   b. Flow is inviscid, steady, and isentropic.

   c. Entropy changes due to discontinuities at the leading and trailing edges are acknowledged but ignored.

   d. Flow is incompressible.

2. The solution of the equation of motion is based upon complete definition of the geometry of the blade surface. A set of meridional streamlines, m, are assumed and the normals, n, are drawn, establishing an orthogonal, axisymmetric coordinate system. This system is corrected by successive approximations. The blade surface is represented by the circular projection on the meridional plane of the lines of intersection of the blade surface with planes θ=constant. θ is the angle measured in the

peripheral direction. The Θ constant planes are planes extending in a radial direction from the axis of rotation, perpendicular to that axis. The peripheral angle, Θ , is referenced to an arbitrary point on the blade surface, usually on the leading edge. The Θ =constant curves are shown in Fig. 1. Assumed coordinate systems are illustrated in Fig. 4.

The angles defined by this family of curves, at an arbitrary point, P, are shown in Figs. 2 and 3. The angle δ is the inclination of a Θ =constant curve from the normal. The angle λ is the inclination of a meridional streamline from the axial direction, Z . The angle β is the flow angle of the relative velocity, W, on the stream surface.

$$\tan \beta = R \frac{d\Theta}{dm} \tag{1}$$

The deviation of a blade section, ϵ , from the radial direction, R, is:

$$\tan \epsilon = \frac{\tan \beta \sin (\lambda - \delta)}{\cos \delta} \tag{2}$$

Thus, the system of streamlines and Θ =constant curves are sufficient to completely define the blade shape.

The relative velocity on a streamline may be expressed vectorially as:

$$\vec{W} = \hat{u} W_m \tan \beta + \hat{m} W_m \tag{3}$$

where: $\hat{u}$ = unit vector in peripheral direction

$\hat{m}$ = unit vector in stream direction

The flow problem is reduced to a solution for the meridional component of the relative velocity, W_m.

3. The Eulerian equation of motion is:

$$\frac{\partial \vec{V}}{\partial t} + \nabla H = \vec{V} \times (\nabla \times \vec{V}) + T \nabla s + \vec{f} \tag{4}$$

For steady, isentropic, relative flows:

$$\nabla H_R = \vec{W} \times (\nabla \times \vec{W} + 2\vec{\omega}) + \vec{f} \tag{5}$$

where,

$$H_R = h + \frac{W^2}{2} - \frac{\omega^2 R^2}{2} \tag{6}$$

For inviscid flow, the friction force, $\vec{f}$, is zero. However, the effect of infinitesimal pressure changes across an infinite number of blades is accounted for by introducing the blade force, $\vec{F}_B$, which is normal to a blade element. Thus:

$$\nabla H_R = \vec{W} \times (\nabla \times \vec{W} + 2\vec{\omega}) + \vec{F}_B \tag{7}$$

Eq. (7) is reduced to its scalar compenents, using:

$$\frac{\partial (\,)}{\partial \Theta} = 0 \tag{8a}$$

$$\vec{F}_B = F_U (\hat{u} - \hat{m} \tan\beta + \hat{n} \tan\beta \tan\delta) \tag{8b}$$

where: $\hat{n}$ = unit vector in normal direction

The $\hat{u}$ component yields:

$$RF_U = W_m \frac{\partial (R W_U + \omega R^2)}{\partial m} \tag{9a}$$

The $\hat{m}$ component, with Eq. (9a) gives:

$$\frac{\partial H_R}{\partial m} = 0 \tag{9b}$$

This relation only holds within the rotor for the assumed theoretical model. Flows outside the rotor are unaffected by such a model.

For all but design conditions, there is a flow discontinuity at the leading edge, since flows ahead of the rotor will not meet the rotor at blade entry angles. It has been assumed that entropy changes caused by these discontinuities are neglected by ignoring the changes in total enthalpy across the leading edge. Conditions ahead of the rotor are derived from Eq. (4) for steady, isentropic flow.

$$\frac{\partial H}{\partial m} = \frac{V_u}{R} \frac{\partial (R V_u)}{\partial m} = 0 \tag{10}$$

A relation between conditions on a streamline ahead of the rotor and within the rotor is established as:

$$H_R = H_e - \omega R_L (W_{uL} + \omega R_L) \tag{11}$$

where e and L denote entrance and leading edge stations. The change of H_R along a normal is:

$$\frac{\partial H_R}{\partial n} = \frac{\partial H_e}{\partial n_e} \frac{\partial n_e}{\partial n} - \omega \frac{\partial (R_L W_{uL} + \omega R_L^2)}{\partial L} \frac{dL}{dn} = K(n) \tag{12}$$

The $\hat{n}$ component of Eq. (7) becomes:

$$W_m \frac{\partial W_m}{\partial n} + W_m^2 k_m + \frac{W_u}{R} \frac{\partial (R W_u + \omega R^2)}{\partial n} + \frac{W_m}{R} \frac{\partial (R W_u + \omega R^2)}{\partial m} \tan\beta \tan\delta = K(n) \tag{9c}$$

where k_m is the curvature of the meridional streamline. From Fig. 3:

$$W_u = W_m \tan\beta \tag{13}$$

Eq. (9c) is reduced to a relation in W_m:

$$\frac{\partial W_m^2}{\partial n}(1+\tan\beta) + \frac{\partial W_m^2}{\partial m}(\tan^2\beta \tan\delta)$$
$$+ W_m^2\left(2k_m + 2\frac{\tan\beta}{R}\left[\frac{\partial(R\tan\beta)}{\partial n} + \tan\delta \frac{\partial(R\tan\beta)}{\partial m}\right]\right) \quad (14)$$
$$+ W_m\left(4\omega\tan\beta\left[\frac{\partial R}{\partial n} + \tan\delta \frac{\partial R}{\partial m}\right]\right)$$
$$= 2K(n)$$

The partial derivatives in brackets are reduced to a total derivative along a Θ =constant curve by:

$$\frac{d(\,)}{dl} = \sin\delta \frac{\partial(\,)}{\partial m} + \cos\delta \frac{\partial(\,)}{\partial n} \quad (15)$$

Eq. (14) becomes:

$$\frac{\partial W_m^2}{\partial n} + \sin^2\beta\tan\delta \frac{\partial W_m^2}{\partial m} + W_m^2\left(2k_m\cos^2\beta\right.$$
$$\left. + \frac{\sin(2\beta)}{R\cos\delta}\frac{d(R\tan\beta)}{dl}\right) + W_m\omega\left(\frac{2\sin(2\beta)}{\cos\delta}\frac{dR}{dl}\right) \quad (16)$$
$$= 2\cos^2\beta\, K(n)$$

Eq. (16) is reduced to an ordinary differential equation along a characteristic, whose tangents at any point satisfy the relation:

$$\tan\gamma = \sin^2\beta\tan\delta \quad (17)$$

According to Ref. 8, these characteristics are regarded as circular projections on a meridional plane of unique spacial lines lying on the blade surface. Introducing Eq. (17) into Eq. (16):

$$\frac{dW_m^2}{dx} + W_m^2 Y_1 + W_m\omega Y_2 = Y_3 \quad (18)$$

where x denotes distance along a characteristic, and:

$$Y_1 = \cos\gamma\left[2k_m\cos^2\beta + \frac{\sin(2\beta)}{R\cos\delta}\frac{d(R\tan\beta)}{dl}\right] \quad (19a)$$

$$Y_2 = 2\cos\gamma\ \frac{\sin(2\beta)}{\cos\delta}\frac{dR}{dl} \quad (19b)$$

$$Y_3 = 2\cos\gamma\cos^2\beta\ K(n) \quad (19c)$$

4. The value of K(n) is dependent upon conditions ahead of the rotor, as shown by Eq. (12). The normal component of the equation of motion for steady, isentropic flows ahead of the rotor blading is:

$$V_m\frac{\partial V_m}{\partial n} + V_m^2 k_m + \frac{V_u}{R}\frac{\partial(RV_u)}{\partial n} - \frac{\partial H}{\partial n} = 0 \quad (20)$$

Eq. (10) shows that for isentropic conditions at the entrance, the total enthalpy and the product RV_u are constant along a meridional streamline. This condition is proved from the $\hat{u}$ and $\hat{m}$ components of Eq. (4). Thus:

$$\frac{\partial V_m^2}{\partial n} + V_m^2 X_1 + X_2 = 0 \quad (21)$$

$$X_1 = 2k_m \quad (22a)$$

$$X_2 = \frac{V_u}{R}\frac{\partial(RV_u)}{\partial n} - \frac{\partial H}{\partial n} = V_{ue}\frac{R_e}{R^2}\left[\frac{\partial(RV_{ue})}{\partial n_e} - \frac{\partial H_e}{\partial n_e}\right]\frac{dn_e}{dn} \quad (22b)$$

The solution of Eq. (21) is:

$$V_m^2 = e^{-\int X_1 dn}\left[V_{mH}^2 - \int X_2 e^{\int X_1 dn}\, dn\right] \quad (23)$$

This solution is solved for given entrance conditions and the volumetric flow rate, Q, by iterating the hub velocity, V_{mH}, until the flow rate is satisfied by:

$$Q = 2\pi \int_H^T R V_m \tan\beta \, dm \tag{24}$$

At the leading edge:

$$W_{uL} = V_m \tan\beta \tag{25}$$

Thus, K(n) is solved for given entrance conditions.

5. The remaining terms of Eqs. (19) are determined from blade geometry and the orientation of the meridional streamlines within the rotor. These streamlines must be assumed and corrected by successive approximations. The location of the streamlines at the leading edge are determined from entrance conditions. Eq. (18) is solved along a characteristic until the flow rate is satisfied by:

$$Q = 2\pi \int_0^{\chi_T} R W_m \cos\gamma \, d\chi \tag{26}$$

B. Blade to Blade Analysis

1. It is assumed that the relative velocity varies linearly across the blade channel. This assumption is taken from thin airfoil theory, where blade profiles are replaced by bound vortices. The relative velocity from the axisymmetric solution is considered to be the mean velocity along the periphery at any point in the meridional plane. These assumptions lead to:

$$W_p = W - \Delta W \tag{27a}$$

$$W_s = W + \Delta W \tag{27b}$$

where p and s refer to the pressure and suction sides of the blade.

2. The difference between relative velocities across the blade is related to the static pressure difference by:

$$p + \rho/2\, W^2 = \text{constant} \tag{28}$$

Thus:

$$\Delta W = \frac{\Delta p}{2\rho W} \tag{29}$$

The pressure difference across a blade element, which is projected onto a meridional plane, is related to the moment about the axis of rotation, exerted by the flow on that element, by:

$$\Delta \vec{M} = -\frac{\vec{\omega}}{\omega}(R\,\Delta p\, dn\, dm) \tag{30}$$

This moment is also derived from the momentum theorem and Eq. (9a):

$$\Delta \vec{M} = -\frac{\vec{\omega}}{\omega}\left[R\,\Delta\Theta\, dn\, dm\, \rho\, \frac{\partial(RW_u + \omega R^2)}{\partial m}\right] \tag{31}$$

The minus sign indicates that the moment oppose the rotation of the rotor. The arc, $\Delta\Theta$, is expressed in terms of an equivalent blade thickness, $\Delta t'$, which is measured perpendicular to the meridional plane.

$$\Delta t' = \frac{\Delta t}{\cos\beta}\sqrt{1 + \sin^2\beta \cos\delta} \tag{32}$$

$$\Delta\Theta = \frac{2\pi}{N} - \frac{\Delta t'}{R} \tag{33}$$

where: N = number of blades

Δt = blade thickness

Equating Eqs. (30) and (31) and combining with Eqs. (29) and (33):

$$\Delta W = \left(\frac{2\pi}{N} - \frac{\Delta t'}{R}\right) \frac{\cos\beta}{2} \frac{\partial (R W_m \tan\beta + \omega R^2)}{\partial m} \quad (34)$$

III. NUMERICAL SOLUTIONS

A. Design or Inverse Solution

1. The application of the preceding theory to impeller design was investigated in an attempt to produce a physical model for the direct solution, or flow analysis. Overall dimensions of an axial entry, mixed flow pump impeller were provided by Professor Vavra, which included:

   a. Hub and tip profiles of meridional contour

   b. Leading and trailing edge contours in a meridional plane

   c. Blade entry and exit angles

The problem was reduced to that of determining blade shapes, which would not only satisfy these boundary conditions, but would conform to practical structural and aerodynamic limitations.

2. A drawing was made of the meridional plane and a series of approximate normals were constructed. A meridional streamline was constructed, dividing the rotor annulus in half.

$$A_{1/2} = \pi (R_m + R_H) \eta_m \tag{35a}$$

Iterations were made on R_m along a normal until:

$$A_{1/2} = \frac{\pi}{2} (R_T + R_H) \eta_T \tag{35b}$$

The slope of this streamline, λ , was measured, plotted, smoothed, and the streamline reconstructed. Normals were corrected.

The distribution of the flow angle, β , along the mean streamline was assumed in the form:

$$\beta = A + Bm^2 \tag{36}$$

A and B were evaluated from initial conditions at the leading and trailing edges. Values of Θ were calculated by numerical integrations (Ref. 11). From Eq. (1):

$$\Theta_i = \Theta_{i-1} + \int_{i-1}^{i} \frac{\tan\beta}{R}\, dm \tag{37}$$

where: $\Theta_L = 0$

The slope of the Θ=constant curves at any point on a streamline may be calculated by Eq. (2), if ϵ is known. The choice of an ϵ distribution is governed by:

a. Maximum ϵ is limited by structural considerations

b. ϵ distribution must be compatible with fabrication tooling practices. An example is given in Ref. 9.

The design problem could have been simplified by using radial blades, where $\epsilon = 0$. However, this is contrary to the intent of this thesis in presenting methods applicable to arbitrary designs. Therefore, several ϵ distributions were assumed, and the angles, δ , computed on the mean streamline.

3. The problem of analytically generating a complete family of Θ =constant curves was as yet unsolved. The β and ϵ distributions on streamlines other than the mean are not independent of the mean distributions. Arbitrary choice of these distributions would, in all probability,

generate impractical blade shapes. These distributions should be assumed as:

$$\beta = \beta(m, n)$$

$$\epsilon = \epsilon(m, n)$$

It appeared that the design problem had become more complex than originally anticipated. It was decided that a complete treatment would detract from the main objective of this thesis. Therefore, the design analysis was discontinued.

B. Meridional Plane Analysis

1. The approach used to solve Eq. (18) along a chosen number of characteristics is, briefly:

a. Assume meridional streamlines in the vicinity of the leading edge which divide the flow into approximately equal increments.

b. Construct normals, thus establishing a coordinate grid system.

c. Measure the necessary blade physical characteristics at each grid point.

d. Generate a characteristic curve within the grid system.

e. Compute the coefficients, Y, of Eqs. (19).

f. Solve Eq. (18) for W_m at the intersections of the characteristic with the streamlines, iterating W_{mH} until the flow rate is satisfied.

g. Correct these intersections until the streamlines divide the flow rate into the prescribed increments.

h. Recompute W_m at the new intersections.

i. Project the corrected streamlines farther into the rotor channel, and repeat the process for a new characteristic.

Thus, the meridional streamlines are generated from leading to trailing edge, and the distribution of the relative velocity on a meridional plane of the rotor is computed. Steps a, b, c, and i are solved by the computer. The remaining steps are carried out by graphical means.

2. There are two categories of initial data required. The first is a complete physical description of the rotor. Finally, flow conditions ahead of the rotor must be prescribed. Normally, sufficient data are available from drawings of the impeller to construct a meridional plane. The Θ =constant curves are best produced by orthogonal projections from a three-view drawing. The meridional plane for the impeller used in this analysis is shown in Fig. 1.

The flow conditions at an entrance station must either be prescribed from an analysis of the machine installation, or assumed. The specific data required are:

a. Thermodynamic data for the fluid
b. Velocity distribution
c. Flow rate
d. Inlet channel contours
e. Impeller RPM

Conditions for this analysis are simplified by assuming:

$$V_L = V_{mL} = \text{const.}$$

$$\frac{\partial H_e}{\partial n_e} = 0$$

This flow is somewhat impractical since it does not reflect actual velocity and energy distributions imposed by intake ducting or guide vanes. However, these distributions do present a definite off-design condition at the leading edge. Design RPM, and a flow rate compatible with actual machine operating conditions, are used. Initial data are listed in Table I. The meridional velocity at the leading edge was computed by:

$$V_{mL} = \frac{Q}{A_L} \tag{38}$$

A_L was computed along the leading edge by Eq. (35b).

3. Streamlines are extended from initial points on the leading edge, such that the flow rate is divided into equal increments. Eight divisions were used for this analysis, as shown in Fig. 4.

A grid system is constructed in the vicinity of the leading edge. A point on the hub streamline is chosen as the starting point of the first characteristic. This point is determined by predicting the approximate alignment of the characteristic. Eq. (17) indicates that the slope of the characteristic, γ , is proportional to, but less than, the slope of the Θ =constant curve which originates from the starting point. γ also has the same sign as δ . These guidelines fix the characteristic within a desired region. These considerations also assist in estimating

the proper grid width. A "starting normal" is constructed from the starting point on the hub to the tip streamline. A second normal is constructed adjacent to the first, in the predicted direction of the characteristic. The distance between the two normals on each streamline is used to fix the remaining grid points. These points do not coincide with true normals, however equal grid spacing on streamlines is used to good advantage in subsequent calculations.

The values of λ , R, and Z are measured at each grid point. The values of Θ were read at the intersections of the Θ =constant curves and the streamlines, plotted, and Θ at the grid points found by interpolation. The angles δ are determined in a similar manner. The deviations of the Θ =constant curves from the radial direction, $\delta-\lambda$, are measured. λ is added to the interpolated results to obtain δ .

4. Each point on a characteristic must satisfy Eq. (17), therefore, the angles β and δ must be calculated for any point on a streamline. β is defined by Eq. (1). The derivative of Θ at a grid point on the j^{th} streamline is approximated by five-point difference formulas from Ref. 12.

Forward Differences

$$\frac{d\Theta_i}{dm_j} = \frac{-25\Theta_i + 48\Theta_{i+1} - 36\Theta_{i+2} + 16\Theta_{i+3} - 3\Theta_{i+4}}{12\,\Delta N_j} \quad (39a)$$

Central Differences

$$\frac{d\Theta_i}{dm_j} = \frac{(\Theta_{i-2} - \Theta_{i+2}) - 8(\Theta_{i-1} - \Theta_{i+1})}{12\,\Delta N_j} \qquad (39b)$$

Backward Differences

$$\frac{d\Theta_i}{dm_j} = \frac{3\Theta_{i-4} - 16\Theta_{i-3} + 36\Theta_{i-2} - 48\Theta_{i-1} + 25\Theta_i}{12\,\Delta N_j} \qquad (39c)$$

ΔN_j is the grid spacing on the j^{th} streamline. The derivative of Θ at points other than grid points, are calculated by interpolating linearly between adjacent normals.

$$\frac{d\Theta^*}{dm_j} = \frac{d\Theta_i}{dm_j} + \left(\frac{d\Theta_{i+1}}{dm_j} - \frac{d\Theta_i}{dm_j}\right)\frac{dN}{\Delta N_j} \qquad (40)$$

dN is the distance from the i^{th} grid point to the point P^*. A consequence of Eqs. (39) and (40) is that the minimum width of the coordinate lattice is six grid points.

The values of R, λ , and δ at a point P^* are also calculated by linear interpolation. β and γ are calculated by Eqs. (1) and (17).

5. A characteristic is approximated by a polygon with each side terminated by adjacent streamlines. Each intersection, P^*, is located from information calculated at the preceeding intersection. In this derivation, the lines between grid points are assumed to be straight. The derivation is shown graphically in Fig. 5.

Assume that P_o is established, and the angle γ , known. A straight line from P_o to P' on the next streamline at the angle γ . The distance, dN' is:

$$dN' = dM \tan\gamma \qquad (41)$$

where:

$$dM = \left| \frac{dR}{\cos \lambda} \right| \tag{42a}$$

or:

$$dM = \left| \frac{dz}{\sin \lambda} \right| \tag{42b}$$

Eq. (42b) is used for λ greater than 45 degrees. The angle γ' is calculated by the methods of paragraph 4. A line is extended from P_o to P'' at this angle. The point P^* is established by:

$$dN = dN' + \frac{\delta N}{2} \tag{43}$$

P* is the reference point for the extension of the characteristic to the next streamline. The polygonal approximation of the completed characteristic is smoothed through the points P*. (Fig. 4)

There are a number of considerations that must be accounted for in generalizing this method for computer programming. dN* originates at the starting normal. The sign of dN' is the same as that of γ . The sign of δN depends on the difference between γ and γ'. The sign of dN* may be plus or minus, and its magnitude may be greater or less than that of dN'. The value of dN in Eq. (40) for a positive dN* is:

$$dN = dN^* \tag{44a}$$

while, for negative dN*:

$$dN = \Delta N - dN^* \tag{44b}$$

6. The coefficients, Y, of Eq. (18) contain four elements which are, as yet, undetermined.

a. R_m

b. $\frac{d}{dl}(R \tan \beta)$

c. dR/dl

d. $K(n)$

The curvature, k, of a given curve is extremely difficult to calculate. If the curve can be expressed analytically:

$$k = \frac{R''}{\left[1 + (R')^2\right]^{3/2}} \qquad (45)$$

where R' and R" are the first and second derivatives, respectively, of the function R = f(Z).

An attempt was made to determine the equations of the hub and tip contours in cartesian coordinates: R = f(Z). Two polynomial approximations of these curves were made using CDC Cooperative Library routines. The coordinates of the curves at each quarter inch along the axis were introduced as data. Only high order polynomials fit these data points properly. The derivatives of these equations were difficult to obtain without frequent interruptions in computer operation. When calculated, the second derivatives reflected the sinuous nature of polynomial approximations, resulting in inaccurate curvatures which varied in sign along a given curve. These methods were considered to be unacceptable for this study.

The derivatives of the hub and tip contours were calculated with various finite difference equations. (Ref. 12) The three and four point calculations were inaccurate. The higher order solutions resulted in erratic second derivatives. It became apparent that all methods were very sensitive to the accuracy of the data. It was found that

inaccuracies in the third decimal place of radius data were sufficient to introduce gross errors in the second derivative.

A semi-graphical approach was used to determine the derivatives. The first derivative was calculated by finite differences, and the results plotted and smoothed. This process was repeated to calculate the second derivative, using the plot of the first derivative for input. Data taken from the two plots were used to calculate the curvature in Eq. (45). Hub and tip curvatures are plotted in Fig. 6.

This procedure is obviously incompatible with continuous computer operations. The computation of the streamline curvatures, k_m, at points P*, would be quite tedious using this method. Therefore, k_m is approximated within the flow passage by linearly interpolating between hub and tip, using the data of Fig. 6. k_m is assumed to vary in equal increments between streamlines:

$$k_{mj} = k_{mH} + \left(k_{mT} - k_{mH}\right) \frac{M_j}{M_T} \tag{46}$$

Linear interpolation, similar to Eq. (40), is used to calculate k_m between grid points on a streamline.

The following derivation defines $\frac{d}{dl}(R \tan\beta)$ in terms of known quantities. From Eq. (15):

$$\frac{d(R\tan\beta)}{dl} = \sin\delta \frac{\partial(R\tan\beta)}{\partial m} + \cos\delta \frac{\partial(R\tan\beta)}{\partial n} \tag{47}$$

$$= R\left(\sin\delta \frac{\partial\tan\beta}{\partial m} + \cos\delta \frac{\partial\tan\beta}{\partial n}\right) + \tan\beta \frac{dR}{dl}$$

From Fig. 2:

$$\frac{dR}{d\ell} = \cos(\delta - \lambda) = D_1 \tag{48}$$

From Eq. (1):

$$\frac{\partial(R\tan\beta)}{\partial m} = R\frac{\partial^2\theta}{\partial m^2} + \frac{\partial\theta}{\partial m}\cdot\frac{\partial R}{\partial m}$$

$$\frac{\partial(R\tan\beta)}{\partial n} = R\frac{\partial^2\theta}{\partial m\partial n} + \frac{\partial\theta}{\partial m}\cdot\frac{\partial R}{\partial N}$$

$$\frac{d(R\tan\beta)}{d\ell} = R^2\left(\sin\delta\frac{d^2\theta}{dm^2} + \cos\delta\frac{d^2\theta}{dmdn}\right) + 2D_1\tan\beta$$

Grouping terms of Eq. (19a):

$$\frac{1}{R\cos\delta}\frac{d(R\tan\beta)}{d\ell} = D_2 = R\left(\tan\delta\frac{d^2\theta}{dm^2} + \frac{d^2\theta}{dmdn}\right) + \frac{2D_1\tan\beta}{R\cos\delta} \tag{49}$$

The term $d^2\theta/dm^2$ at a point P* is computed by assuming a parabolic distribution of $d\theta/dm$ between grid points.

$$\frac{d\theta}{dm} = a + bm + cm^2 \tag{50}$$

$$a = \frac{d\theta}{dm} \text{ at } P^* = \frac{\tan\beta}{R}$$

$$b = \frac{d^2\theta}{dm^2} \text{ at } P^* \tag{51}$$

Fig. 7 will assist in following the derivation for b.

$$m_2^2\left(\frac{d\theta}{dm}\right)_1 = \left(a + bm_1 + cm_1^2\right)m_2^2 \tag{52a}$$

$$m_1^2\left(\frac{d\theta}{dm}\right)_2 = \left(a + bm_2 + cm_2^2\right)m_1^2 \tag{52b}$$

Subtracting Eq. (52b) from (52a):

$$b = \frac{m_2^2\left[\left(\frac{d\theta}{dm}\right)_1 - \left(\frac{d\theta}{dm}\right)_0\right] - m_1^2\left[\left(\frac{d\theta}{dm}\right)_2 - \left(\frac{d\theta}{dm}\right)_0\right]}{m_1 m_2^2 - m_2 m_1^2} \qquad (53)$$

m_1 and m_2 are defined in Fig. 8.

The function, $\frac{d^2\Theta}{dmdn}$, is calculated by differentiating $\frac{d\Theta}{dm}$ along the normal nearest the point P*. A parabolic distribution of $\frac{d\Theta}{dm}$ over three streamlines along the normal is assumed. The coefficient, b, is derived in the same manner as that described in the preceding paragraph. In this derivation the two succeeding grid points from the origin are used, instead of adjacent points. Calculations for points on the last two streamlines are made by using the two preceding grid points.

Forward Differentiation

$$b = \frac{n_2^2\left[\left(\frac{d\theta}{dm}\right)_1 - \left(\frac{d\theta}{dm}\right)_0\right] - n_1^2\left[\left(\frac{d\theta}{dm}\right)_2 - \left(\frac{d\theta}{dm}\right)_0\right]}{n_1 n_2^2 - n_2 n_1^2} \qquad (54a)$$

Backward Differentiation

$$b = \frac{n_{-2}^2\left[\left(\frac{d\theta}{dm}\right)_{-1} - \left(\frac{d\theta}{dm}\right)_0\right] - n_{-1}^2\left[\left(\frac{d\theta}{dm}\right)_{-2} - \left(\frac{d\theta}{dm}\right)_0\right]}{n_{-1} n_{-2}^2 - n_{-2} n_{-1}^2} \qquad (54b)$$

The increments n_j are functions of the grid spacing, dM.

The values of K(n) are required for the calculation of Y_3. Initial conditions have simplified Eq. (12). With Eq. (25):

$$K(n) = -\omega \frac{\partial\left(R_L V_m \tan\beta_L + \omega R_L^2\right)}{\partial L} \frac{dL}{dn} \qquad (55)$$

$$\omega = \frac{\pi}{30} \cdot RPM \qquad (56)$$

$$\frac{dL}{dn} = \frac{dL}{dR} \cdot \frac{dR}{dn} = \frac{\cos\lambda}{\sin\alpha} \qquad (57)$$

where α is the slope of the leading edge. β_L is calculated, using the forward difference formula of Eq. (54a) in conjunction with Eq. (1). The terms in parentheses in Eq. (55) are grouped, and the derivative calculated using the parabolic distribution methods of Eqs. (54).

$$F(L) = R_L V_m \tan \beta_L + \omega R_L^2 \tag{58}$$

In summary, the coefficients, Y, are reduced to:

$$Y_1 = \cos\gamma \left[2 R_m \cos^2\beta + \sin(2\beta) \cdot D_2 \right] \tag{59a}$$

$$Y_2 = 2\cos\gamma \frac{\sin(2\beta)}{\cos\delta} \cdot D_1 \tag{59b}$$

$$Y_3 = 2\cos\gamma \cos^2\beta \, K(n) \tag{59c}$$

7. The equation of motion, Eq. (18), is solved by successive approximations, until the distribution of W_m along the characteristic satisfies the flow rate of Eq. (26). The steps in this solution are:

a. Assume W_{mH}

b. Solve Eq. (18) for $\frac{dW_{mH}^2}{dx}$

c. Let:

$$W_{m2}^2 = W_{mH} + \frac{dW_{mH}^2}{dx} \, dx_2 \tag{60}$$

$$dx_2 = \frac{dM_2}{\cos\gamma_H} \tag{61}$$

d. Solve Eq. (18) for $\frac{dW_{m2}^2}{dx}$

e. Let:

$$W_{M2}^2 = W_{mH} + \frac{1}{2}\left(\frac{dW_{mH}^2}{dx} + \frac{dW_{m2}^2}{dx} \right) dx_2 \tag{62}$$

f. Repeat for W_{m3}, using W_{m2} in (a).

The variables under the integral sign in Eq. (26) are grouped.

$$E(x) = R W_m \cos\gamma$$

$$Q = 2\pi \int_H^T E(x)\, dx \tag{63}$$

Numerical integrations are performed over two adjacent streamlines at a time, and the results are successively summed. A parabolic distribution is assumed for E(x).

$$E(x) = a + bx + c x^2 \tag{64}$$

The coefficients are derived in the same manner as that used for the development for the difference equations.

$$a = E_o \tag{65a}$$

$$b = \frac{X_2^2 (E_1 - E_o) - X_1^2 (E_2 - E_o)}{X_1 X_2^2 - X_2 X_1^2} \tag{65b}$$

$$c = \frac{X_2 (E_1 - E_o) - X_1 (E_2 - E_o)}{X_1^2 X_2 - X_2^2 X_1} \tag{65c}$$

where:

$$X_1 = dX_1$$

$$X_2 = dX_1 + dX_2$$

The integral of E(x) is:

$$\int_k^{k+2} E(x)dx = a(X_{k+2} - X_k) + \frac{b}{2}(X_{k+2}^2 - X_k^2) + \frac{c}{3}(X_{k+2}^3 - X_k^3) \tag{66}$$

where:

$$X_k = \sum_{i=2}^{k} dX_i \tag{67}$$

In case there exists an odd number of streamtubes, the final integral is calculated by:

$$E(x) = a + bx \tag{68}$$

$$a = E_o \tag{69a}$$

$$b = \frac{E_1 - E_0}{dX_1} \tag{69b}$$

$$\int_K^{K+1} E(x)\,dx = a(X_{K+1} - X_K) + \frac{b}{2}\left(X_{K+1}^2 - X_K^2\right) \tag{70}$$

8. The intersection of the characteristic with each streamline, excluding hub and tip, is connected until adjacent streamlines divide the flow rate into M-1 equal increments. Calculations progress from streamline M-1 to streamline 2. Each calculation iterates the increment δx until:

$$Q\left(\frac{K}{M}\right) = 2\pi \int_T^K E(X+\delta X)\ (dX+\delta X) \tag{71}$$

$$K = M-1, M-2, \cdots\cdots 2$$

The variables in E(x) are corrected by δx.

$$\begin{aligned} R_K &= R_i + \left(\frac{dR}{dx}\right)_i \delta x \\ &= R_i + \delta x \cos(\gamma_i - \lambda_i) \end{aligned} \tag{72}$$

$$\begin{aligned} W_{mK} &= W_{mi} + \left(\frac{dW_m}{dx}\right)_i \delta x \\ &= W_{mi} + \frac{\delta x}{2W_{mi}}\left(\frac{dW_m^2}{dx}\right)_i \end{aligned} \tag{73}$$

$$\gamma_K = \gamma_i + \left(\gamma_{i\pm1} - \gamma_i\right)\frac{\delta x}{dx_{i\pm1}} \tag{74}$$

K indicates the new point of intersection, and i, the original point. Eq. (71) is solved by introducing the proper limits into Eqs. (66) or (70).

9. Preliminary calculations for the blade to blade solution are included in the computer program for the meridional plane analysis. Variables of Eq. (34) are grouped,

and the groupings computed at the corrected intersections of the characteristic and streamlines.

$$DW_{coes} = \left(\frac{2\pi}{N} - \frac{\Delta t'}{R}\right) \cos\beta \qquad (75a)$$

$$DW_{func} = RW_m \tan\beta + \omega R^2 \qquad (75b)$$

C. Computer Programs; ROTOR 1 and LEDGE 1

1. The preceding methods are translated into FORTRAN computer language compatible with the CDC 1604 digital computer. Program ROTOR 1 calculates a complete solution for one characteristic, from the location of the characteristic to the correction of assumed streamlines and the relative velocity profile. The solution procedes in an orderly fashion, much like the development of the preceding section. Subroutines are used for repetitive calculations. Control of decisions, iterations, and progressive development is maintained in the main program. Subroutine PSTAR locates the characteristic, accounting for all signs of dN*. Subroutine DDM calculates the first derivative of Θ, $\frac{d\Theta}{dm}$, by finite differences. Subroutine ANGLE calculates β and γ. Subroutine COY calculates the elements of the coefficients, Y, except K(n). The coefficients, Y, are calculated in the main program. The relative velocities are calculated in subroutine RELVEL, and the flow rate in subroutine FLOW. Control of the iterations is maintained in the main program. Iterations for streamline corrections are made in the main program, using subroutine FLOW.

2. Entrance conditions are calculated in a separate program, since these computations are not required after the locations of streamlines on the leading edge are determined. Program LEDGE 1 calculates K(n) as defined by Eqs. (55), (56), and (57), with the exception that cos λ is omitted. This variable is a function of position on a streamline, and therefore is included in the calculations for Y_3. The results of LEDGE 1 are used as inputs to ROTOR 1.

It should be noted that the first term of K(n) in Eq. (12) is omitted, since $\frac{\partial He}{\partial ne} = 0$ in this analysis. This term is introduced as input (DHEDN) into ROTOR 1. It is intended that this term would be calculated separately from given thermodynamic data at the entrance.

3. Definitions, flow diagrams, and program listings are included in the Appendix. Many control, indexing, and grouping names are undefined. Their usage may be interpreted from the developments of the preceding section or from the program listings.

D. Results of ROTOR 1

This program computed properly, but the results were unacceptable. Streamline corrections were large (up to 1/2 inch), imposing improbable velocity distributions. The characteristics appeared to be properly located, however, the flow angles, β , were somewhat arbitrarily distributed along normals and characteristics.

A number of test print-outs were made in order to locate the inaccuracies. (The listing of Rotor 1 in the Appendix includes test print-out instructions.) It was discovered that the derivatives of Θ , calculated by Eqs. (39), (40), (53), and (54) were inaccurate. The second derivatives were particularly incorrect. The methods used are considered to be sound, however, the degree of accuracy primarily depends on the accuracy of the input data. In this analysis, the Θ =constant lines were originally plotted from approximations. Errors introduced in plotting were compounded by graphical interpolations (and extrapolations) for Θ values at grid points. The erroneous Θ derivatives were introduced in the computations for the coefficients, Y, resulting in an improbable flow solution.

E. Alternate Meridional Plane Analysis

1. It was decided to eliminate the derivatives of Θ from the calculations, therefore, it was necessary to introduce known values of β . It is reasonable to assume that these data would be available, or could be computed, from detailed drawings of the impeller. For this analysis, β distributions along the hub and tip contours were obtained from data used in the original design work. However, β cannot be specified on the internal streamlines until the streamline is constructed. A distribution of β from hub to tip must be assumed.

2. β along the hub and tip contours is shown in Fig. 9.

It is assumed that β varies linearly along normals between these contours.

$$\beta_j = \beta_H + \left(\beta_T - \beta_H\right) \frac{M_j}{M_T} \tag{76}$$

The function D_2 of Eq. (49) becomes:

$$D_2 = \frac{1}{R\cos\delta} \frac{d\left(R\tan\beta\right)}{dl}$$

$$= \tan\delta \frac{\partial \tan\beta}{\partial m} + \frac{\partial \tan\beta}{\partial n} + \frac{D_1 \tan\beta}{R\cos\delta} \tag{77}$$

The distribution of $\tan\beta$ between two grid points on a streamline or normal is assumed to be linear.

$$\frac{\partial \tan\beta}{\partial m_j} = \frac{\tan\beta_{i+1} - \tan\beta_i}{\Delta N_j} \tag{78a}$$

$$\frac{\partial \tan\beta}{\partial n_i} = \frac{\tan\beta_{j+1} - \tan\beta_j}{dM_i} \tag{78b}$$

At the i^{th} grid point:

$$\frac{\partial \tan\beta_i}{\partial m_j} = \frac{\tan\beta_{i+1} - \tan\beta_{i-1}}{2\,\Delta N_j} \tag{79}$$

At a point, P*:

$$\frac{\partial \tan\beta}{\partial n} = \left(\frac{\partial \tan\beta}{\partial n_{i+1}} - \frac{\partial \tan\beta}{\partial n_i}\right) \frac{dN}{\Delta N_j} \tag{80}$$

The angle δ is still measured on the Θ=constant curves.

Leading edge calculations are also modified. A linear distribution of β along the leading edge is assumed in the same manner as Eq. (76).

F. Computer Programs: ROTOR 2 and LEDGE 2

1. Program ROTOR 2 is a modification of ROTOR 1, with the new calculations for β replacing the Θ derivatives. The

order of some solutions has been changed to simplify the mechanics of the program. Subroutines DTD and ANGLE are eliminated. The values of the angles, γ, are computed in the main program or in subroutine PSTAR. Subroutine PSTAR is modified to reflect these changes. Subroutine DDL replaces COY, and calculates the derivatives along the Θ=constant curves. Curvatures are calculated in PSTAR. Subroutines RELVEL and FLOW are unchanged. Program LEDGE 2 is a simplification of LEDGE 1, reflecting the introduction of β data.

Both programs are diagrammed and listed in the Appendix. Only new or modified variable names are defined.

G. Results of ROTOR 2

1. The complete meridional plane analysis was solved by ROTOR 2. Nine characteristics were generated. Fig. 4 is a tracing of the actual construction for the first two characteristics. The grid networks for both solutions are indicated. Two modifications are made to the first set of estimated streamlines. The first modification reflects the changes effected by the calculations for characteristic C1. Each change required recalculations in LEDGE 2. The results of the last calculation were held constant throughout the remaining solutions.

Data for each characteristic are listed in Tables II-1 through II-9. The "starting normal" originates from the "starting point" for each calculation. The "starting point number" indicates the position of the normal in the grid

system for each solution. The intersection of a characteristic with each streamline is located by measuring the distance DNSTAR (dN*) from the intersection of the starting normal with the streamline. Streamlines are corrected by measuring the distance DELTA (δx) along the characteristic from the original intersection, P*. Relative velocities are listed for the final intersection point. Additional data are listed as checks on the calculations.

For example, the calculations for characteristic C8 showed a discrepancy between the correction length, δx, and the computed radius, in locating the new streamlines. Test print-outs revealed errors in the calculated grid lengths, dM. These errors had accumulated, resulting in somewhat radical streamline deviations and questionable velocities. dM had been calculated by Eq. (42a), which, at the time, was used for angles, λ , of 60 degrees or less. This limit was changed to 45 degrees and Eq. (42b) applied. The results were satisfactory.

2. The completed system of computer characteristics and streamlines is shown in Fig. 10. True normals are constructed perpendicular to these streamlines. Streamlines have been faired and extended to the trailing edge. Data points are indicated.

The distributions of relative velocity along odd numbered streamlines are plotted in Fig. 11. Values at the leading edge were hand calculated. Velocities at the trailing edge were extrapolated on a large scale plot. Curves

are faired through data points without smoothing. The relative velocity profiles on the odd numbered normals of Fig. 10 are cross plotted in Fig. 12.

3. Computer run time for one ROTOR 2 solution was approximately two minutes. Construction and data preparation time was about four hours. Total preparation and computer time for LEDGE is approximately two hours.

H. Blade to Blade Analysis

1. Most of the preliminary calculations have been accomplished in the hub to tip solution. The values of W, DW_{coef}, and DW_{func} are plotted from the results in Tables II, and the curves smoothed. Data are read from these curves at equal increments along each streamline. Extrapolated data are used at the leading and trailing edges. An increment of 1/2 inch is used in this solution.

The derivatives of DW_{func} are computed by the five-point difference formulas of Eqs. (39). The relative velocity difference, ΔW, is computed by a form of Eq. (34):

$$\Delta W = \frac{DW_{coef}}{2} \cdot \frac{d(DW_{func})}{dm} \qquad (81)$$

The relative velocity distributions on the pressure and suction blade surfaces (driving and trailing surfaces in a compressor) are calculated by Eqs. (27).

2. Program BLADE performs these calculations along each streamline, from leading edge to trailing edge. Computer run time was approximately 30 seconds. Preparation time was about six hours.

3. Results are compiled in Tables III-1 through III-9. The relative velocity distributions along the hub, tip, and mean streamlines are plotted in Figs. 13, 14, and 15. The linear velocity profiles across the blade channel, at various stations along the mean streamline, are shown in Fig. 16.

IV. DISCUSSION

A. Theoretical Assumptions

1. The assumption of axial symmetry is in keeping with sound engineering practice. Although changes in the circumferential direction are ignored, incremental pressure changes across the blades are considered by introducing the blade force, F_B. This assumption is also made in Refs. 1 and 2. The general theory, postulated by Wu in Ref. 4, does not admit to axial symmetry. Wu modifies the development of Ref. 2 to allow for deviations from axial symmetry, accounting for these deviations with a thickness factor, B. This factor is conveniently used as an integrating parameter in defining a flow function. B is interpreted as being proportional to the thickness of a stream sheet containing an arbitrary stream surface, and to blade thickness distribution.

This theory is sound, and would produce accurate results if explicitly applied. However, the factor B must be assumed, either arbitrarily or from available data. An example of an assumed distribution of B is found in Ref. 6. A blade to blade analysis is made, using the distribution as input. This report states that such data are obtained from a meridional plane analysis, presumably by the methods of Ref. 4. Yet, Ref. 4 states that B is best calculated from the results of a blade to blade analysis. Wu, in Ref. 13, uses a value of B equal to one, which imposes axial symmetry. He states that methods for estimating B were

unavailable at the time. This reference also shows that the changes effected by this assumption are small. The advantage of using approximate values of B, over the axisymmetric approach, is doubtful.

2. The assumption of a steady, inviscid, adiabatic flow is generally accepted. Exclusion of any one of these factors introduces highly complex theoretical considerations, which are difficult, if not impossible to apply. The assumption of isentropic flow within the rotor is reasonable, since known exceptions are considered. The specific exceptions, included in this theory, are the entropy changes caused by discontinuities of the leading and trailing edges. The analysis of this thesis is based upon the premise that these entropy changes are small and can be ignored. This is also implied in Ref. 1, which analyzes flows which conform to the prescribed blade angles at the leading and trailing edges. The analysis of this thesis is not limited by this implication. Entrance conditions are not restricted to design conditions, and Eq. (25) is generally applicable.

3. An incompressible solution was developed in this thesis in order to simplify the presentation. Compressible solutions can be solved by this method if the volumetric flow rate is replaced by the mass flow rate. Density changes along a characteristic can be computed by thermodynamic relations which equate the equilibrium conditions at any point, P*, to known or computed entrance conditions.

4. A simplified blade to blade solution is used in this

thesis. The assumption of a linear velocity distribution is not unique. Ref. 1 assumes a linear pressure variation across the blade channel. Ref. 6 validates this assumption for design conditions. The results of Ref. 3 show near-linear velocity distributions for both the compressible and incompressible solutions.

B. The Design Analysis

1. The design analysis was discontinued because of time considerations. However, it was shown that the theory could be applied to the design solution as well as the direct solution. Difficulty arose in prescribing practical blade characteristics. One method would be to assume various β and ϵ distributions as functions of streamline and normal directions; then generate a blade shape for each combination, and select the most practical solution. Selection would be contingent upon the results of a direct analysis, similar to the method developed in this thesis. This approach appears to be quite long.

The question is whether or not this development is warranted. A design method, based on the theoretical development of Ref. 1, is presented in Ref. 5. The hub profile is calculated from successive flow solutions. This approach is modified by Ref. 7 to provide for arbitrary entrance and discharge conditions. In effect, the initial conditions establish the Θ =constant curves. The solution provided the upper limit of these curves. The design

problem is practically solved by the initial conditions. All that remains is a system of repetitive calculations, which produces an acceptable tip profile. In comparison, the method proposed in this thesis would generate blade shapes, rather than tip contours. It seems more logical, and perhaps more expeditious, to establish feasible physical contours and analyze the flow under prescribed conditions. The contours could then be altered to eliminate undesirable flow phenomena, and to produce the desired performance. This is precisely what is done in the direct approach. Therefore, the design, or indirect, method is considered to be unnecessary.

C. Methods of Solution

1. The developments of Refs. 8 and 9 present a relatively simple approach to the direct problem when compared to Ref. 4. The establishment of characteristic solutions provides a method, compatible with high speed machine computations. A limited number of applications of Ref. 4 have been presented. None have attempted a solution of the complete theory, but have reduced the problem to solutions for specific applications. Ref. 6 deals with the blade to blade analysis. Refs. 5 and 7 are concerned with the design problem, and consider the methods proposed in Ref. 4 to be impractical for engineering applications. In Ref. 13 the methods of Ref. 4 are simplified by assuming axial symmetry, and an incompressible solution is used as a basis for the compressible solution. It is concluded, therefore,

that the approach presented in this thesis is theoretically sound.

2. The accuracy of the solution of any theoretical analysis depends upon the precision of the numerical methods used in computations, and in the accuracy of the input data. It is difficult to assess the inaccuracies introduced by the numerical approximations in this method. It would be impossible to isolate each error, even if test results were available for comparison. Gross inaccuracies, such as those revealed by ROTOR 1, can be detected. Small errors may cancel, or large errors may ensue from an accumulation of small inaccuracies.

For example, the assumptions of linear distributions of curvature and flow angles are questionable in the vicinity of the axial midpoint of the test impeller. Hub and tip curvatures (Fig. 6) follow different patterns in this region. The odd distribution of hub curvature is difficult to explain. The difference between hub and tip blade angles is a maximum in this region. (Fig. 9) These two quantities are multiplied in the calculations of the coefficient, Y. Difficulties were encountered in obtaining accurate results along characteristics in this region, indicating that the errors introduced by these assumptions may have multiplied. Such reasoning is not conclusive, however, since the results of the complete solution do not indicate excessive errors.

Many interpolations were used in this solution. The accuracy of each depends on the grid spacing. The spacing

of normals was limited to a maximum of .3 inches. Nine streamlines are considered sufficient. A finer network would certainly increase the accuracy of each calculation, however, the process of measuring data would become tedious.

The reliability of all calculations also depends upon the accuracy of the measured data. The meridional plane was drawn to double scale. Lengths were measured to an accuracy of about .05 inches. The angles, λ , were measured with a drafting machine to an accuracy of 5 minutes. (.1 degree) This accuracy is reduced to about .3 degrees, since measurements were made on curved lines. Interpolations were made for δ to the nearest tenth of a degree, but an accuracy of 1/2 degree is more reasonable.

3. The general approach to the meridional plane solution can be applied to obtain the desired degree of accuracy, within the limits outlined in the preceding discussion. A finer grid will increase accuracy for a particular characteristic solution. A solution can be repeated, using the previous results to establish new initial conditions. The number of characteristic solutions used is arbitrary. Therefore, a detailed investigation can be conducted in discrete regions in a rotor channel, or a complete solution can be rapidly calculated, using a few characteristics.

Theoretically, the method can be used to calculate characteristic solutions outside the rotor channel. In this case the defining angles of the blade are set equal to zero, and the characteristics coincide with normals. In stationary

cascades, the rotational effects are eliminated. These solutions are excluded in the computer solutions of this thesis, because of the schemes adapted in performing numerical interpolations. Solutions can be calculated in close proximity to the leading and trailing edges if fictitious blade characteristics are used outside these boundaries.

D. Results

1. The results of the first method of solution (ROTOR 1) were unacceptable. This was partially due to the numerical methods used in calculating the Θ-derivatives. However, inaccuracies of the Θ=constant curves are considered to be the primary fault. It is believed that accurate Θ=constant curves can be constructed from three-view drawings. Under this assumption, ROTOR 1 can be utilized with acceptable accuracy.

2. The results of ROTOR 2 are considered valid. Although test results are not available for comparison, the logic of the preceding discussion is sufficient proof, in that:

   a. The theory is sound.
   b. The assumptions are justified for engineering applications.
   c. Numerical methods are designed to minimize inaccuracies in each calculation, so that errors will not accumulate.
   d. Data are accurately measured.

3. The computed system of streamlines is regular and follows

a logical development through the rotor. Fig. 10 is a smooth plot of this system. Deviations from data points are small. Maximum deviations occur in the region of rapid curvature and blade angle changes.

4. The acceptable system of streamlines demonstrates the consistency of the solution. The accuracy of the method is measured by the resultant relative velocity distribution. This distribution completely defines the flow. Both pressure distribution and power delivered, or required, are calculated directly from the velocities. Variations in relative velocity indicate areas of possible flow separation.

The accuracy of the relative velocities at the leading edge are computed directly from entrance conditions, and are accurate. Variations of velocities along selected streamlines are shown in Fig. 11. Proper trends are indicated for a compressor with deleaded type blades. Most of the work input is accomplished in the forward section of the rotor, diminishing towards the trailing edge. It should be noted that the energy level of the fluid is not affected by velocity alone. Eq. (6), together with Eq. (9b), shows that the local enthalpy is also a function of peripheral speed, ωR. Therefore, the deloaded blade effectively reduces the deceleration of the relative velocity at high radii, so that the work input, thus blade loading, will not become excessive. The irregular nature of the velocity distributions in Fig. 11 might be attributed to inaccuracies in the calculations; however, similar presentations

in Refs. 5, 6, and 13 support the existence of these irregularities. In contrast, the velocity profiles along normals in Fig. 12 are quite regular.

5. The applicability of these results can be illustrated by an investigation of flow separation along a contour. Relative velocity changes along the hub, near the leading edge, appear to be conducive to separation. The rapid decrease in velocity implies an adverse pressure gradient. A separation parameter, K, is derived in Ref. 14. A value of K greater than .045 indicates probable separation.

$$K = \frac{l \frac{dp}{dl}}{\rho W^2 R_e^{1/5}} \tag{82}$$

Reynold's Number is defined as:

$$R_e = \frac{Wl}{\nu}$$

Let:

$$l = \frac{m}{\cos \bar{\beta}}$$

where: l = length along blade from stagnation point

$\bar{\beta}$ = average blade angle

Along a streamline, from Eqs. (6) and (9b):

$$\frac{dh}{dm} = -W \frac{dW}{dm} + \omega^2 R \frac{dR}{dm} \tag{83}$$

For incompressible flow:

$$dh = \frac{dp}{\rho}$$

$$K = \frac{m^{.8}\left(-W \frac{dW}{dm} + \omega^2 R \frac{dR}{dm}\right) \cdot \left(\nu \cos \bar{\beta}\right)^{.2}}{W^{2.2}} \tag{84}$$

At a point on the hub, m = 2 inches:

W = 106 ft./sec.

$\frac{dW}{dm} \doteq$ -216 ft./sec.-ft.

$\frac{dR}{dm} = \sin \lambda = .165$

$R = .5$ ft.

$\nu \doteq .00016$ ft.^{2}/sec. for air

$\bar{\beta} \doteq 49^\circ$ from Fig. 9

Therefore: $K = .0138$

Thus, flow at this particular point, which appears to be in one of the more critical regions for separation, should not separate. The relatively high value of K does indicate possible separation farther along the hub; however, the change of velocity decreases beyond this point. The effects of peripheral speed and curvature on separation are illustrated in Eq. (84). The value of K is approximately .0092 at the point of maximum curvature, at a distance of about .4 inches along the tip streamline. The velocity gradient at this point is practically zero. Although the value of K is low, it can be surmised that a nominal negative velocity gradient might induce separation.

6. The results of the blade to blade analysis are extensions of the more exact meridional plane analysis. The relative velocity distributions along streamlines (Figs. 13, 14, and 15) can also be analyzed for local phenomena, which may be aggrevated by the correction, ΔW. This velocity difference is used to calculate the fluid forces on the blade with the relations of Section II. A presentation of the type shown in Fig. 16 is adequate for these calculations.

An attempt was made to indicate the correlation between the trailing edge velocities in Fig. 14, in order to

establish some initial conditions for a wake analysis. The dashed line indicates a possible velocity distribution, but this is only a guess. Figs. 13 and 15 do not demonstrate this convergence. In addition, the velocities at the trailing edge are calculated from extrapolated data. Therefore, this type of correlation is inconclusive.

E. Extensions of the Method

1. The meridional plane analysis sufficiently describes the flow for an incompressible analysis. The results might be extended to include the calculations of:

   a. Pressure distribution
   b. Power input or power required
   c. Separation parameter
   d. Cavitation parameter
   e. Blade forces

Most of these calculations depend upon the results of several characteristic solutions, and would be included in a separate computer program. Many preliminary calculations of point functions (pressure, enthalpy, etc.) can be included in the main solution.

2. The methods should be modified to include characteristic calculations outside the rotor passage. This would permit continuous solutions through multi-stage machines and in unbladed passages. Major modifications would be required, since a number of decisions would be needed to insure the use of proper blade properties in the vicinity of blade boundaries. Input requirements would necessarily

become more complex.

3. The theory and methods could be modified to use non-dimensional variables. This would be particularly applicable to design studies, where non-dimensional results of preliminary rotor configurations could be directly compared.

4. This method should be extended to include the compressible solution. A method is outlined in Ref. 9.

5. The blade to blade method used in this thesis is practical in its simplicity, and is sufficiently accurate when used in conjunction with the meridional plane analysis. It would be interesting to compare the results of this solution with a more exact approach, such as the method of Ref.

6. The extensions to the meridional plane analysis should also be included in the blade to blade solution.

V. CONCLUSIONS AND RECOMMENDATIONS

A. It is concluded that:

1. Theoretical assumptions are based on practical consideration, and do not impose excessive limitations on the solution.

2. The meridional plane analysis is developed from sound theoretical derivations, which provide a relatively rapid and accurate method of solution.

3. The methods which are applied in solving this problem are good approximations. The degree of accuracy of each characteristic solution depends on the size of the coordinate grid and on the accuracy of data measurements.

4. The progressive method employed in the meridional plane solution can be applied at arbitrary intervals to obtain the desired accuracy.

5. The accuracy of the results, based primarily upon theoretical considerations, is sufficient for engineering purposes.

6. Results are not sufficiently accurate to compute detailed analyses at the trailing edge.

7. The results of this method are sufficient to completely describe the flow within the rotor, and predict the performance of the machine.

8. This solution is restricted to flows within the rotor passage.

9. The computer program, ROTOR 1, can be used if Θ=constant curves are accurately specified.

10. The use of a direct flow analysis is preferrable to the inverse method in design studies.

11. The blade to blade analysis is limited by the assumption of a linear velocity distribution, but the results are acceptable for engineering purposes.

B. It is recommended that:

1. The method be non-dimensionalized.

2. Computations be added to describe pressure distribution, blade force, power, and critical flow phenomena.

3. The solution be modified to include compressible flows, and calculations beyond rotor boundaries.

4. A more accurate blade to blade analysis be used in conjunction with this meridional plane solution.

REFERENCES

1. Hamrick, Joseph T., Ginsburg, Ambrose, and Osborn, Walter M.: Method of Analysis for Compressible Flow Through Mixed-Flow Centrifugal Impellers of Arbitrary Design. NACA Rep. 1082, 1952.

2. Wu, Chung-Hua: A General Through-Flow Theory of Fluid Flow with Subsonic or Supersonic Velocity in Turbomachines of Arbitrary Hub and Casing Shapes. NACA TN 2302, 1951.

3. Wu, Chung-Hua, Brown, Curtis A.: Method of Analysis for Compressible Flow Past Arbitrary Turbomachine Blades on General Surface of Revolution. NACA TN 2407, 1951.

4. Wu, Chung-Hua: A General Theory of Three-Dimensional Flow in Subsonic and Supersonic Turbomachines of Axial-, Radial-, and Mixed-Flow Types. NACA TN 2604, 1952.

5. Smith, Kenneth J., and Hamrick, Joseph T.: A Rapid Approximation Method for the Design of Hub Shroud Profiles of Centrifugal Impellers of Given Blade Shape. NACA TN 3399, 1955.

6. Kramer, James J., Stockman, Norbert O., and Bean, Ralph J.: Nonviscous Flow Through a Pump Impeller on a Blade-to-Blade Surface of Revolution. NASA TN D-1108, 1962.

7. Stockman, Norbert O., and Kramer, James J.: Method for Design of Pump Impellers Using a High Speed Digital Computer. NASA TN D-1562, 1963.

8. Meyer, Rudolph X.: A General Method for the Computation of the Compressible Flow in Turbo Machines of Prescribed Boundaries and Blades. Naval Research Project 24748, Rep. 1, U. S. Naval Postgraduate School, Annapolis, Md., 1949.

9. Vavra, M. H.: Aero-Thermodynamics and Flow in Turbomachines, Chapt. 11, John Wiley and Sons, Inc., New York, 1960.

10. Vavra, M. H., and Gawain, T. H.: Compressor Test Rig for Investigation of Flow Phenomena in Turbo-Machines. ONR Project NR 061-058, Rep. 12, U. S. Naval Postgraduate School, Monterey, California, 1955.

11. Salvadori, Mario G., and Baron, Melvin L.: Numerical Methods in Engineering. Prentice-Hall Inc., Englewood Cliffs, N. J., 1952.

12. Southwell, R. V.: Relaxation Methods in Theoretical Physics. pp. 229-233, Oxford Press, 1946.

13. Wu, Chung-Hua; Brown, Curtis A., and Costilow, Eleanor L.: Analysis of Flow in a Subsonic Mixed-Flow Impeller. NACA TN 2749, 1952.

14. Ban-Zelikowitsch, G. M., Iswestia Acadamia Nauk SSR, No. 12, 1954. (In Russian) Referenced in: Developments on Stream Turbine Bladings. Escher-Wyss Review, Vol. 33, 1960.

TABLE I

INITIAL DATA FOR TEST IMPELLER

No. of Blades.	23
Blade Thickness, in.	.3
RPM.	1800
Volumetric Flow Rate, cu. ft./sec.	128.212
Annulus Area at L.E., sq. in.	196.22
Meridional Velocity, V_{mL}, ft./sec.	94.09

Air at Standard Temperature and Pressure

TABLE II-1

DATA FOR CHARACTERISTIC C1

LOCATION OF CHARACTERISTIC CURVE

STARTING NORMAL NO. = 4

M =	1	2	3	4	5
DNSTAR =	.0000	-.0342	-.0778	-.1268	-.1842
GAM-LAM =	-11.3400	-10.9150	-10.4652	-10.4767	-10.1701
GAMMA =	-2.5900	-3.7924	-5.2378	-5.7088	-7.3777
BETA(P) =	-49.3000	-49.5236	-49.7943	-50.0899	-50.4328
RADIUS =	6.0100	6.6160	7.1639	7.6701	8.1727

LOCATION OF NEW STREAMLINES

M =	1	2	3	4	5
DELTA X =	.0000	.0443	.0805	.0220	-.0166
BETA(X) =	-49.3000	-49.5414	-49.8367	-50.1027	-50.4215
RADIUS =	6.0100	6.6595	7.2431	7.6917	8.1563

VELOCITY PROFILE

M =	1	2	3	4	5
WM(P) =	86.4590	88.7083	90.0108	90.6751	90.8116
WM(X) =	86.4590	88.8395	90.1501	90.6938	90.8169
REL VEL =	132.5857	136.9081	139.7742	141.3968	142.5392
DW COEF =	.1281	.1320	.1345	.1359	.1368
DW FUNC =	-441.	35.	605.	1139.	1787.

TABLE II-1

DATA FOR CHARACTERISTIC C1

LOCATION OF CHARACTERISTIC CURVE

STARTING NORMAL NO. = 4

M =	6	7	8	9
DNSTAR =	-.2471	-.3166	-.3881	-.4679
GAM-LAM =	-9.8294	-9.7783	-9.5601	-9.5577
GAMMA =	-8.5532	-9.0037	-10.8228	-12.3382
BETA(P) =	-50.8637	-51.3793	-51.8894	-52.4967
RADIUS =	8.6200	9.0700	9.4878	9.9023

LOCATION OF NEW STREAMLINES

M =	6	7	8	9
DELTA X =	-.0684	-.0935	-.1196	.0000
BETA(X) =	-50.7988	-51.2735	-51.7424	-52.4967
RADIUS =	8.5526	8.9779	9.3699	9.9023

VELOCITY PROFILE

M =	6	7	8	9
WM(P) =	90.3799	89.4412	88.1390	86.3790
WM(X) =	90.4889	89.6787	88.5868	86.3790
REL VEL =	143.1683	143.3472	143.0669	141.8821
DW COEF =	.1370	.1368	.1363	.1349
DW FUNC =	2401.	3145.	3917.	5108.

TABLE II-2

DATA FOR CHARACTERISTIC C2

LOCATION OF CHARACTERISTIC CURVE

STARTING NORMAL NO. = 3

M =	1	2	3	4	5
DNSTAR =	.0000	.0221	.0311	.0320	.0326
GAM-LAM =	-9.4547	-8.8207	-7.1870	-7.1506	-5.6883
GAMMA =	2.2953	1.6850	.1174	.1087	.0426
BETA(P) =	-43.7000	-43.6597	-43.6947	-43.7616	-43.8372
RADIUS =	6.2100	6.8346	7.3839	7.8343	8.2730

LOCATION OF NEW STREAMLINES

M =	1	2	3	4	5
DELTA X =	.0000	.0691	.1202	.1068	.1089
BETA(X) =	-43.7000	-43.6548	-43.7039	-43.7778	-43.8600
RADIUS =	6.2100	6.9029	7.5031	7.9402	8.3813

VELOCITY PROFILE

M =	1	2	3	4	5
WM(P) =	77.3222	81.5205	84.3795	86.1041	87.3991
WM(X) =	77.3222	81.9309	84.8900	86.4604	87.6694
REL VEL =	106.9511	113.2405	117.4265	119.7464	121.5882
DW COEF =	.1491	.1542	.1575	.1595	.1612
DW FUNC =	1763.	2506.	3307.	3990.	4768.

TABLE II-2

DATA FOR CHARACTERISTIC C2

LOCATION OF CHARACTERISTIC CURVE

STARTING NORMAL NO. = 3

M =	6	7	8	9
DNSTAR =	.0329	.0303	.0217	.0048
GAM-LAM =	-4.7525	-5.3110	-6.0772	-5.9846
GAMMA =	.0575	-.7670	-1.7137	-2.5034
BETA(P) =	-43.9181	-44.0091	-44.1269	-44.2784
RADIUS =	8.6330	9.0528	9.4521	9.9105

LOCATION OF NEW STREAMLINES

M =	6	7	8	9
DELTA X =	.1141	.1013	.0315	.0000
BETA(X) =	-43.9400	-44.0321	-44.1350	-44.2784
RADIUS =	8.7467	9.1537	9.4834	9.9105

VELOCITY PROFILE

M =	6	7	8	9
WM(P) =	88.1297	88.5673	88.5827	88.0851
WM(X) =	88.3047	88.6192	88.5680	88.0851
REL VEL =	122.6340	123.2617	123.4050	123.0314
DW COEF =	.1624	.1636	.1644	.1653
DW FUNC =	5489.	6383.	7173.	8299.

TABLE II-3

DATA FOR CHARACTERISTIC C3

LOCATION OF CHARACTERISTIC CURVE

STARTING NORMAL NO. = 2

M =	1	2	3	4	5
DNSTAR =	.0000	.0728	.1355	.1760	.2206
GAM-LAM =	-11.0921	-10.3759	-9.5373	-9.0372	-7.8418
GAMMA =	5.6079	5.9430	5.9027	5.5052	5.9803
BETA(P) =	-38.2000	-38.2507	-38.3586	-38.5683	-38.7540
RADIUS =	6.4700	7.1808	7.7735	8.1744	8.6075

LOCATION OF NEW STREAMLINES

M =	1	2	3	4	5
DELTA X =	.0000	.0072	.0242	.0569	.0480
BETA(X) =	-38.2000	-38.2513	-38.3650	-38.5950	-38.7793
RADIUS =	6.4700	7.1879	7.7973	8.2306	8.6550

VELOCITY PROFILE

M =	1	2	3	4	5
WM(P) =	70.9010	76.6468	80.8738	83.2348	85.4015
WM(X) =	70.9010	76.7004	81.0299	83.5263	85.6207
REL VEL =	90.2212	97.6698	103.3449	106.8691	109.8314
DW COEF =	.1677	.1722	.1752	.1766	.1778
DW FUNC =	3559.	4523.	5458.	6185.	6976.

TABLE II-3

DATA FOR CHARACTERISTIC C3

LOCATION OF CHARACTERISTIC CURVE

STARTING NORMAL NO. = 2

M =	6	7	8	9
DNSTAR =	.2578	.2997	.3324	.3751
GAM-LAM =	-7.0684	-5.6366	-5.6294	-5.6032
GAMMA =	6.1473	6.1015	6.0736	5.8575
BETA(P) =	-38.9747	-39.2207	-39.5066	-39.6997
RADIUS =	8.9586	9.3394	9.6484	10.0450

LOCATION OF NEW STREAMLINES

M =	6	7	8	9
DELTA X =	.0492	.0318	.0331	.0000
BETA(X) =	-39.0023	-39.2461	-39.5297	-39.6997
RADIUS =	9.0074	9.3710	9.6814	10.0450

VELOCITY PROFILE

M =	6	7	8	9
WM(P) =	86.8675	88.2065	89.0356	89.7898
WM(X) =	87.0509	88.3039	89.1115	89.7898
REL VEL =	112.0172	114.0234	115.5348	116.7006
DW COEF =	.1785	.1791	.1793	.1799
DW FUNC =	7673.	8441.	9124.	10034.

TABLE II-4

DATA FOR CHARACTERISTIC C4

LOCATION OF CHARACTERISTIC CURVE

STARTING NORMAL NO. = 2

M =	1	2	3	4	5
DNSTAR =	.0000	.1156	.2132	.2938	.3709
GAM-LAM =	-15.1727	-14.4958	-12.7895	-11.6315	-10.3907
GAMMA =	9.5773	8.7551	10.1163	10.9301	10.8506
BETA(P) =	-32.0000	-32.2773	-32.6731	-33.1846	-33.7038
RADIUS =	6.9900	7.6851	8.2632	8.6847	9.0741

LOCATION OF NEW STREAMLINES

M =	1	2	3	4	5
DELTA X =	.0000	-.0004	.0228	.0156	.0086
BETA(X) =	-32.0000	-32.2771	-32.6935	-33.2041	-33.7162
RADIUS =	6.9900	7.6847	8.2854	8.6999	9.0825

VELOCITY PROFILE

M =	1	2	3	4	5
WM(P) =	66.5165	72.9600	77.6404	80.8896	83.6173
WM(X) =	66.5165	72.9568	77.8154	80.9992	83.6713
REL VEL =	78.4348	86.2908	92.4644	96.8051	100.5909
DW COEF =	.1866	.1903	.1917	.1920	.1923
DW FUNC =	5723.	6882.	7974.	8732.	9464.

TABLE II-4

DATA FOR CHARACTERISTIC C4

LOCATION OF CHARACTERISTIC CURVE

STARTING NORMAL NO. = 2

M =	6	7	8	9
DNSTAR =	.4394	.5076	.5698	.6407
GAM-LAM =	-9.6181	-9.4840	-9.0488	-8.3707
GAMMA =	11.0479	11.5039	11.9500	12.9363
BETA(P) =	-34.3802	-35.1071	-35.9127	-36.7628
RADIUS =	9.4277	9.7770	10.0699	10.3860

LOCATION OF NEW STREAMLINES

M =	6	7	8	9
DELTA X =	-.0056	-.0078	-.0114	.0000
BETA(X) =	-34.3697	-35.0909	-35.8826	-36.7628
RADIUS =	9.4222	9.7694	10.0586	10.3860

VELOCITY PROFILE

M =	6	7	8	9
WM(P) =	85.7169	87.5236	89.0085	90.4841
WM(X) =	85.6873	87.4843	88.9556	90.4841
REL VEL =	103.8114	106.9175	109.7919	112.9469
DW COEF =	.1918	.1910	.1896	.1879
DW FUNC =	10108.	10784.	11304.	11908.

TABLE II-5

DATA FOR CHARACTERISTIC C5

LOCATION OF CHARACTERISTIC CURVE

STARTING NORMAL NO. = 2

M =	1	2	3	4	5
DNSTAR =	.0000	.1411	.2609	.3466	.4271
GAM-LAM =	-19.6662	-19.0712	-18.3910	-16.4404	-15.7630
GAMMA =	11.5838	11.5338	11.3148	12.0517	12.8821
BETA(P) =	-27.8000	-28.5343	-29.3978	-30.4472	-31.6027
RADIUS =	7.5900	8.2556	8.8105	9.2064	9.5618

LOCATION OF NEW STREAMLINES

M =	1	2	3	4	5
DELTA X =	.0000	.0046	.0032	.0092	.0419
BETA(X) =	-27.8000	-28.5399	-29.4043	-30.4730	-31.7408
RADIUS =	7.5900	8.2599	8.8135	9.2152	9.6021

VELOCITY PROFILE

M =	1	2	3	4	5
WM(P) =	63.0930	70.0131	75.2679	78.5352	81.1981
WM(X) =	63.0930	70.0553	75.2940	78.6023	81.4914
REL VEL =	71.3253	79.7456	86.4278	91.1999	95.8230
DW COEF =	.1985	.2005	.2012	.2001	.1982
DW FUNC =	7829.	9084.	10154.	10892.	11571.

TABLE II-5

DATA FOR CHARACTERISTIC C5

LOCATION OF CHARACTERISTIC CURVE

STARTING NORMAL NO. = 2

M =	6	7	8	9
DNSTAR =	.5103	.6037	.6952	.8083
GAM-LAM =	-15.2153	-14.5683	-14.7957	-14.1805
GAMMA =	14.4943	15.7970	18.0082	19.5109
BETA(P) =	-32.8655	-34.2872	-35.8854	-37.7208
RADIUS =	9.8964	10.2519	10.5742	10.8850

LOCATION OF NEW STREAMLINES

M =	6	7	8	9
DELTA X =	.0389	-.0040	-.0084	.0000
BETA(X) =	-33.0031	-34.2713	-35.8425	-37.7208
RADIUS =	9.9339	10.2480	10.5660	10.8850

VELOCITY PROFILE

M =	6	7	8	9
WM(P) =	83.5503	85.8377	87.8115	89.7423
WM(X) =	83.7991	85.8120	87.7596	89.7423
REL VEL =	99.9224	103.8407	108.2609	113.4539
DW COEF =	.1956	.1930	.1890	.1842
DW FUNC =	12113.	12605.	13006.	13267.

TABLE II-6

DATA FOR CHARACTERISTIC C6

LOCATION OF CHARACTERISTIC CURVE

STARTING NORMAL NO. = 2

M =	1	2	3	4	5
DNSTAR =	.0000	.1462	.2716	.3765	.4888
GAM-LAM =	-28.8995	-27.4739	-25.9103	-24.1102	-24.9668
GAMMA =	11.0505	12.8221	14.0721	15.8992	16.1083
BETA(P) =	-23.7000	-25.5592	-27.5695	-29.7262	-31.9938
RADIUS =	8.7000	9.3214	9.8034	10.1755	10.5488

LOCATION OF NEW STREAMLINES

M =	1	2	3	4	5
DELTA X =	.0000	-.0620	-.0409	-.0278	-.0713
BETA(X) =	-23.7000	-25.3956	-27.4165	-29.5774	-31.5970
RADIUS =	8.7000	9.2664	9.7665	10.1501	10.4842

VELOCITY PROFILE

M =	1	2	3	4	5
WM(P) =	61.6410	68.8717	74.0780	77.6503	80.9685
WM(X) =	61.6410	68.2392	73.7027	77.4126	80.4159
REL VEL =	67.3185	75.5386	83.0281	89.0118	94.4121
DW COEF =	.2118	.2102	.2076	.2035	.2000
DW FUNC =	11442.	12583.	13499.	14068.	14496.

TABLE II-6

DATA FOR CHARACTERISTIC C6

LOCATION OF CHARACTERISTIC CURVE

STARTING NORMAL NO. = 2

M =	6	7	8	9
DNSTAR =	.5852	.6687	.7762	.9022
GAM-LAM =	-23.5395	-22.0885	-21.0109	-19.2679
GAMMA =	17.5715	19.0663	21.3290	22.7489
BETA(P) =	-34.3762	-36.8106	-39.4102	-42.3090
RADIUS =	10.8624	11.1154	11.4175	11.7516

LOCATION OF NEW STREAMLINES

M =	6	7	8	9
DELTA X =	-.0661	.0530	.0501	.0000
BETA(X) =	-33.9009	-37.2278	-39.7999	-42.3090
RADIUS =	10.8018	11.1645	11.4642	11.7516

VELOCITY PROFILE

M =	6	7	8	9
WM(P) =	83.4560	85.2295	87.0504	88.5593
WM(X) =	82.9763	85.5546	87.3327	88.5593
REL VEL =	99.9711	107.4487	113.6722	119.7514
DW COEF =	.1949	.1865	.1791	.1719
DW FUNC =	14766.	14786.	14764.	14664.

TABLE II-7

DATA FOR CHARACTERISTIC C7

LOCATION OF CHARACTERISTIC CURVE

STARTING NORMAL NO. = 2

M =	6	7	8	9
DNSTAR =	.6225	.7263	.8381	.9475
GAM-LAM =	-29.5988	-27.9648	-28.2480	-28.9740
GAMMA =	18.5752	20.1474	21.3246	21.9428
BETA(P) =	-37.6563	-40.4622	-43.3651	-46.2584
RADIUS =	11.8069	12.1087	12.4042	12.6870

LOCATION OF NEW STREAMLINES

M =	6	7	8	9
DELTA X =	-.0185	.0040	-.0122	.0000
BETA(X) =	-37.5028	-40.4982	-43.2526	-46.2584
RADIUS =	11.7908	12.1122	12.3935	12.6870

VELOCITY PROFILE

M =	6	7	8	9
WM(P) =	79.6489	81.5500	83.2322	84.4272
WM(X) =	79.5300	81.5733	83.1723	84.4272
REL VEL =	100.2490	107.2731	114.1944	122.1092
DW COEF =	.1877	.1793	.1711	.1618
DW FUNC =	17570.	17528.	17315.	16909.

TABLE II-7

DATA FOR CHARACTERISTIC C7

LOCATION OF CHARACTERISTIC CURVE

STARTING NORMAL NO. = 2

M =	1	2	3	4	5
DNSTAR =	.0000	.1578	.3039	.4101	.5172
GAM-LAM =	-32.2487	-33.2812	-31.5112	-30.3829	-29.9231
GAMMA =	15.0513	14.4762	15.7760	16.4842	16.9608
BETA(P) =	-24.0000	-26.6517	-29.3615	-32.0475	-34.8028
RADIUS =	9.8100	10.3442	10.8314	11.1799	11.5049

LOCATION OF NEW STREAMLINES

M =	1	2	3	4	5
DELTA X =	.0000	-.0096	-.0400	-.0250	-.0108
BETA(X) =	-24.0000	-26.6106	-29.1671	-31.8716	-34.7224
RADIUS =	9.8100	10.3361	10.7972	11.1583	11.4955

VELOCITY PROFILE

M =	1	2	3	4	5
WM(P) =	58.0370	65.4298	71.1053	74.5236	77.3497
WM(X) =	58.0370	65.3268	70.7192	74.3173	77.2744
REL VEL =	63.5294	73.0666	80.9884	87.5111	94.0167
DW COEF =	.2129	.2107	.2065	.2012	.1949
DW FUNC =	15098.	16079.	16861.	17282.	17522.

TABLE II-8

DATA FOR CHARACTERISTIC C8

LOCATION OF CHARACTERISTIC CURVE

STARTING NORMAL NO. = 2

M =	1	2	3	4	5
DNSTAR =	.0000	.1863	.3537	.4777	.5875
GAM-LAM =	-38.3072	-36.3681	-36.9234	-36.9877	-37.0683
GAMMA =	17.4928	18.9027	18.1034	18.1761	17.5196
BETA(P) =	-26.4000	-29.3276	-32.2429	-35.0748	-37.9632
RADIUS =	10.9200	11.3957	11.8267	12.1581	12.4577

LOCATION OF NEW STREAMLINES

M =	1	2	3	4	5
DELTA X =	.0000	.0100	.0013	-.0190	-.0090
BETA(X) =	-26.4000	-29.3831	-32.2524	-34.9396	-37.8908
RADIUS =	10.9200	11.4037	11.8277	12.1429	12.4505

VELOCITY PROFILE

M =	1	2	3	4	5
WM(P) =	52.9880	61.1183	67.2976	71.1384	73.8746
WM(X) =	52.9880	61.2480	67.3112	70.9712	73.8168
REL VEL =	59.1574	70.2902	79.5918	86.5760	93.5358
DW COEF =	.2110	.2059	.2013	.1955	.1885
DW FUNC =	19031.	19793.	20341.	20569.	20637.

TABLE II-8

DATA FOR CHARACTERISTIC C8

LOCATION OF CHARACTERISTIC CURVE

STARTING NORMAL NO. = 2

M =	6	7	8	9
DNSTAR =	.6883	.7986	.8831	.9746
GAM-LAM =	-37.0218	-37.5553	-38.2758	-40.9817
GAMMA =	18.8401	19.8310	19.3823	17.7669
BETA(P) =	-40.7806	-43.7548	-46.4951	-49.3487
RADIUS =	12.7323	12.9993	13.2607	13.5496

LOCATION OF NEW STREAMLINES

M =	6	7	8	9
DELTA X =	.0038	.0275	.0503	.0000
BETA(X) =	-40.8126	-44.0789	-46.9727	-49.3487
RADIUS =	12.7354	13.0215	13.3002	13.5496

VELOCITY PROFILE

M =	6	7	8	9
WM(P) =	75.7367	77.3583	78.3727	79.1673
WM(X) =	75.7561	77.4854	78.5444	79.1673
REL VEL =	100.0937	107.8603	115.1091	121.5238
DW COEF =	.1802	.1703	.1614	.1539
DW FUNC =	20574.	20237.	19914.	19615.

TABLE II-9

DATA FOR CHARACTERISTIC C9

LOCATION OF CHARACTERISTIC CURVE

STARTING NORMAL NO. = 2

M =	1	2	3	4	5
DNSTAR =	.0000	.1820	.3319	.4518	.5673
GAM-LAM =	-45.4285	-45.3287	-44.7492	-45.0907	-46.5900
GAMMA =	18.3715	17.8140	18.3051	18.6397	17.2144
BETA(P) =	-31.8000	-34.7985	-37.6903	-40.3692	-43.0088
RADIUS =	12.4200	12.8306	13.1770	13.4616	13.7247

LOCATION OF NEW STREAMLINES

M =	1	2	3	4	5
DELTA X =	.0000	-.0607	-.0757	-.0746	-.1057
BETA(X) =	-31.8000	-34.4885	-37.2367	-39.8407	-42.2680
RADIUS =	12.4200	12.7880	13.1233	13.4089	13.6521

VELOCITY PROFILE

M =	1	2	3	4	5
WM(P) =	55.1540	61.8969	66.3989	69.3353	71.6441
WM(X) =	55.1540	61.2727	65.7637	68.8022	71.1038
REL VEL =	64.8952	74.3385	82.6028	89.6061	96.0853
DW COEF =	.2036	.1982	.1915	.1845	.1779
DW FUNC =	23980.	24365.	24591.	24654.	24544.

TABLE III-9

DATA FOR CHARACTERISTIC C9

LOCATION OF CHARACTERISTIC CURVE

STARTING NORMAL NO. = 2

M =	6	7	8	9
DNSTAR =	.6681	.7596	.8385	.9061
GAM-LAM =	-47.6141	-47.3437	-45.6471	-44.5153
GAMMA =	16.3507	16.3615	16.4971	16.7489
BETA(P) =	-45.5308	-47.9953	-50.2033	-52.3203
RADIUS =	13.9669	14.2071	14.3925	14.5853

LOCATION OF NEW STREAMLINES

M =	6	7	8	9
DELTA X =	-.1353	-.1049	-.0744	.0000
BETA(X) =	-44.5559	-47.1992	-49.6145	-52.3203
RADIUS =	13.8757	14.1360	14.3405	14.5853

VELOCITY PROFILE

M =	6	7	8	9
WM(P) =	73.2304	74.4063	75.2378	75.7349
WM(X) =	72.6960	74.0611	75.0393	75.7349
REL VEL =	102.0200	109.0013	115.8142	123.9022
DW COEF =	.1711	.1628	.1546	.1450
DW FUNC =	24374.	24100.	23583.	22936.

TABLE III-1

VELOCITY PROFILE

MERIDIONAL STREAMLINE NO. 1

M	W	DW	W SUCTION	W PRESSURE
.00	160.2000	10.1043	170.3043	150.0957
.50	144.7000	11.3940	156.0940	133.3060
1.00	130.2000	11.4028	141.6028	118.7972
1.50	117.0000	11.8866	128.8866	105.1134
2.00	106.8000	11.5423	118.3423	95.2577
2.50	97.2000	10.9433	108.1433	86.2567
3.00	91.3000	11.1128	102.4128	80.1872
3.50	86.4000	10.5962	96.9962	75.8037
4.00	82.4000	10.4334	92.8334	71.9666
4.50	78.8000	11.6713	90.4713	67.1287
5.00	75.6000	12.6603	88.2603	62.9397
5.50	72.9000	13.3047	86.2047	59.5953
6.00	70.9000	14.2076	85.1076	56.6924
6.50	69.6000	15.1219	84.7219	54.4781
7.00	68.5000	16.5328	85.0328	51.9672
7.50	67.5000	18.3021	85.8021	49.1979
8.00	66.8000	19.1616	85.9616	47.6384
8.50	65.8000	19.6617	85.4617	46.1383
9.00	64.5000	21.3834	85.8834	43.1166
9.50	63.2000	23.5927	86.7927	39.6073
10.00	61.7000	24.9452	86.6452	36.7548
10.50	60.0000	24.9541	84.9541	35.0459
11.00	59.2000	24.9375	84.1375	34.2625
11.50	60.0000	24.9381	84.9381	35.0619
12.00	62.2000	24.7177	86.9177	37.4823
12.50	65.5000	23.9489	89.4489	41.5511
13.00	69.0000	23.0313	92.0313	45.9688
13.50	73.0000	23.6601	96.6601	49.3399
14.00	77.0000	22.2040	99.2040	54.7960

TABLE III-2

VELOCITY PROFILE

MERIDIONAL STREAMLINE NO. 2

M	W	DW	W SUCTION	W PRESSURE
.00	156.7000	11.2554	167.9554	145.4446
.50	143.9000	11.8948	155.7948	132.0052
1.00	133.0000	12.7219	145.7219	120.2781
1.50	121.0000	13.2414	134.2414	107.7586
2.00	111.4000	13.3102	124.7102	98.0898
2.50	103.1000	13.1943	116.2943	89.9057
3.00	97.1000	12.5589	109.6589	84.5411
3.50	92.4000	12.3531	104.7531	80.0469
4.00	88.6000	13.0225	101.6225	75.5775
4.50	85.5000	13.7728	99.2728	71.7272
5.00	82.7000	14.2125	96.9125	68.4875
5.50	80.3000	14.7261	95.0261	65.5739
6.00	78.5000	15.5826	94.0826	62.9174
6.50	77.2000	16.6498	93.8498	60.5502
7.00	76.2000	18.3017	94.5017	57.8983
7.50	75.4000	19.5005	94.9005	55.8995
8.00	74.6000	19.6812	94.2813	54.9187
8.50	73.8000	20.2202	94.0202	53.5798
9.00	72.9000	21.5470	94.4470	51.3530
9.50	72.0000	23.0556	95.0556	48.9444
10.00	71.0000	23.4652	94.4652	47.5348
10.50	70.2000	23.5125	93.7125	46.6875
11.00	70.4000	23.6410	94.0410	46.7590
11.50	71.4000	23.3800	94.7800	48.0200
12.00	74.3000	23.1866	97.4866	51.1134
12.50	78.2000	22.2397	100.4397	55.9603
13.00	83.0000	22.5898	105.5898	60.4102

TABLE III-3

VELOCITY PROFILE

MERIDIONAL STREAMLINE NO. 3

M	W	DW	W SUCTION	W PRESSURE
.00	155.2000	13.2444	168.4444	141.9556
.50	143.8000	12.9910	156.7910	130.8090
1.00	133.3000	14.0600	147.3600	119.2400
1.50	123.3000	14.6491	137.9491	108.6509
2.00	114.5000	14.6679	129.1679	99.8321
2.50	107.5000	14.3500	121.8500	93.1500
3.00	102.0000	13.9765	115.9765	88.0235
3.50	97.7000	14.0631	111.7631	83.6369
4.00	94.1000	14.3938	108.4938	79.7062
4.50	90.7000	14.4722	105.1722	76.2278
5.00	87.9000	14.7451	102.6451	73.1549
5.50	85.8000	15.5713	101.3713	70.2287
6.00	84.6000	16.3908	100.9908	68.2092
6.50	83.7000	17.1630	100.8630	66.5370
7.00	83.1000	18.9291	102.0291	64.1709
7.50	82.3000	19.3504	101.6504	62.9496
8.00	81.6000	18.7687	100.3687	62.8313
8.50	81.0000	20.4359	101.4359	60.5641
9.00	80.5000	22.4865	102.9865	58.0135
9.50	80.0000	23.2128	103.2128	56.7872
10.00	79.5000	22.5787	102.0787	56.9213
10.50	79.7000	22.0301	101.7301	57.6699
11.00	80.6000	22.0323	102.6323	58.5677
11.50	82.5000	21.7964	104.2964	60.7036
12.00	85.7000	21.6038	107.3038	64.0962
12.50	90.0000	20.9741	110.9741	69.0259

TABLE III-4

VELOCITY PROFILE

MERIDIONAL STREAMLINE NO. 4

M	W	DW	W SECTION	W PRESSURE
.00	154.6000	12.6731	167.2731	141.9269
.50	143.4000	13.3948	156.7948	130.0052
1.00	132.8000	14.5162	147.3162	118.2837
1.50	123.2000	15.1505	138.3505	108.0495
2.00	116.0000	15.2259	131.2259	100.7741
2.50	110.0000	14.8893	124.8893	95.1107
3.00	105.0000	14.2543	119.2543	90.7457
3.50	101.1000	14.4224	115.5224	86.6776
4.00	97.6000	15.0151	112.6151	82.5849
4.50	94.6000	15.3777	109.9777	79.2223
5.00	92.3000	15.5216	107.8216	76.7784
5.50	90.8000	15.7555	106.5555	75.0445
6.00	89.9000	16.2322	106.1322	73.6678
6.50	89.2000	16.8063	106.0063	72.3937
7.00	88.7000	17.6029	106.3029	71.0971
7.50	88.3000	18.6923	106.9923	69.6077
8.00	87.8000	19.1391	106.9391	68.6609
8.50	87.5000	20.2892	107.7892	67.2108
9.00	87.0000	21.7247	108.7247	65.2753
9.50	86.7000	22.0298	108.7298	64.6702
10.00	86.6000	21.6809	108.2809	64.9191
10.50	87.3000	21.2212	108.5212	66.0788
11.00	88.8000	21.1551	109.9551	67.6449
11.50	91.8000	20.8495	112.6495	70.9505
12.00	96.1000	20.8327	116.9327	75.2673

TABLE III-5

VELOCITY PROFILE

MERIDIONAL STREAMLINE NO. 5

M	W	DW	W SUCTION	W PRESSURE
.00	152.7000	13.0122	165.7122	139.6878
.50	143.0000	14.6320	157.6320	128.3680
1.00	133.7000	15.3426	149.0426	118.3574
1.50	125.0000	15.7981	140.7981	109.2019
2.00	118.2000	15.8833	134.0833	102.3167
2.50	112.2000	15.5870	127.7870	96.6130
3.00	107.4000	14.7262	122.1262	92.6738
3.50	103.7000	14.3023	118.0023	89.3977
4.00	100.8000	14.7846	115.5846	86.0154
4.50	98.3000	15.0312	113.3312	83.2687
5.00	96.4000	15.2025	111.6025	81.1975
5.50	95.4000	15.4751	110.8751	79.9249
6.00	95.0000	15.4599	110.4599	79.5401
6.50	94.7000	15.8551	110.5551	78.8449
7.00	94.4000	15.8689	110.2689	78.5311
7.50	94.1000	16.9366	111.0366	77.1634
8.00	93.9000	19.5936	113.4936	74.3064
8.50	93.8000	20.7099	114.5099	73.0901
9.00	93.6000	20.6857	114.2857	72.9143
9.50	93.8000	20.5208	114.3208	73.2792
10.00	94.3000	20.4300	114.7300	73.8700
10.50	95.2000	21.4977	116.6977	73.7023
11.00	96.6000	22.9335	119.5335	73.6665
11.50	99.1000	15.7829	114.8829	83.3171

TABLE III-6

VELOCITY PROFILE

MERIDIONAL STREAMLINE NO. 6

M	W	DW	W SUCTION	W PRESSURE
.00	151.3000	14.9754	166.2754	136.3246
.50	142.1000	15.0663	157.1663	127.0337
1.00	133.3000	15.7379	149.0379	117.5621
1.50	126.0000	16.2337	142.2337	109.7663
2.00	118.9000	16.3429	135.2429	102.5571
2.50	113.8000	15.7706	129.5706	98.0294
3.00	109.6000	13.8396	123.4396	95.7604
3.50	106.5000	13.1380	119.6380	93.3620
4.00	103.7000	13.9661	117.6661	89.7339
4.50	101.5000	13.9572	115.4572	87.5428
5.00	100.4000	14.1321	114.5321	86.2679
5.50	99.8000	14.4612	114.2612	85.3388
6.00	99.5000	14.5626	114.0626	84.9374
6.50	99.5000	14.8687	114.3688	84.6312
7.00	99.5000	15.6544	115.1544	83.8456
7.50	99.5000	16.4922	115.9922	83.0078
8.00	99.5000	17.5373	117.0373	81.9627
8.50	99.7000	17.8737	117.5737	81.8263
9.00	100.0000	18.0790	118.0790	81.9210
9.50	100.4000	19.4753	119.8753	80.9247
10.00	101.0000	21.1580	122.1580	79.8420
10.50	101.9000	24.7289	126.6289	77.1711
11.00	103.0000	39.8627	142.8627	63.1373

TABLE III -7

VELOCITY PROFILE

MERIDIONAL STREAMLINE NO. 7

M	W	Dw	W SUCTION	W PRESSURE
.00	149.8000	7.2347	157.0347	142.5653
.50	140.8000	20.6986	161.4986	120.1014
1.00	132.4000	17.4489	149.8489	114.9511
1.50	125.0000	15.4627	140.4627	109.5373
2.00	119.5000	14.9104	134.4104	104.5896
2.50	115.3000	13.2504	128.5504	102.0496
3.00	111.5000	13.9944	125.4944	97.5056
3.50	108.9000	15.0037	123.9037	93.8963
4.00	106.8000	13.7119	120.5119	93.0881
4.50	105.2000	12.6254	117.8254	92.5746
5.00	104.0000	12.0089	116.0089	91.9911
5.50	104.6000	11.5333	116.1333	93.0667
6.00	106.2000	12.0001	118.2001	94.1999
6.50	107.2000	13.1771	120.3771	94.0229
7.00	107.5000	14.2603	121.7603	93.2397
7.50	107.5000	16.1911	123.6911	91.3089
8.00	107.5000	17.9708	125.4708	89.5292
8.50	107.7000	17.8199	125.5199	89.8801
9.00	108.0000	17.7962	125.7962	90.2038
9.50	108.3000	19.3903	127.6903	88.9097
10.00	108.7000	22.1214	130.8214	86.5786
10.50	109.2000	30.7068	139.9068	78.4932

TABLE III-8

VELOCITY PROFILE

MERIDIONAL STREAMLINE NO. 8

M	W	DW	W SUCTION	W PRESSURE
.00	147.8000	15.5906	163.3906	132.2094
.50	139.2000	14.9572	154.1572	124.2428
1.00	131.3000	15.7562	147.0562	115.5438
1.50	124.2000	15.2227	139.4227	108.9773
2.00	119.9000	13.8629	133.7629	106.0371
2.50	116.4000	11.8239	128.2239	104.5761
3.00	113.3000	12.9087	126.2087	100.3913
3.50	111.8000	14.5964	126.3964	97.2036
4.00	109.4000	13.0625	122.4625	96.3375
4.50	108.6000	11.7237	120.3237	96.8763
5.00	105.8000	10.2004	116.0004	95.5996
5.50	109.8000	8.4688	118.2688	101.3312
6.00	112.0000	9.2796	121.2796	102.7204
6.50	113.3000	11.9992	125.2992	101.3008
7.00	113.7000	14.2146	127.9146	99.4854
7.50	114.1000	15.8650	129.9650	98.2350
8.00	114.5000	16.0562	130.5562	98.4438
8.50	114.9000	16.1184	131.0184	98.7816
9.00	115.1000	17.0096	132.1096	98.0904
9.50	115.5000	18.5037	134.0038	96.9962
10.00	115.7000	22.1589	137.8589	93.5411
10.50	116.1000	32.4139	148.5139	83.6861

TABLE III-9

VELOCITY PROFILE

MERIDIONAL STREAMLINE NO. 9

M	W	DW	W SUCTION	W PRESSURE
.00	144.1000	15.1797	159.2797	128.9203
.50	136.2000	15.1771	151.3771	121.0229
1.00	129.1000	14.7211	143.8211	114.3789
1.50	123.1000	13.4406	136.5406	109.6594
2.00	119.9000	12.0860	131.9860	107.8140
2.50	117.2000	10.1354	127.3354	107.0646
3.00	115.0000	11.8577	126.8577	103.1423
3.50	113.5000	12.9722	126.4722	100.5278
4.00	112.5000	10.3646	122.8646	102.1354
4.50	112.6000	8.9383	121.5383	103.6617
5.00	114.0000	6.9374	120.9374	107.0626
5.50	116.5000	6.5427	123.0427	109.9573
6.00	118.0000	8.5094	126.5094	109.4906
6.50	120.2000	10.8457	131.0457	109.3543
7.00	121.4000	13.2845	134.6845	108.1155
7.50	121.9000	14.6543	136.5543	107.2457
8.00	122.0000	15.5320	137.5320	106.4680
8.50	122.1000	17.4360	139.5360	104.6640
9.00	122.6000	17.8984	140.4984	104.7016
9.50	123.2000	16.2431	139.4431	106.9569
10.00	124.2000	20.4772	144.6772	103.7227

Fig. 1
Meridional Plane
with
Physical Surfaces

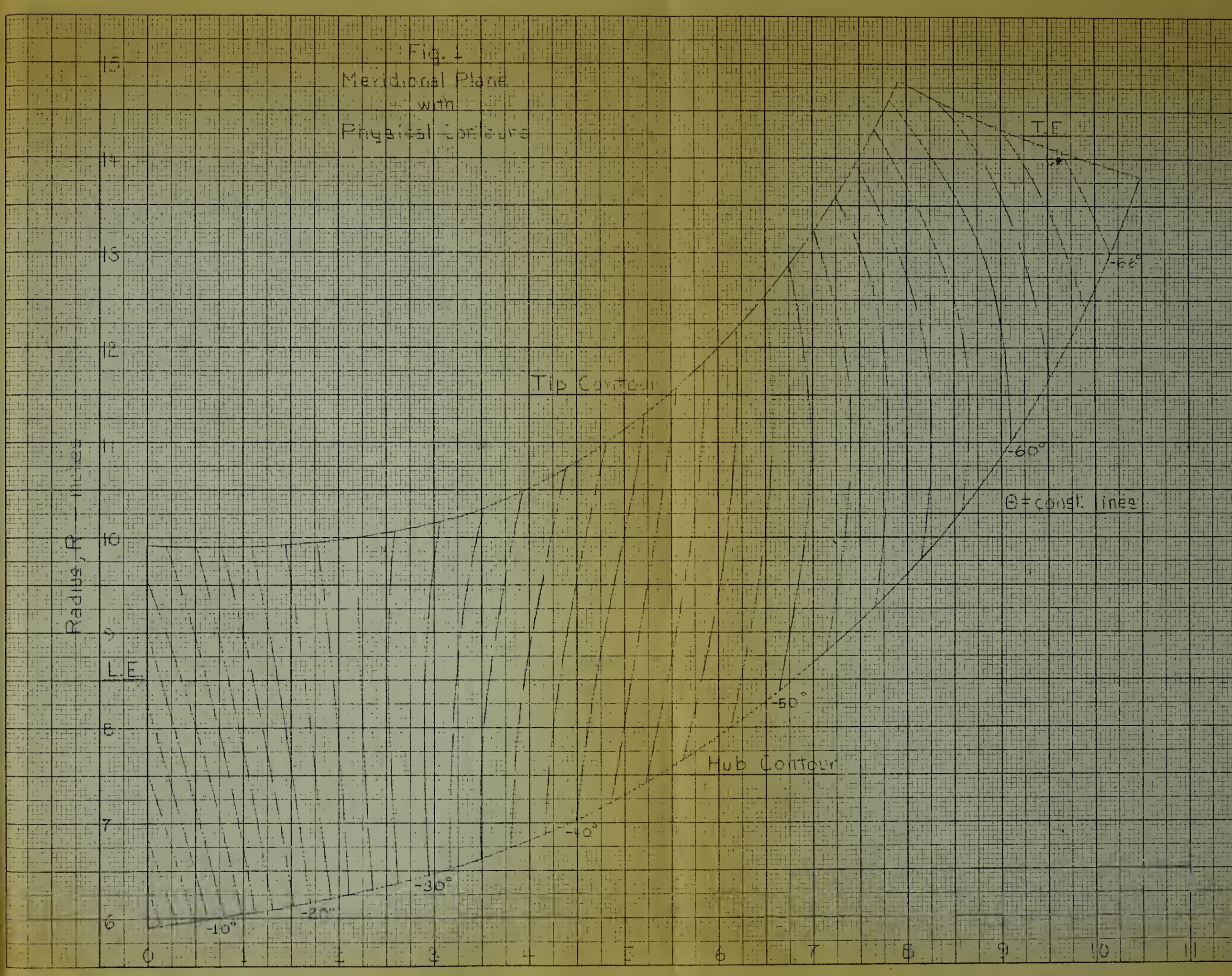

Fig. 2
Definition of Angles
on a
Meridional Plane

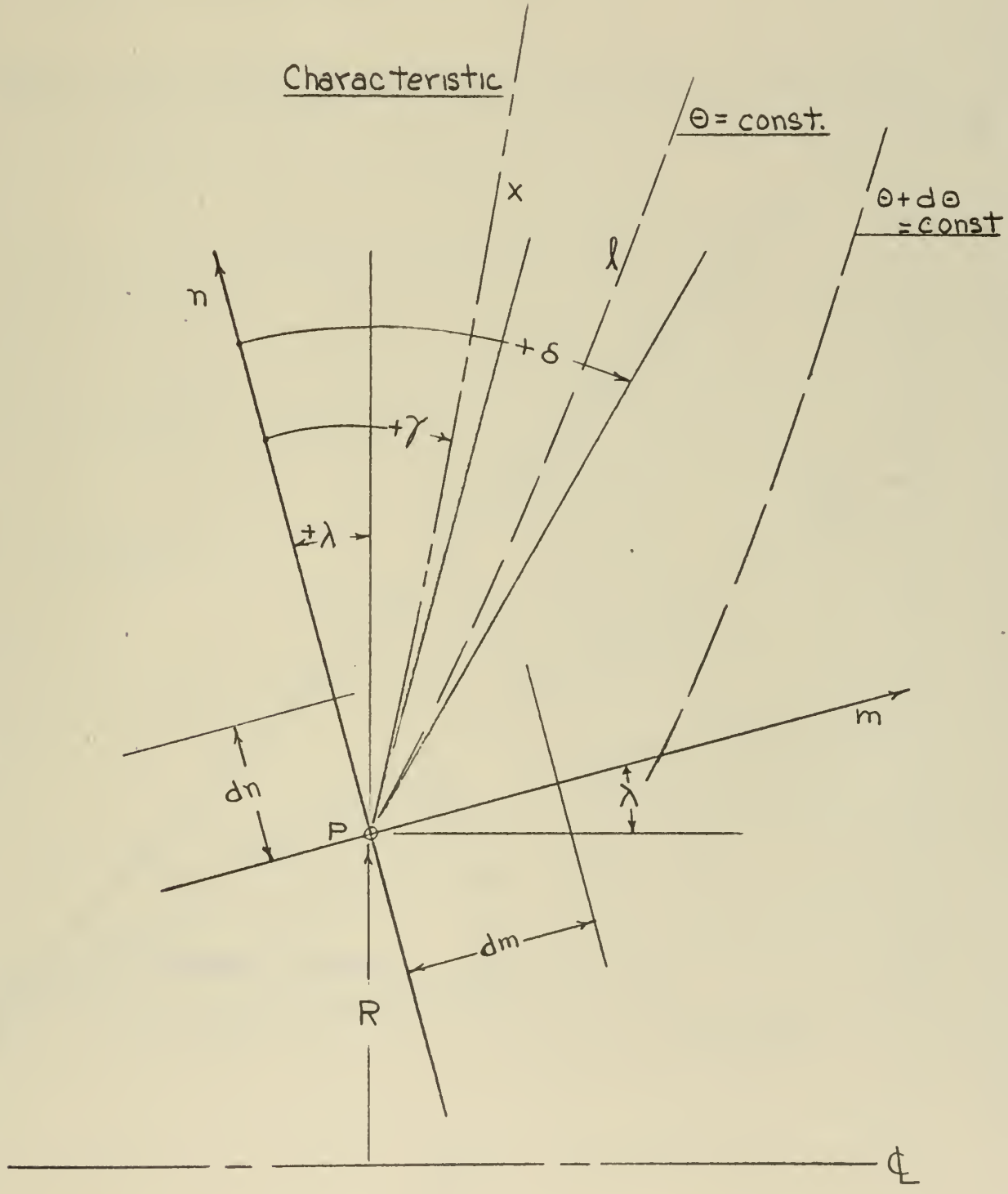

Fig. 3
Velocity Triangle
on the
Tangent Plane of a Stream Surface

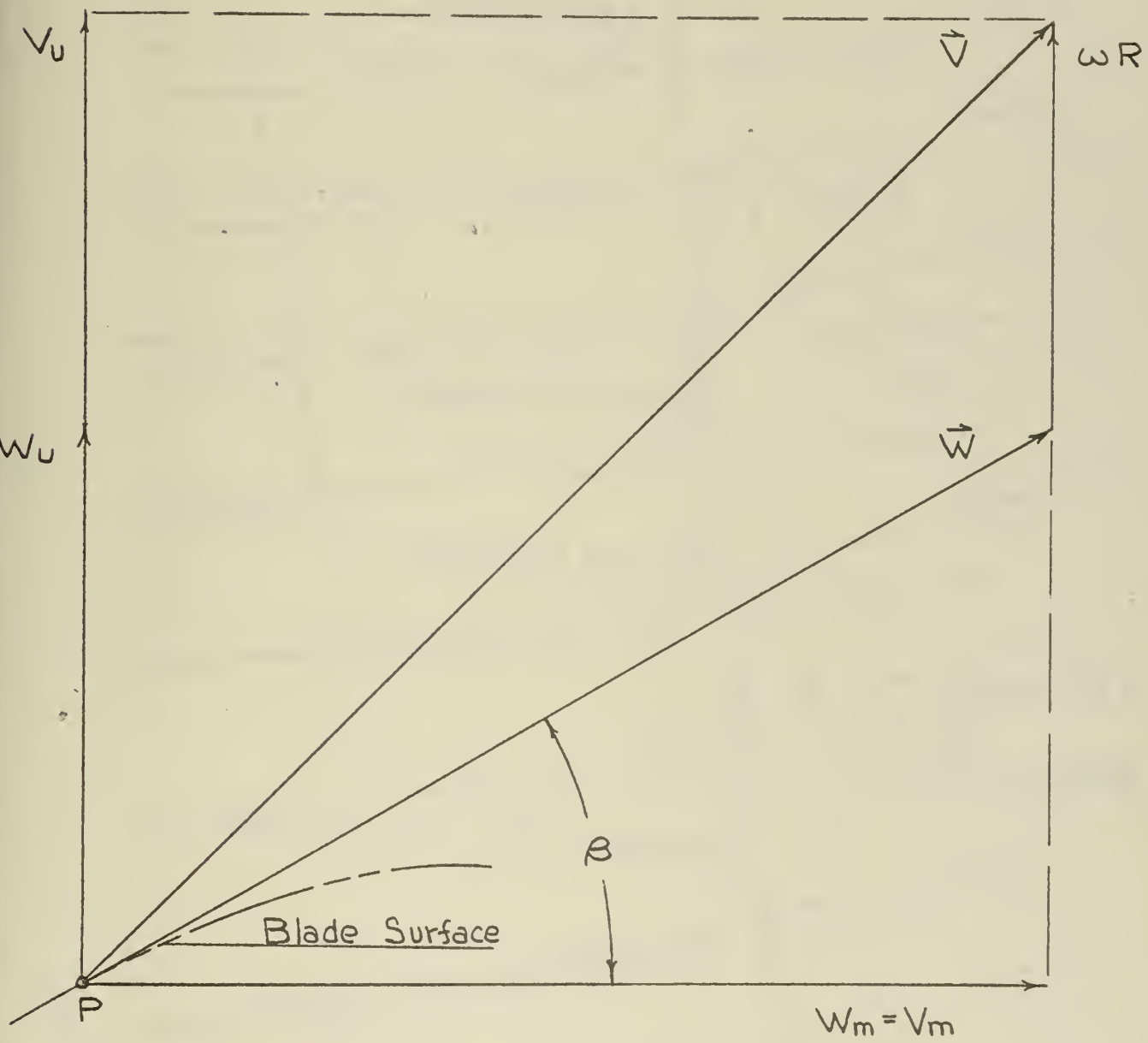

Fig. 4

Location of Streamlines

Characteristics Nos. 1 & 2

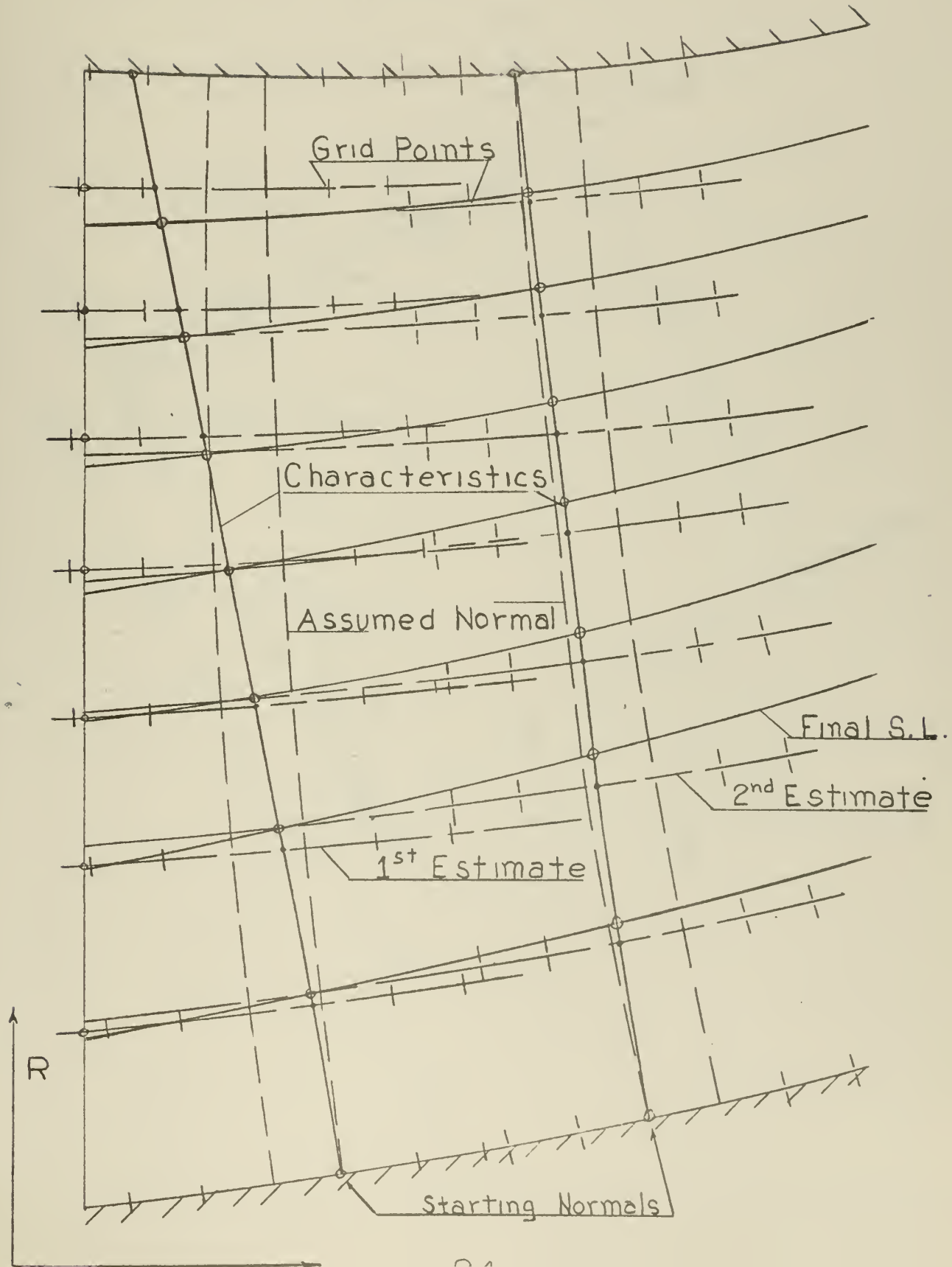

Fig 5
Location of a Point
P*
on a Characteristic

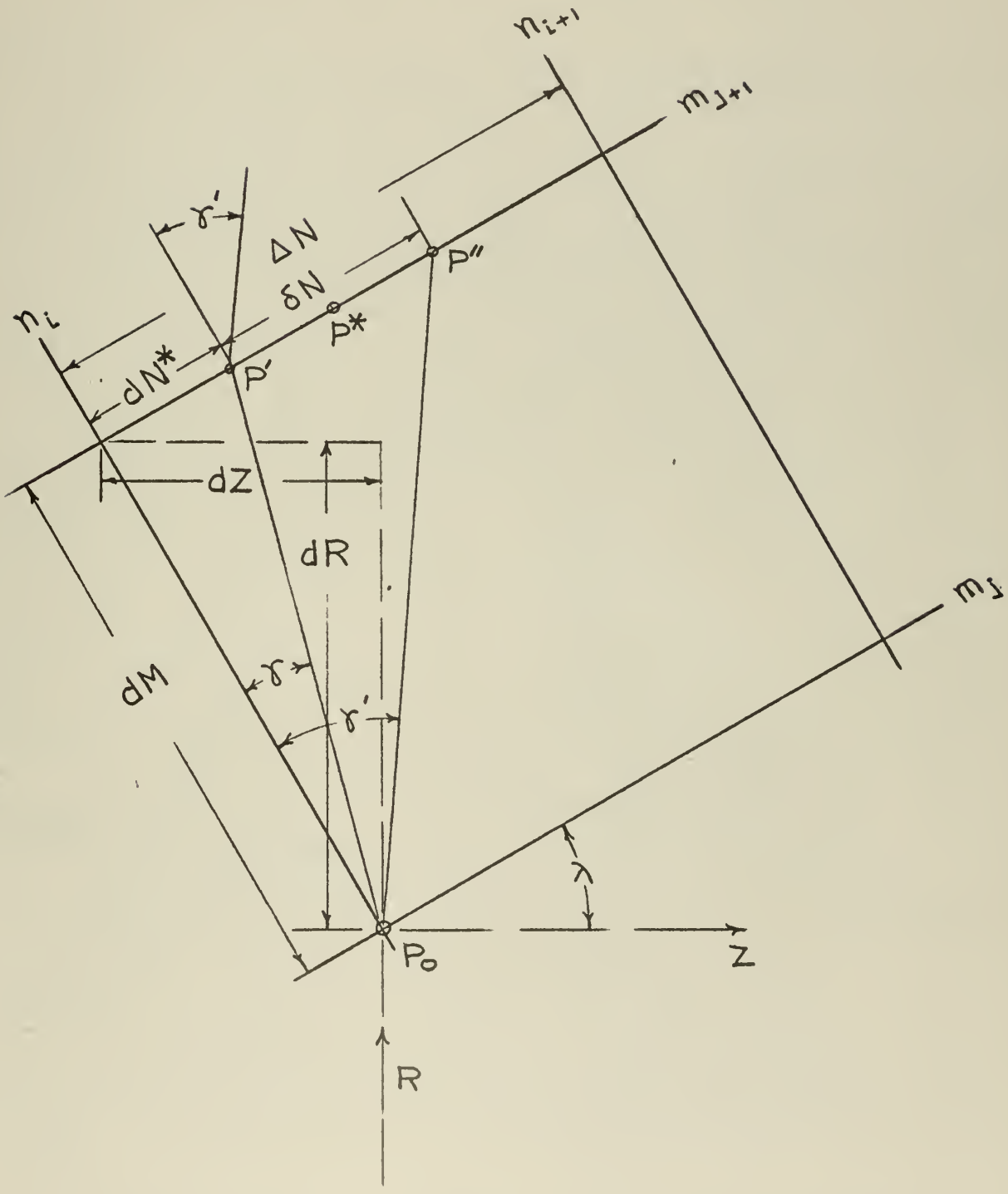

Fig. 6

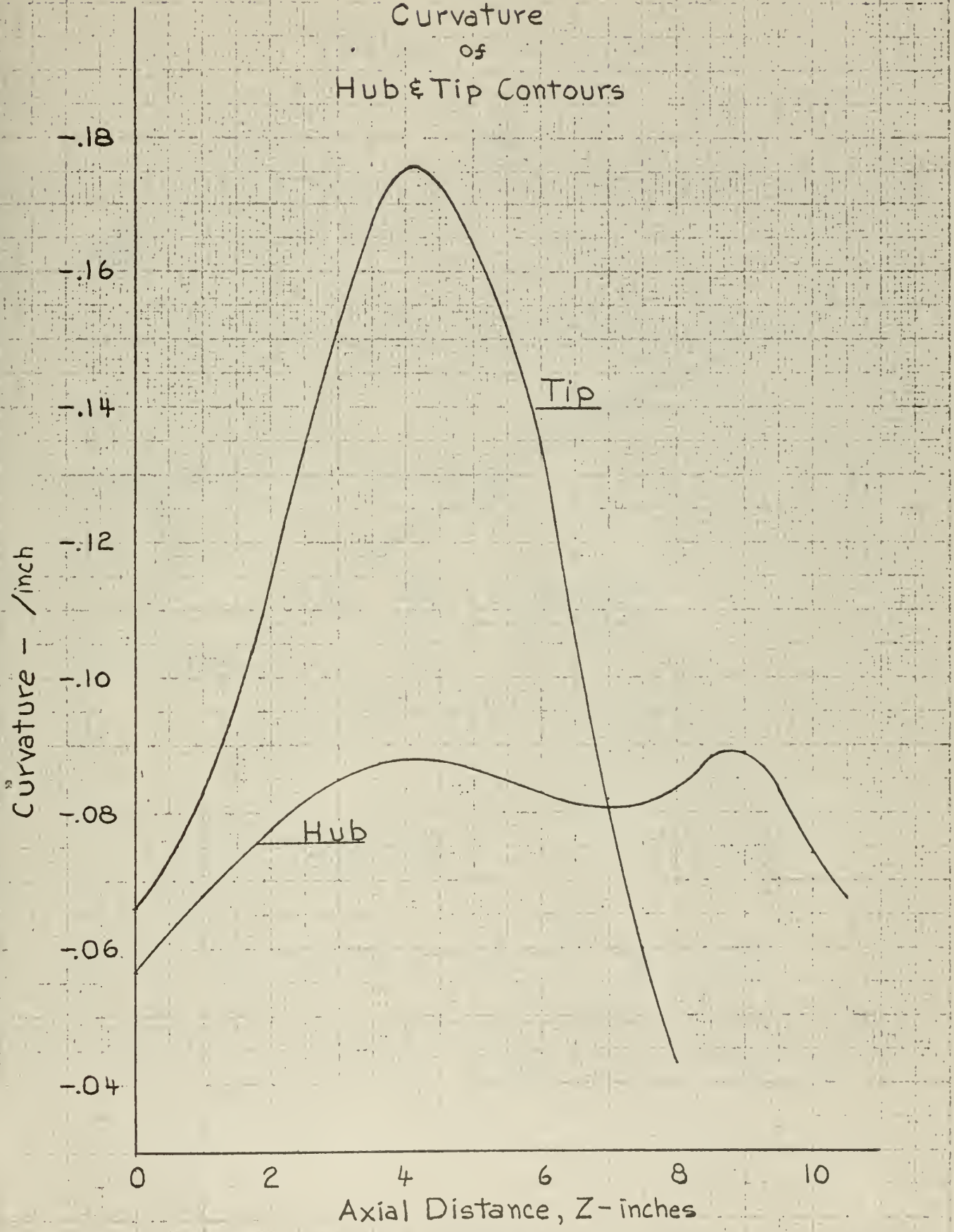
Curvature
of
Hub & Tip Contours
-.18
-.16
-.14
-.12
-.10
-.08
-.06
-.04
Curvature - "/inch
Tip
Hub
0
2
4
6
8
10
Axial Distance, Z - inches

Fig. 7

Parabolic Interpolation

for

$\frac{d^2\theta}{dm^2}$

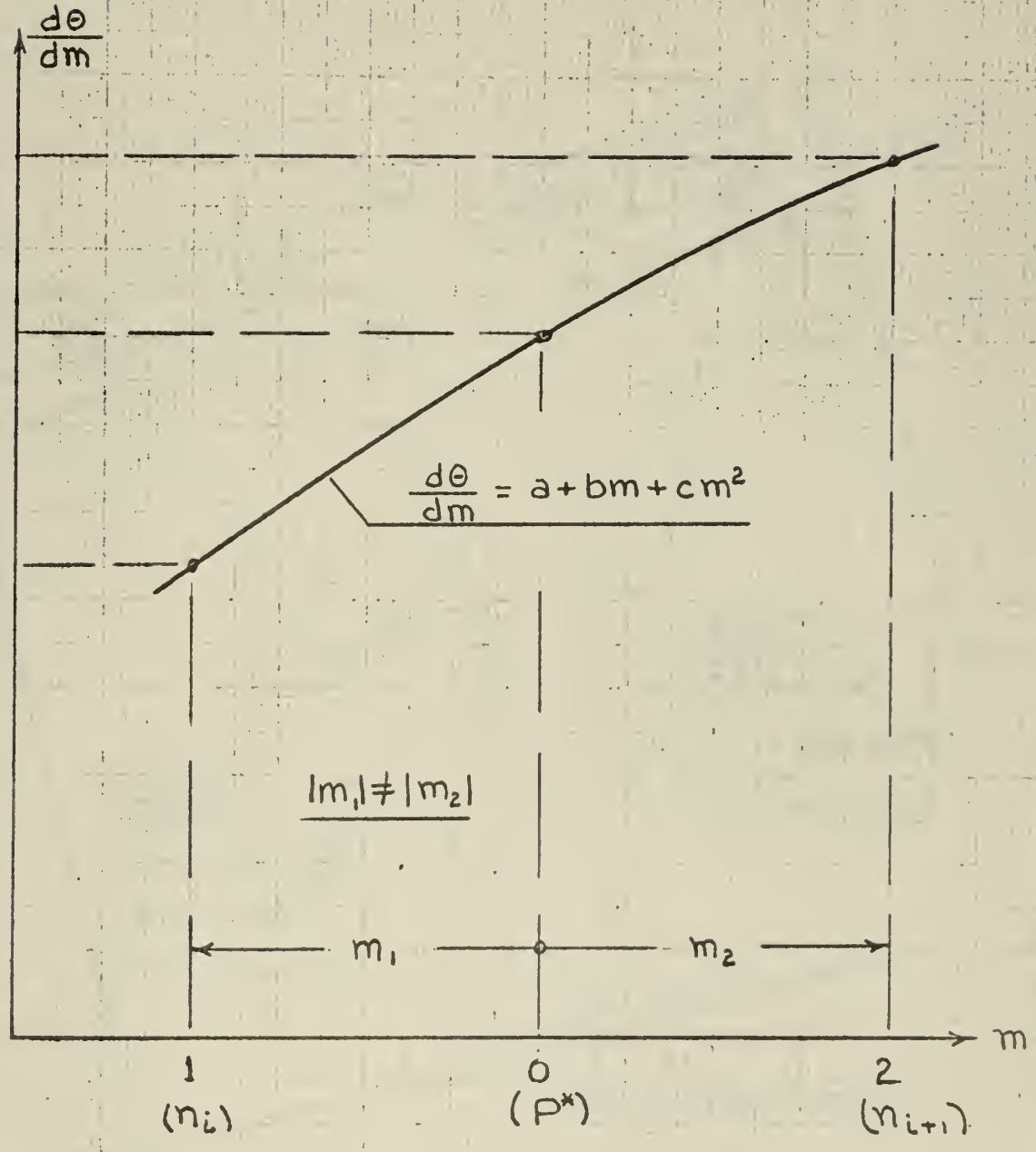

Fig. 8

Determination of Increments

for

Parabolic Interpolation

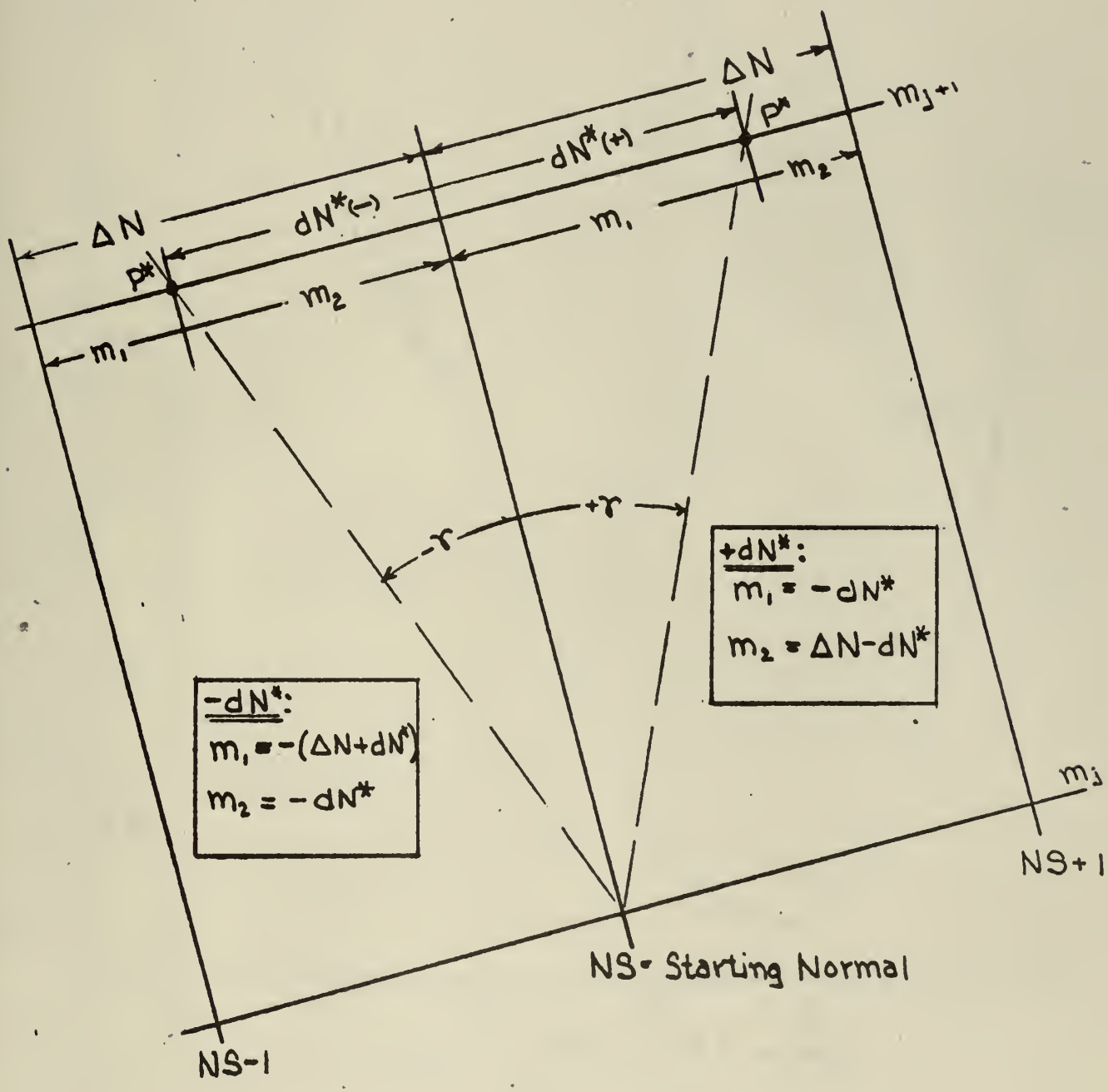

Fig. 9

Blade Angle, β

on

Hub & Tip Contours

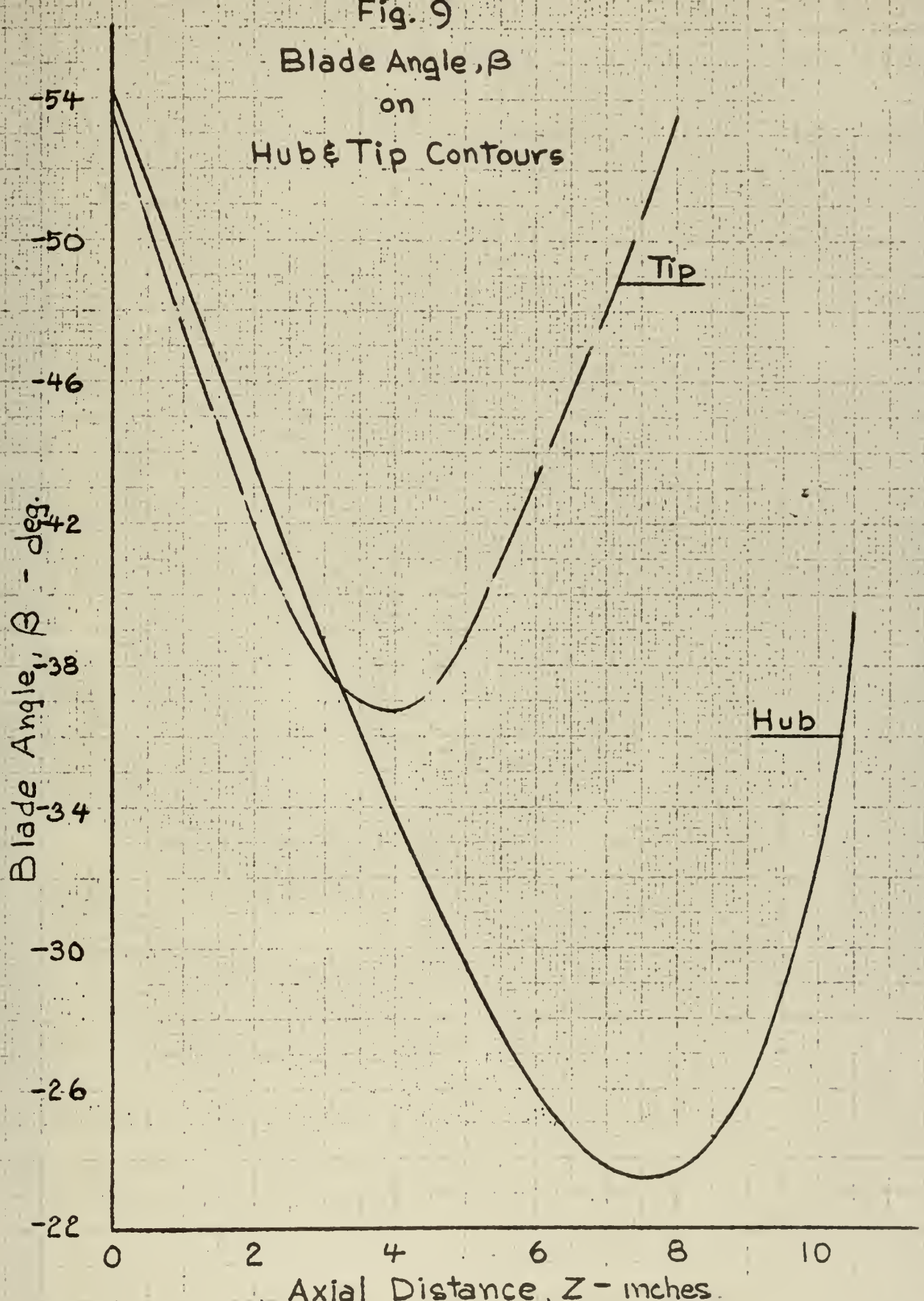

Fig. 10

Computed Streamlines

Constant V_θ alternate rows

Radius = 12

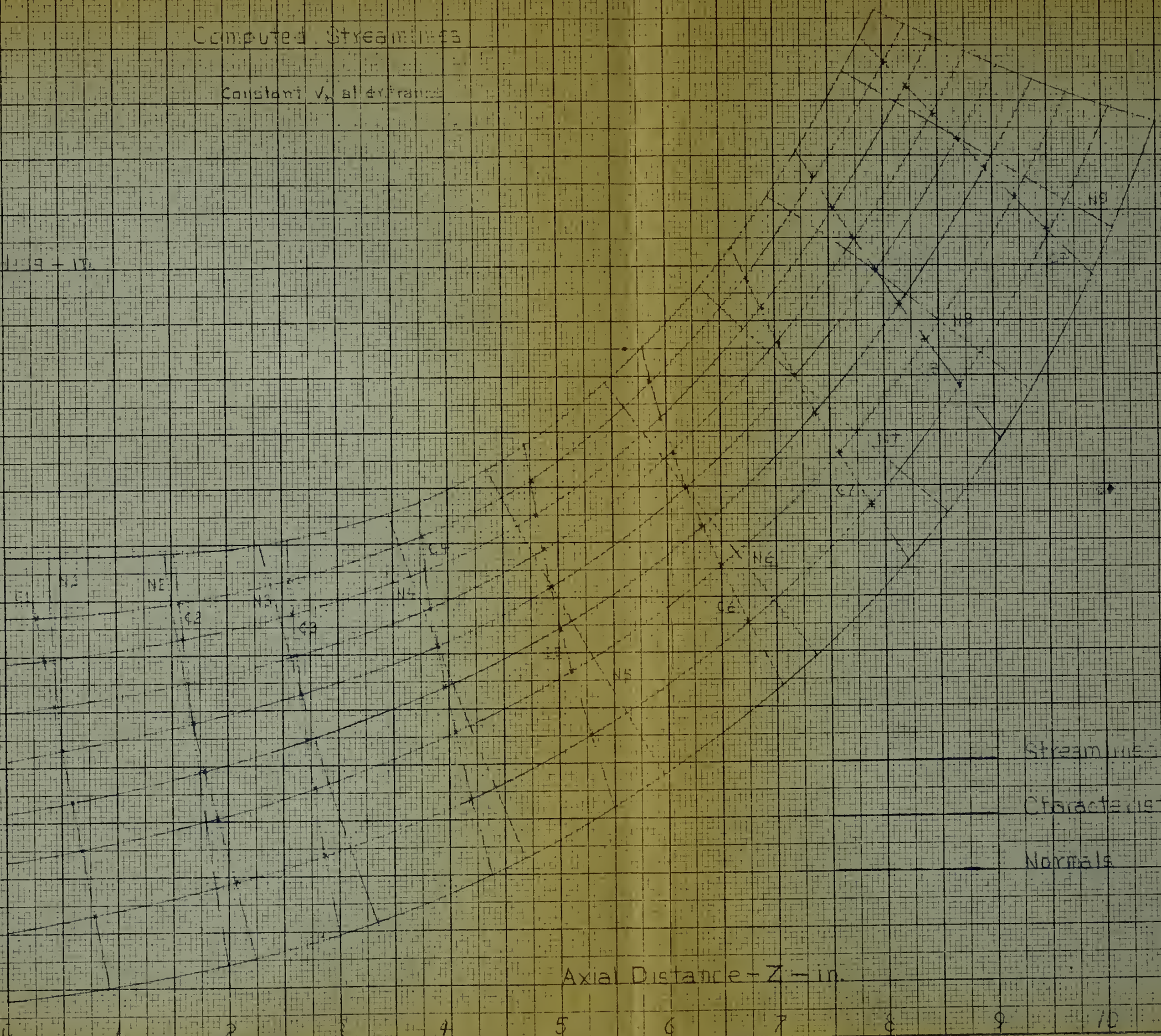

Fig. 11

Velocity Distribution
on
Streamlines

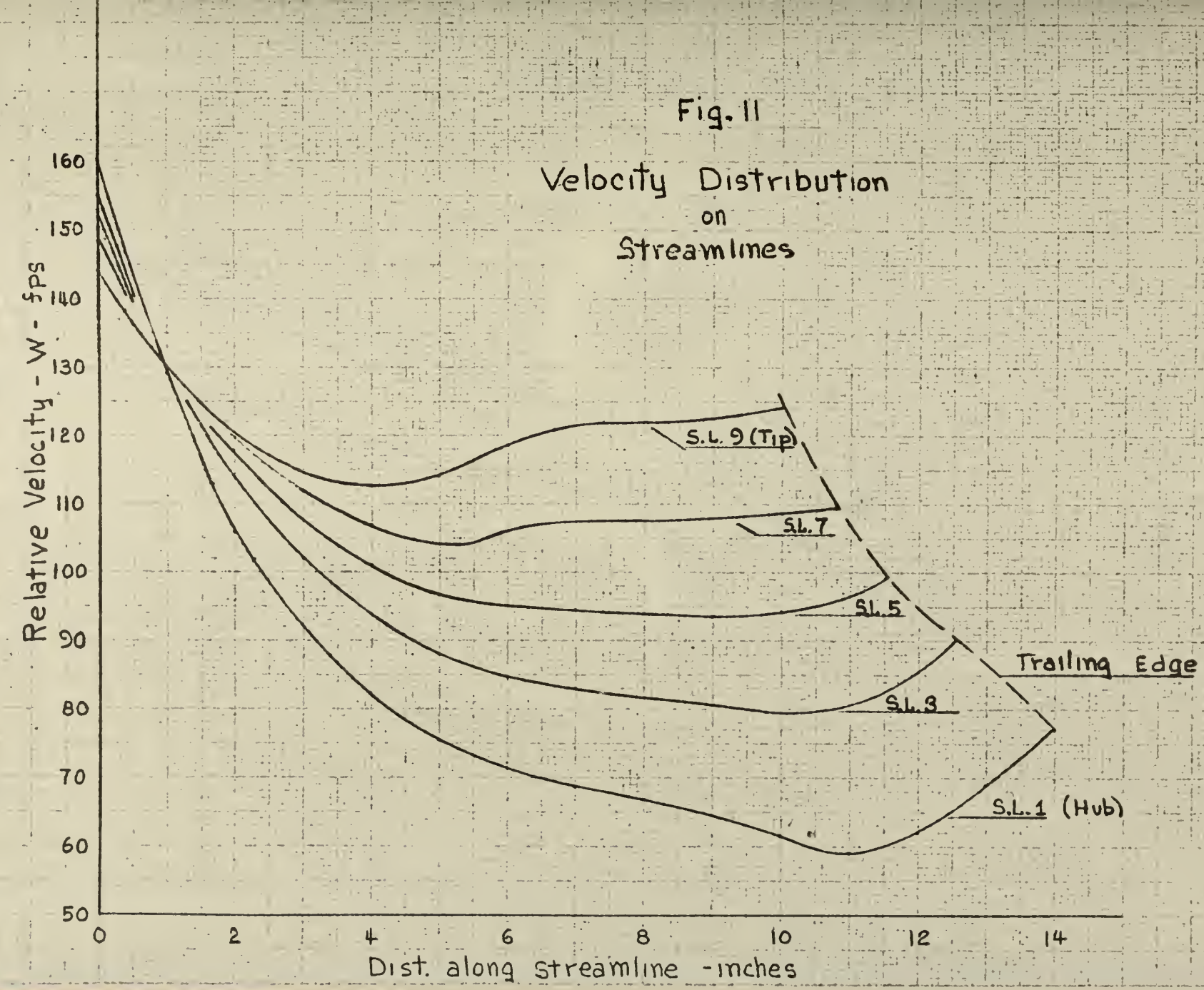

Fig. 12
Velocity Distribution
on
Normals

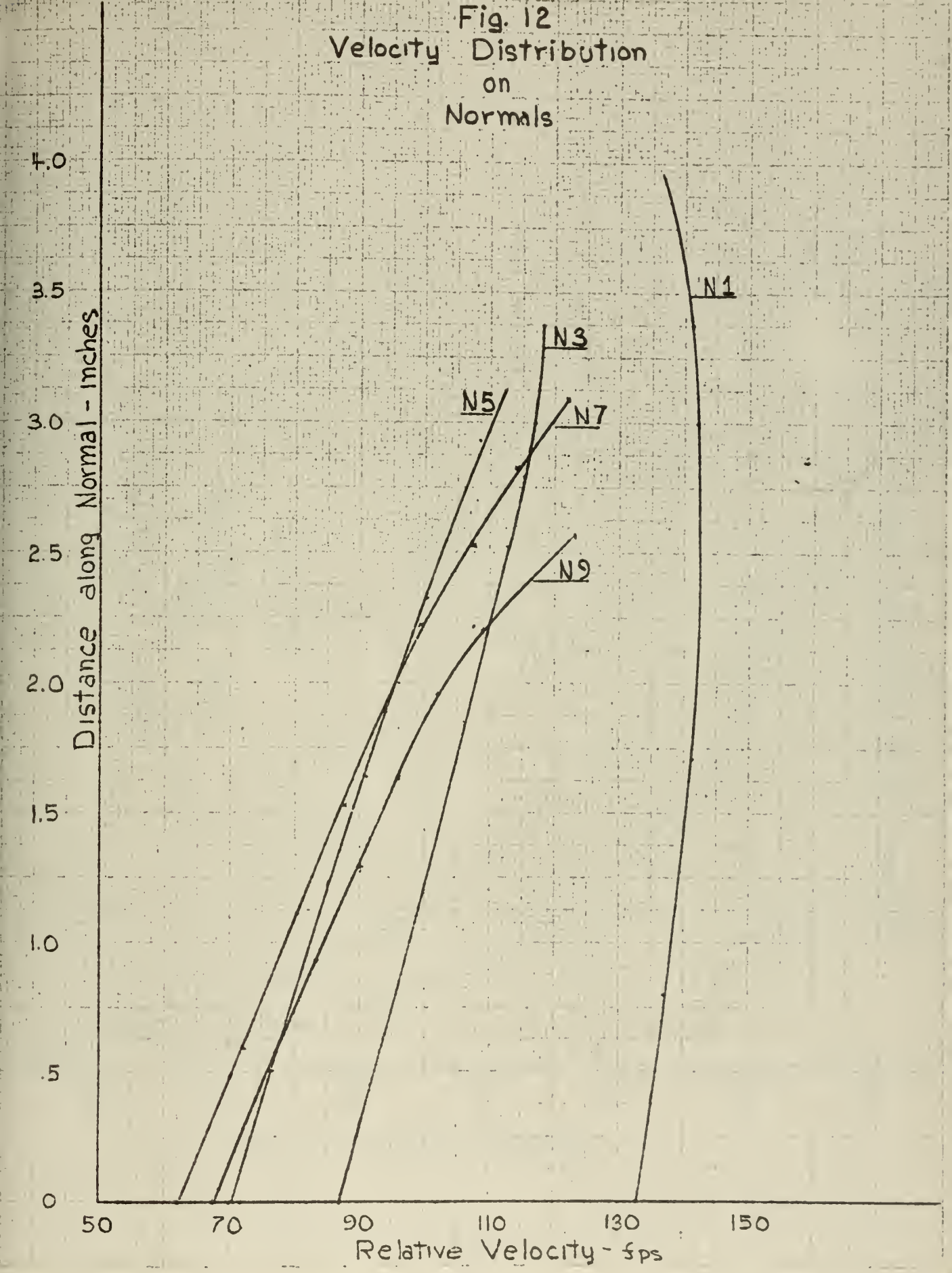

Fig. 13
Blade to Blade
Velocity Distribution
along
Hub Streamline

S. L. No. 1

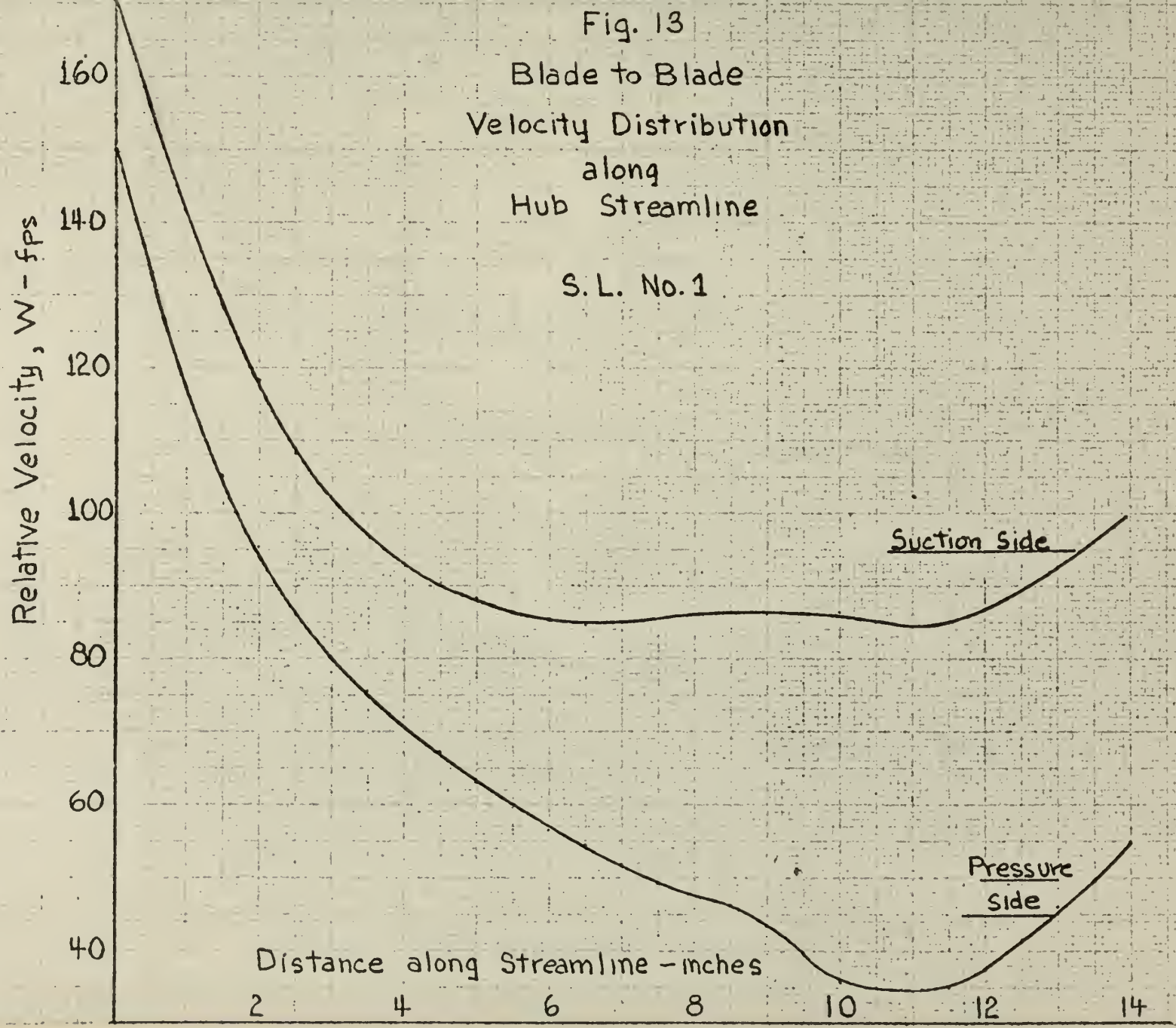

Fig. 14

Blade to Blade Velocity Distibution along Mean Streamline

S. L. No. 5

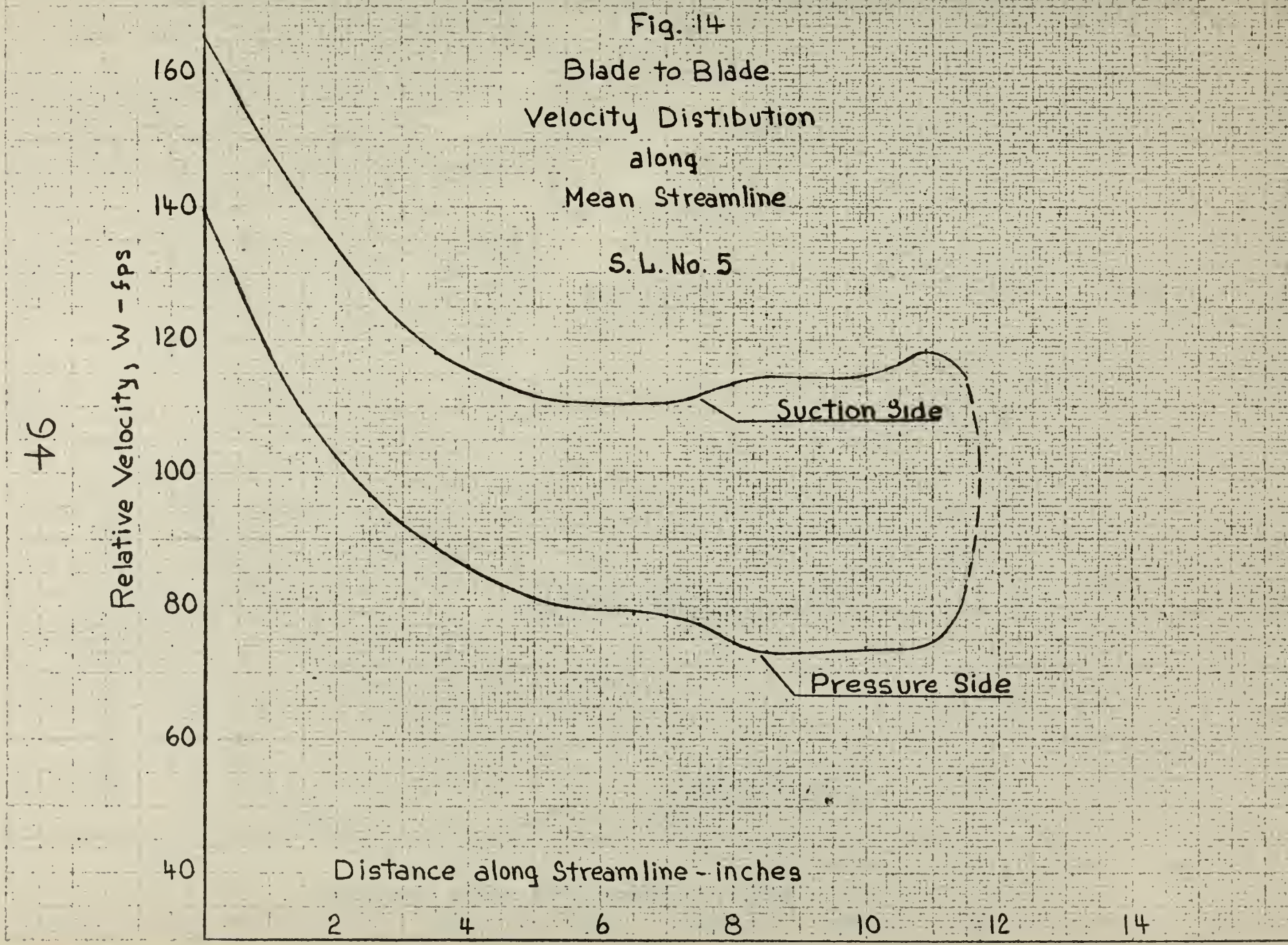

Fig. 15

Blade to Blade

Velocity Distribution

along

Tip Streamline

S.L. No. 9

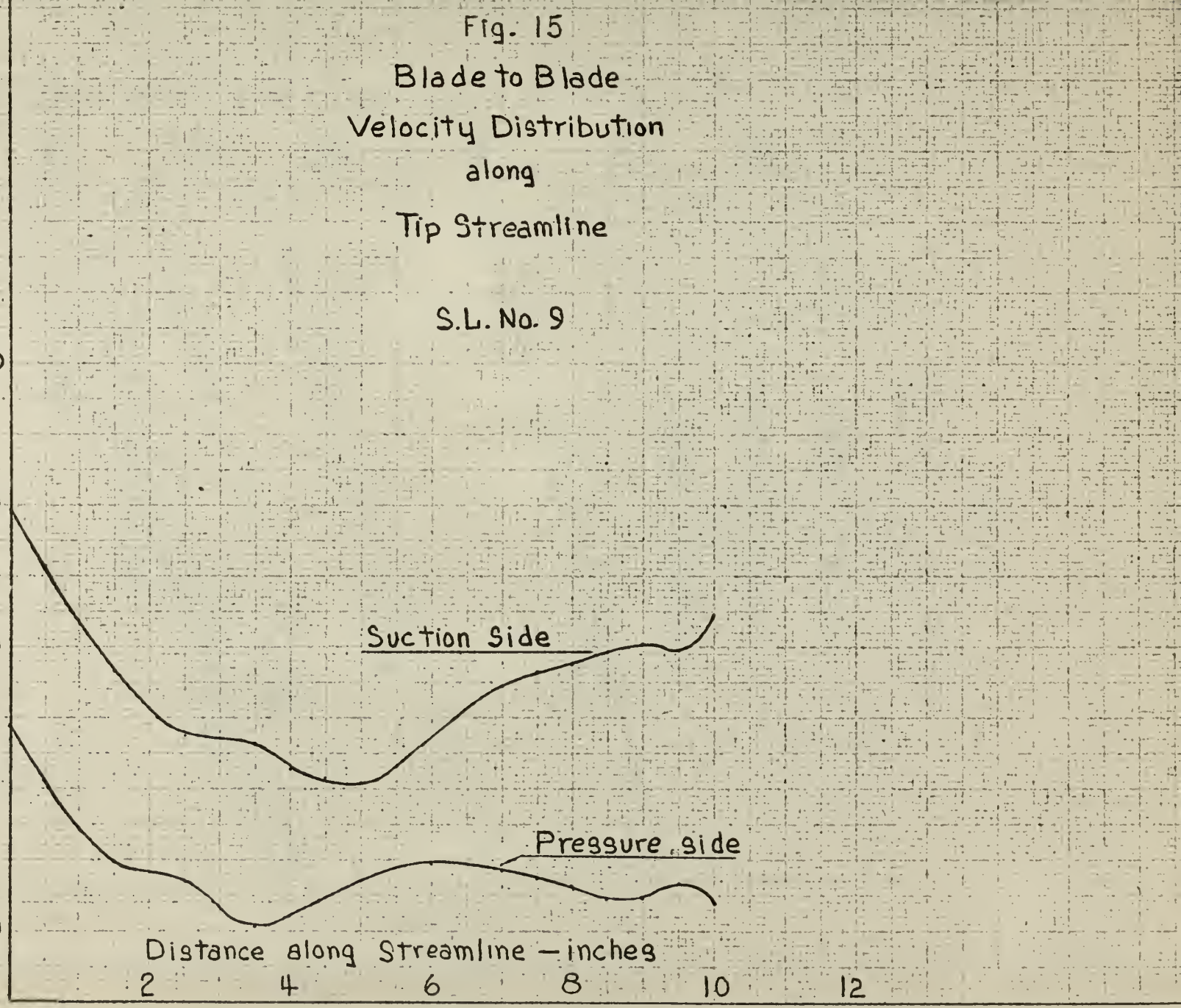

Fig. 16

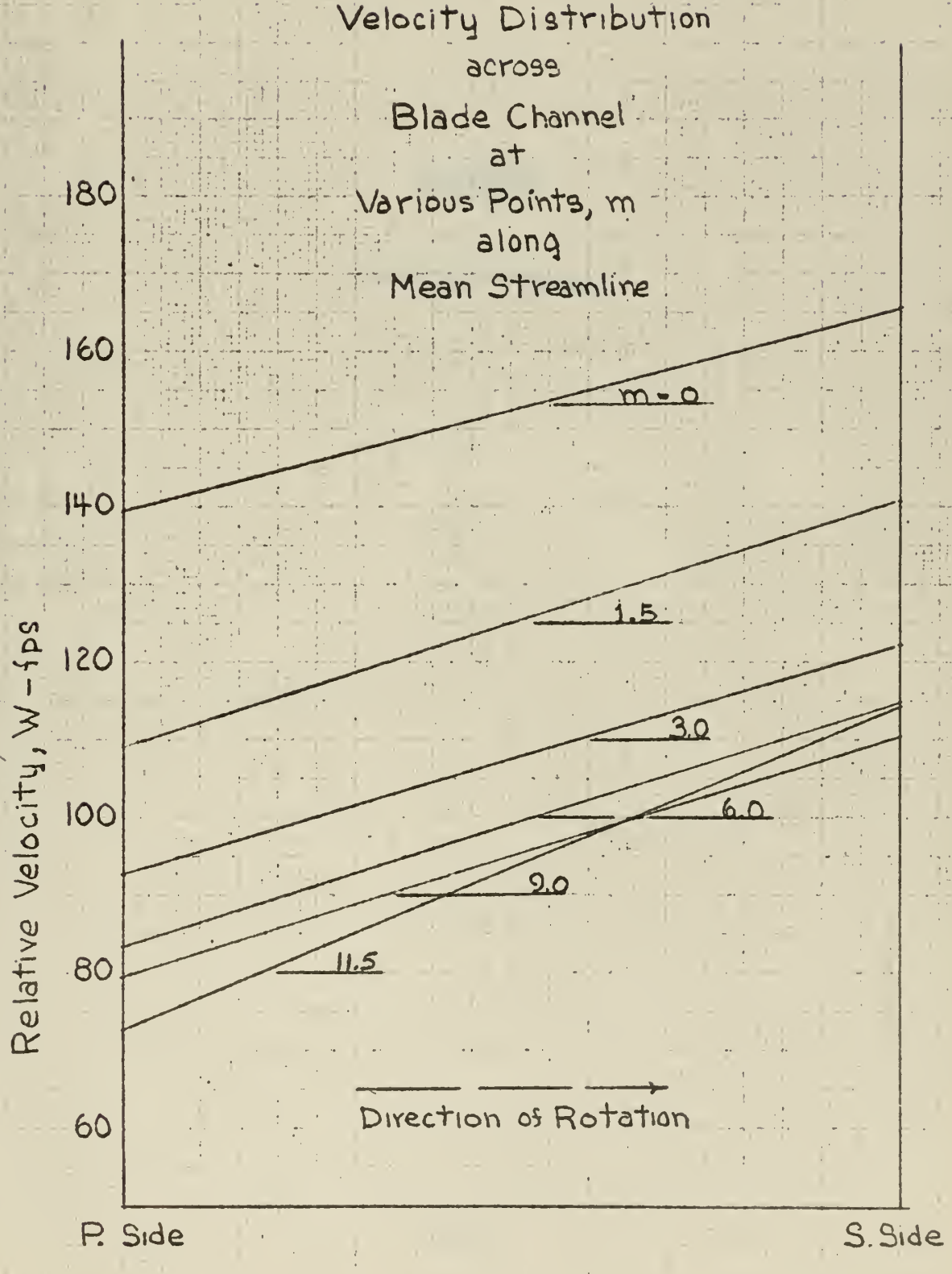
Velocity Distribution
across
Blade Channel
at
Various Points, m
along
Mean Streamline
180
160
140
120
100
80
60
Relative Velocity, W - fps
m = 0
1.5
3.0
6.0
9.0
11.5
Direction of Rotation
P. Side
S. Side

APPENDIX

COMPUTER PROGRAMS

PROGRAMS LEDGE 1 AND LEDGE 2

VARIABLE NAMES

Name	Equivalent to	Units
ALFA	α	deg.
AALFA	α	rad.
DELN	ΔN	in.
DFL	$dF(L)/dL$	
DTDM	$d\theta/dm$	rad./in.
F	$F(L)$	
MO	M_T	
OMEGA	ω	rad./sec.
RL	R_L	in.
THETA	θ	deg.
ATHETA	θ	rad.
VM	V_m	ft./sec.
Additions for LEDGE 2		
BETA	β	deg.
ABETA	β	rad.

Program LEDGE I

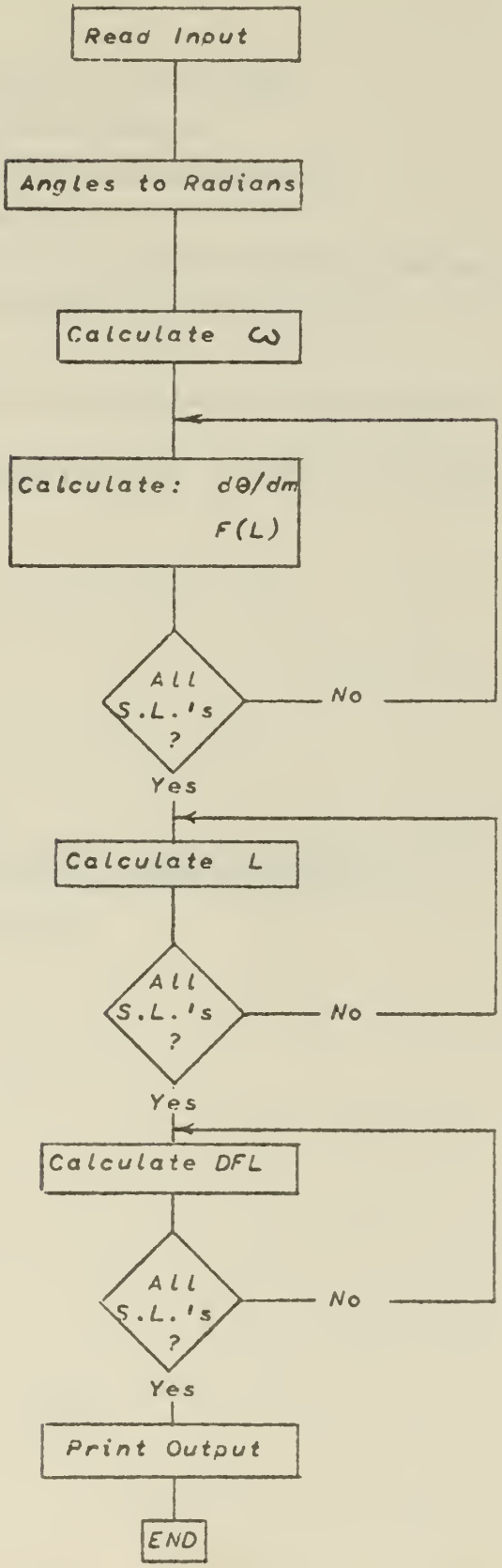

```
      PROGRAM LEDGE 1
      DIMENSION RL(9),ALFA(9),DELN(9),F(9),EL(9),VM(9),
     1THETA(9,3),AALFA(9),ATHETA(9)
      READ 10,MO,RPM
   10 FORMAT(I10,F10.0)
      READ 11,RL
   11 FORMAT(6F10.0)
      READ 11,ALFA
      READ 11,DELN
      READ 11,VM
      READ 11,((THETA(M,K),K=1,3),M=1,MO)
      DO 12 M=1,MO
      AALFA(M) = ALFA(M)*3.14159/180.
      DO 12 K=1,3
      ATHETA(M,K) = THETA(M,K)*3.14159/180.
   12 CONTINUE
      OMEGA = RPM*3.14159/30.
      DO 13 M=1,MO
      DTDM = (-3.*ATHETA(M,1)+4.*ATHETA(M,2)-ATHETA(M,3))
     1/(2.*DELN(M))
      F(M) =(VM(M)*12.*DTDM+OMEGA)*RL(M)*RL(M)
   13 CONTINUE
      EL(1) = 0.
      DO 14 M=2,MO
      EL(M)=EL(M-1)+(RL(M)-RL(M-1))*SINF(AALFA(M-1))
   14 CONTINUE
      PRINT 21
   21 FORMAT(///10X,21HLEADING EDGE FUNCTION///11X1HM11X3HDFL)
      DO 22 M=1,MO
      IF(M-1) 15,15,16
   15 MA = 1
      MB = 2
      MC = 3
      GO TO 19
   16 IF(M-MO) 17,18,18
   17 MA = M
      MB = M+1
      MC = M-1
      GO TO 19
   18 MA = MO
      MB = MO-1
      MC = MO-2
   19 XA = EL(MB)-EL(MA)
      XB = EL(MC)-EL(MA)
      DFL = (XB*XB*(F(MB)-F(MA))-XA*XA*(F(MC)-F(MA)))
     1/((XA*XB*XB-XA*XA*XB)*12.*SINF(AALFA(M)))
      PRINT 20,M,DFL
   20 FORMAT(/10X,I2,5X,F15.5)
   22 CONTINUE
      END
      END
```

Program LEDGE 2

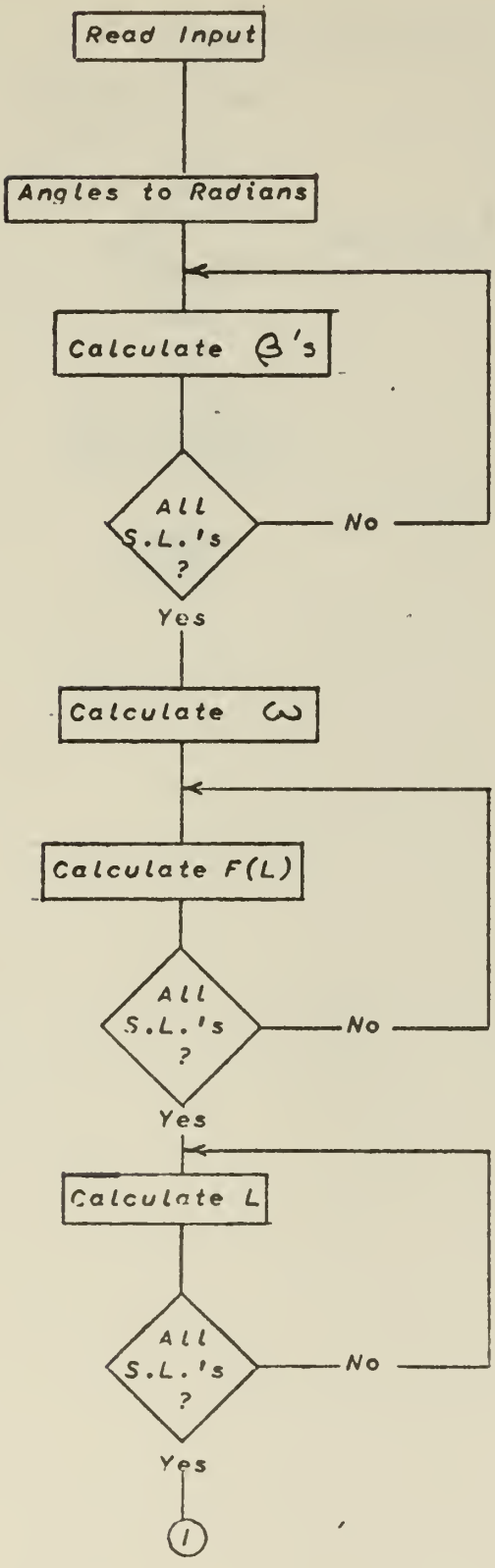

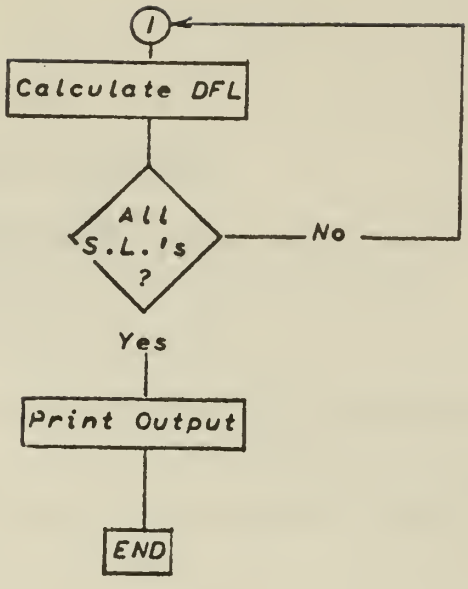
1
Calculate DFL
All S.L.'s ?
No
Yes
Print Output
END

```
      PROGRAM LEDGE 2
      DIMENSION RL(9),ALFA(9),F(9),EL(9),VM(9),
     1BETA(9),ABETA(9),AALFA(9)
      READ 10,MO,RPM
   10 FORMAT(I10,F10.0)
      READ 11,RL
   11 FORMAT(6F10.0)
      READ 11,ALFA
      READ 11,VM
      READ 32,BETA(1),BETA(9)
   32 FORMAT(2F10.0)
      ABETA(1)  = BETA(1)*3.14159/180.
      ABETA(9) = BETA(9)*3.14159/180.
      DO 12 M=1,MO
      AM = FLOATF(M-1)/FLOATF(MO-1)
      AALFA(M) = ALFA(M)*3.14159/180.
   12 ABETA(M) = ABETA(1)+(ABETA(9)-ABETA(1))*AM
      OMEGA = RPM*3.14159/30.
      DO 91 M=1,MO
      BETA(M) = ABETA(M)*180./3.14159
   91 CONTINUE
      DO 13 M=1,MO
      F(M) = VM(M)*RL(M)*TANF(ABETA(M))*12.+OMEGA*RL(M)*RL(M)
   13 CONTINUE
      EL(1) = 0.
      DO 14 M=2,MO
      EL(M)=EL(M-1)+(RL(M)-RL(M-1))*SINF(AALFA(M-1))
   14 CONTINUE
      PRINT 31
   31 FORMAT(1H1)
      PRINT 21
   21 FORMAT(///10X,21HLEADING EDGE FUNCTION///11X1HM11X3HDFL)
      DO 22 M=1,MO
      IF(M-1) 15,15,16
   15 MA = 1
      MB = 2
      MC = 3
      GO TO 19
   16 IF(M-MO) 17,18,18
   17 MA = M
      MB = M+1
      MC = M-1
      GO TO 19
   18 MA = MC
      MB = MC-1
      MC = MO-2
   19 XA = EL(MB)-EL(MA)
      XB = EL(MC)-EL(MA)
      DFL = (XB*XB*(F(MB)-F(MA))-XA*XA*(F(MC)-F(MA)))
     1/((XA*XB*XB-XA*XA*XB)*12.*SINF(AALFA(M)))
      PRINT 20,M,DFL
   20 FORMAT(/10X,I2,5X,F15.5)
   22 CONTINUE
      END
      END
```

PROGRAMS ROTOR 1 AND ROTOR 2

VARIABLE NAMES

Name	Equivalent to	Units
BETA	β at P*	deg.
PBETA	β at P*	rad.
TBETA	tan β	
XBETA	β at (P*+ δx)	rad.
ZBETA	β at (P*+ δx)	deg.
BLNO	N	
CURV	k_m	$in.^{-1}$
PCURV	k_m at P*	$in.^{-1}$
D1	D_1	
D2	D_2	
D2TDM2	$d^2\theta/dm^2$	
D2TDNM	$d^2\theta/dndm$	
DELN	ΔN	in.
DELTA	δ	deg.
ADELTA	δ	rad.
DDELTA	δ at P*	deg.
PDELTA	δ at P*	rad.
YDELTA	δ at (P*+ δx)	rad.
DHEDN	$\partial H_e/\partial n_e$	
DM	dM	in.
DNSTAR	dN*	in.
DTDM, DT1, DT2	$d\theta/dm$	
DWCO	$DW_{coef.}$	

Name	Equivalent to	Units
DWFUNC	DW_{func}	
DX	dx	in.
EN	$\delta N/2$	in.
FX	$E(x)$	
GAMMA	γ at P*	deg.
GAMX	γ at (P*+ δx)	deg.
PGAMMA	γ at P*	rad.
TGAMMA	$\tan \gamma$	
XGAMMA	γ at (P*+ δx)	rad.
ALAM	λ	rad.
DLAM	λ	deg.
PLAM	λ at P*	rad.
XLAM	λ at (P*+ δx)	rad.
OMEGA	ω	per sec.
QA	Q (actual)	cu. ft./sec.
QC	Q (calculated)	cu. ft./sec.
QDEL	ΔQ	cu. ft./sec.
DQ	$\int E(x)dx$	cu. ft./sec.
R	R	in.
AR	R at P*	in.
RX	R at (P*+ δx)	in.
THETA	Θ	deg.
ATHETA	Θ	rad.
THICK	Δt	in.
TKEQV	$\Delta t'$	in.

Name	Equivalent to	Units
W	W	ft./sec.
WDEL	dW	ft./sec.
WM	W_m at P*	ft./sec.
WX	W_m at (P*+ δx)	ft./sec.
WSQ	W_m^2 at P*	$ft.^2/sec.^2$
DWSQ	dW_m^2/dx	$ft.^2/sec.^2$-in.
X, AX	x	in.
XDEL	δx	in.
Y1, Y2, Y3	Y_1, Y_2, Y_3	
Z	Z	in.

INDEX NAMES

N, NN, etc.	=	Normal number
M, MM, etc.	=	Streamline number
MO	=	Total number of streamlines
NO	=	Total number of normals
NS	=	Starting normal

Changes and additions for ROTOR 2

ABETA	β	rad.
APBETA	β at P*	deg.
DTBN	$d(\tan\beta)/dn$	
DTBM	$d(\tan\beta)/dm$	

Program ROTOR I

Main Program

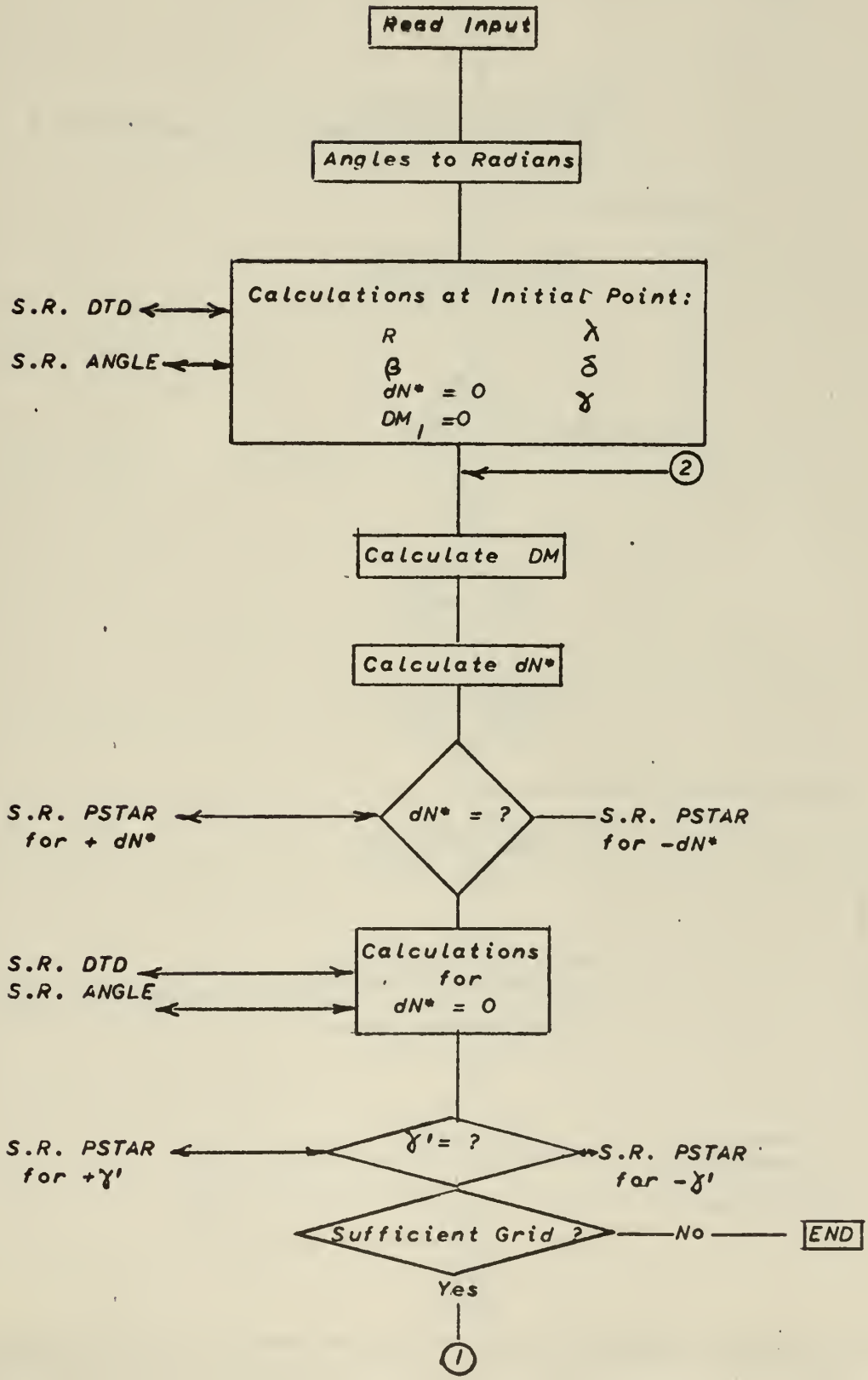

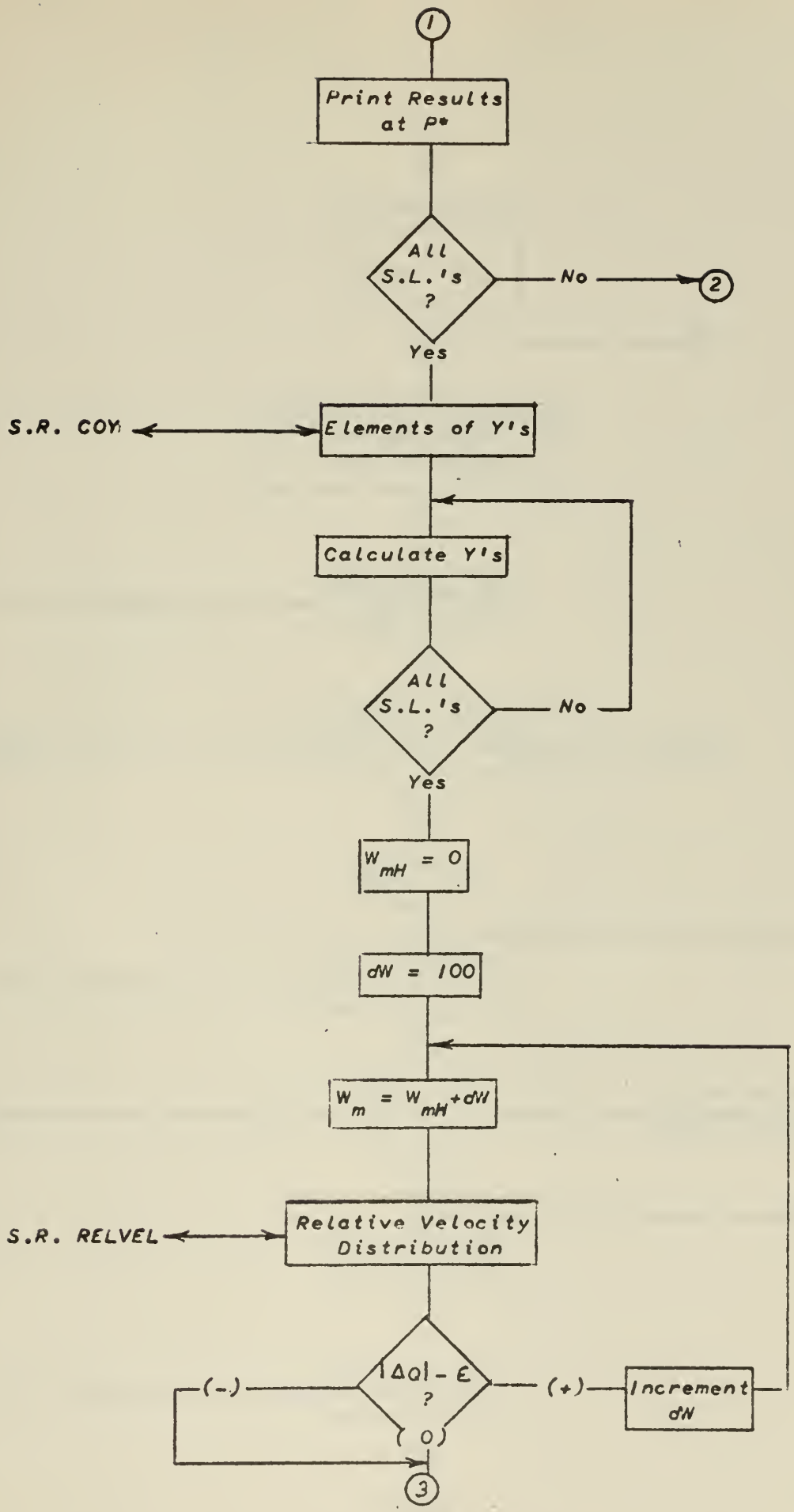
1
Print Results at P*
All S.L.'s ?
No
2
Yes
S.R. COY
Elements of Y's
Calculate Y's
All S.L.'s ?
No
Yes
$W_{mH} = 0$
dW = 100
$W_m = W_{mH} + dW$
S.R. RELVEL
Relative Velocity Distribution
$|\Delta a| - \epsilon$?
(-)
(+)
Increment dW
(0)
3

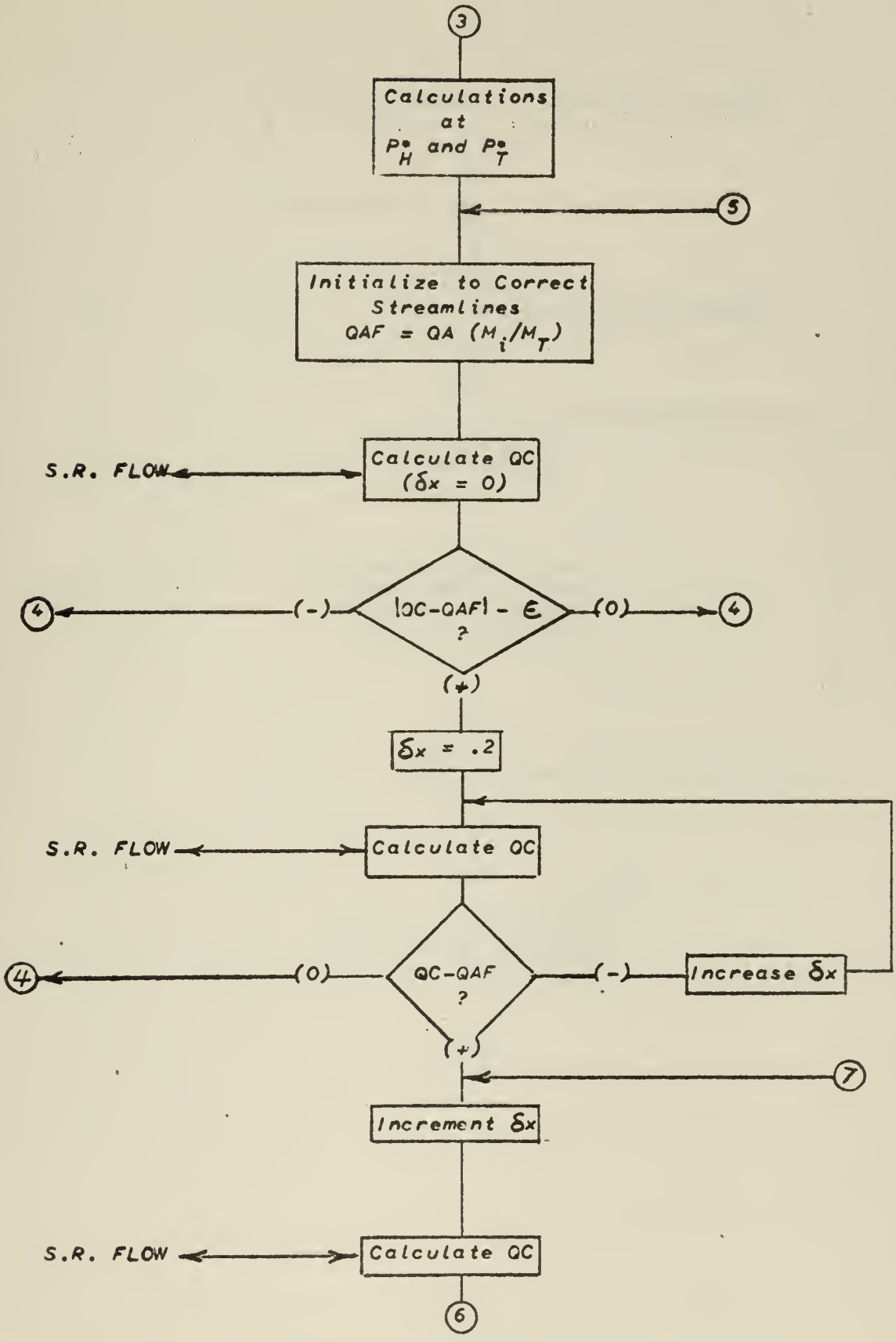
3
Calculations at P_H^* and P_T^*
5
Initialize to Correct Streamlines
QAF = QA (M_i/M_T)
S.R. FLOW
Calculate QC ($\delta x = 0$)
4
(-)
|QC-QAF| - ϵ ?
(0)
4
(+)
δx = .2
S.R. FLOW
Calculate QC
4
(0)
QC-QAF ?
(-)
Increase δx
(+)
7
Increment δx
S.R. FLOW
Calculate QC
6

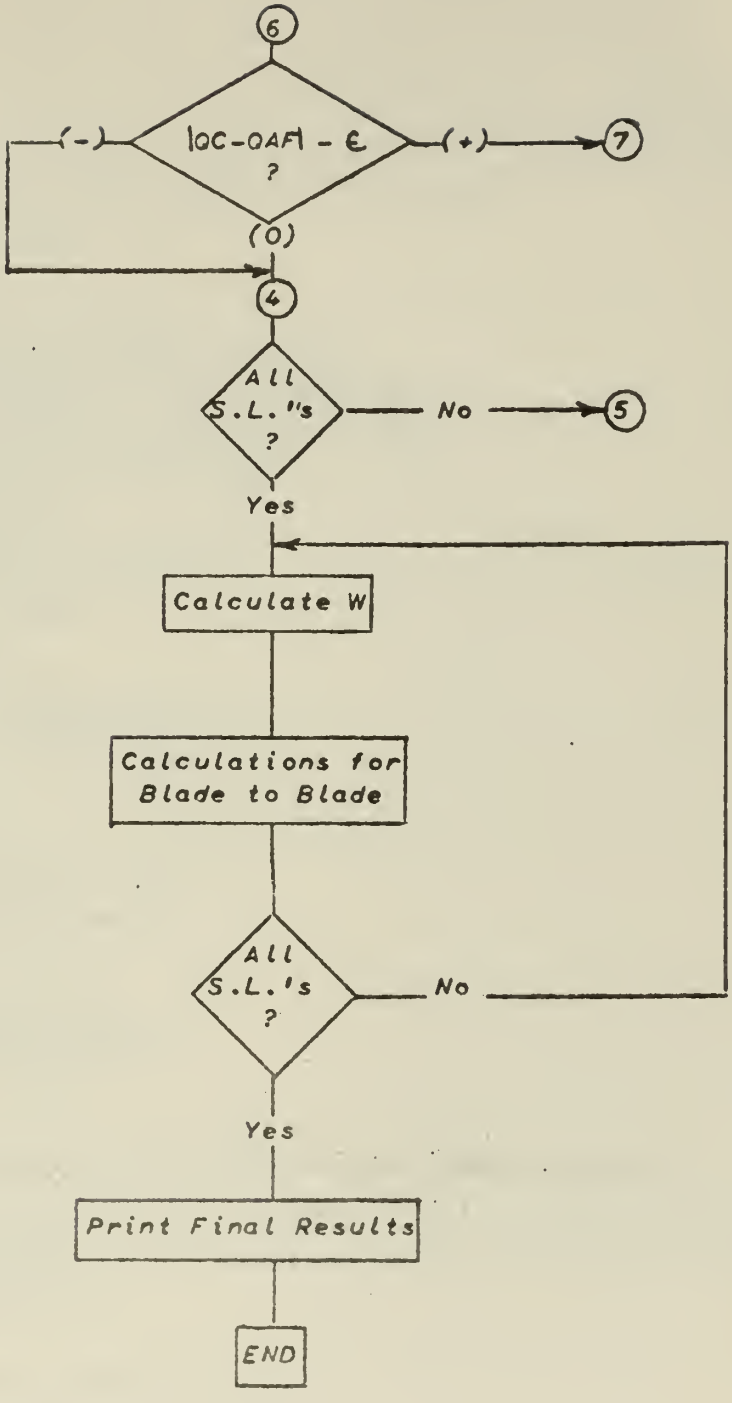
6
|QC-QAF| - ε
?
(-)
(+)
7
(0)
4
All
S.L.'s
?
No
5
Yes
Calculate W
Calculations for
Blade to Blade
All
S.L.'s
?
No
Yes
Print Final Results
END

```
      PROGRAM ROTOR 1
      DIMENSION DLAM(9,10),R(9,10),Z(9,10),THETA(9,10) ,
     1ALAM(9,10),ATHETA(9,10),DELTA(9,10),ADELTA(9,10),
     2AR(9),PLAM(9),GAMMA(9),PGAMMA(9),PBETA(9),DELN(9),
     3PDELTA(9),DNSTAR(9),DM(9),D1(9),D2(9),CURV(9,10),
     4PCURV(9),Y1(9),Y2(9),Y3(9),DHEDN(9),DFL(9),WM(9),
     5DWSQ(9),LX(9),AX(9),FX(9),BETA(9),DDELTA(9),XLAM(9),
     6RX(9),WX(9),XGAMMA(9),XBETA(9),GAMX(9),W(9),XDEL(9),
     7ZBETA(9),GML(9),YDELTA(9),DWCC(9),DWFUNC(9),TKEQV(9)
      COMMON M,DELN,ATHETA,NO,DTDM,PBETA,PDELTA,PGAMMA,PLAM,
     1AR,R,DM,DNSTAR,ADELTA,NOCO,ALAM,NS,D1,D2,CURV,PCURV,MO,
     2Y1,Y2,Y3,WM,QDEL,DWSQ,OMEGA,DX,AX,QA,QC,
     3WX,RX,XGAMMA,XBETA,YDELTA
      READ 10,MC,NO,NS
   11 FORMAT(6F10.0)
   10 FORMAT(3I10)
      READ 11,(DELN(M),M=1,MC)
      READ 11,((R(M,N),N=1,NO),M=1,MC)
      READ 11,((Z(M,N),N=1,NO),M=1,MC)
      READ 11,((DLAM(M,N),N=1,NO),M=1,MO)
      READ 11,((THETA(M,N),N=1,NO),M=1,MO)
      READ 11,((DELTA(M,N),N=1,NO),M=1,MO)
      READ 11, (CURV(1,N),N=1,NO)
      READ 11, (CURV(9,N),N=1,NO)
      READ 90,OMEGA,QA
   90 FORMAT(2F15.0)
      READ 11,(DHEDN(M),M=1,MO)
      READ 11,(DFL(M),M=1,MC)
      READ 11,THICK,BLNC
      DO 12 M=1,MO
      DO 12 N=1,NO
      C = 3.14159/180.
      ALAM(M,N) = DLAM(M,N)*C
      ATHETA(M,N) = THETA(M,N)*C
      ADELTA (M,N) = DELTA(M,N)*C
   12 CONTINUE
      M = 1
      CALL DTD(NS)
      AR(M) = R(M,NS)
      PDELTA(M) = ADELTA(M,NS)
      CALL ANGLE
      GAMMA(M) = PGAMMA(M)/C
      DNSTAR(1) =0.
      DM(1) = C.
      PLAM(M) =ALAM(M,NS)
      BETA(M) = PBETA(M)/C
      DDELTA(M) = PDELTA(M)/C
      XLAM(M) = PLAM(M)/C
      PRINT 929
  929 FORMAT(1H1)
      PRINT 13
   13 FORMAT(10X39HLOCATION OF POINTS ON CHARACTERISTIC   ///)
      PRINT 14
   14 FORMAT(2H M8X5HGAMMA10X6HDNSTAR9X4HBETA11X5HDELTA10X5HLAMDA
     1 12X1HR14X2HDM//)
      PRINT 15,M,GAMMA(M),DNSTAR(M),BETA(M),DDELTA(M),XLAM(M),AR(M),
     1 DM(M)
   15 FORMAT(I2,7F15.4//)
      DO 16 M=2,MC
      NOGO = 0
      NP = DNSTAR(M-1)/DELN(M-1)
      NE = NS+NP
      IF(PLAM(M-1)-.7854) 17,17,18
   17 ADM = (R(M,NE)-R(M-1,NE))/COSF(PLAM(M-1))
      DM(M) = ABSF(ADM)
      GO TO 19
   18 ADM = (Z(M,NE)-Z(M-1,NE))/SINF(PLAM(M-1))
      DM(M) = ABSF(ADM)
   19 DNSTAR(M) = DNSTAR(M-1)+DM(M)*TANF(PGAMMA(M-1))
      IF(DNSTAR(M)) 20,21,22
   20 CALL PSTAR(NS,-1,-1.)
      GO TO 23
   22 CALL PSTAR(NO-NS,1,1.)
```

```
      GO TO 23
   21 CALL CTO(NS)
      PLAM(M) = ALAM(M,NS)
      PDELTA(M) = ADELTA(M,NS)
      AR(M) = R(M,NS)
      CALL ANGLE
      IF(PGAMMA(M)) 24,23,25
   24 CALL PSTAR(NS,-1,-1.)
      GO TO 23
   25 CALL PSTAR(NO-NS ,1,1.)
   23  CONTINUE
      IF(1-NCGO) 26,26,28
   26 PRINT 27,M
   27 FORMAT(27HINSUFFICIENT GRID WIDTH  M=,I2)
      GO TO 55
   28 GAMMA(M) = PGAMMA(M)/C
      BETA(M) = PBETA(M)/C
      DDELTA(M) = PDELTA(M)/C
      XLAM(M) = PLAM(M)/C
      PRINT 15,M,GAMMA(M),DNSTAR(M),BETA(M),DDELTA(M),XLAM(M),AR(M),
     1 DM(M)
   16 CONTINUE
      PRINT 951
  951 FORMAT(1H1,20X12HTEST FOR COY//)
      PRINT 952
  952 FORMAT(2H M3X2HNX8X6HD2TDM29X6HD2TDNM11X2HD113X2HD212X4HCURV//)
      CALL COY
      CONTINUE
      PRINT 970
  970 FORMAT(1H1,5X,6HY TEST//)
      DO 31 M=1,MO
      Y1(M) = COSF(PGAMMA(M))*(2.*PCURV(M)*(COSF(PBETA(M)))**2
     1+SINF(2.*PBETA(M))*D2(M))*12.
      Y2(M) = 2.*COSF(PGAMMA(M))*SINF(2.*PBETA(M))*D1(M)
     1/COSF(PDELTA(M))
      Y3(M) =  (DHEDN(M)-OMEGA*DFL(M))*COSF(PLAM(M))*2.*
     1COSF(PGAMMA(M))*( COSF(PBETA(M)))**2
      PRINT 971,M,Y1(M),Y2(M),Y3(M)
  971 FORMAT(I10,3F15.5)
   31 CONTINUE
      PRINT 972
  972 FORMAT(1H1,5X,8HVEL TEST//)
      EE = .001
      WM(1) = 0.
      I = 1
   32 WDEL = 100.*(-.1**(I-1))
      WM(1) = WM(1)+WDEL
      CALL RELVEL
      IF(ABSF(QDEL)-EE ) 38,38,33
   33 IF(QDEL) 32,38,34
   34 I = I+1
   35 WDEL = 100.*(-.1**(I-1))
      WM(1) = WM(1)+WDEL
      CALL RELVEL
      IF(ABSF(QDEL)-EE) 38,38,36
   36 IF(QDEL) 37,38,35
   37 I = I+1
      GO TO 32
   38 CONTINUE
      PRINT 981
  981 FORMAT(1H1,13HTEST FOR XDEL//)
      PRINT 982
  982 FORMAT(3H  M,3H  J,15H FLOW FRACTION ,15H CAL FLOW RATE ,
     115H     DELTA X     //)
  983 FORMAT(36X,F15.4)
      WX(1) = WM(1)
      WX(MO) = WM(MO)
      RX(1) = AR(1)
      RX(MO) = AR(MO)
      XBETA(1) = PBETA(1)
      XBETA(MO) = PBETA(MO)
      XGAMMA(1) = PGAMMA(1)
      XGAMMA(MO) = PGAMMA(MO)
```

```
      YDELTA(1) = PDELTA(1)
      YDELTA(MO) = PDELTA(MO)
      MO1=MO-1
      DO 950 K=2,MO1
      KK = MO+1-K
      F = FLOATF(MO-K)/FLOATF(MO-1)
      QAF = QA*F
      EE = .001
      CALL FLOW(KK,0.)
      IF(ABSF(QC-QAF)-EE) 50,50,40
   40 XDEL(KK) = .2
      PRINT 983,XDEL(KK)
      DDD = XDEL(KK)
   41 CALL FLOW(KK,DDD)
      IF(QC-QAF) 42,50,43
   42 XDEL(KK) = XDEL(KK)+.1
      DDD = XDEL(KK)
      PRINT 983,XDEL(KK)
C... DRIVES QC GREATER THAN QA TO START
      GO TO 41
   43 J = 1
   44 XDEL(KK) = XDEL(KK)-.1*(-.1**(J-1))
      DDD = XDEL(KK)
      PRINT 983,XDEL(KK)
      CALL FLOW(KK,DDD)
      IF(ABSF(QC-QAF)-EE) 50,50,45
   45 IF(QC-QAF) 46,50,44
   46 J = J+1
   47 XDEL(KK) = XDEL(KK)-.1*(-.1**(J-1))
      DDD=XDEL(KK)
      PRINT 983,XDEL(KK)
      CALL FLOW(KK,DDD)
      IF(ABSF(QC-QAF)-EE) 50,50,48
   48 IF(QC-QAF) 47,50,49
   49 J = J+1
      GO TO 44
   50 CONTINUE
      PRINT 980,KK,J,F,QC,XDEL(KK)
  980 FORMAT(2I3,3F15.4)
  950 CONTINUE
      PRINT 984
  984 FORMAT(1H1,16HVELOCITY PROFILE//)
      PRINT 985
  985 FORMAT(2H M8X6HRADIUS4X10HBLADE ANGLE8X5HGAMMA9X2HWM
     115H REL VELOCITY W //)
      DO 51 M=1,MO
      ZBETA(M) = XBETA(M)/C
      GAMX(M) = PGAMMA(M)/C
      W(M) = WX(M)*SQRTF(1.+(TANF(XBETA(M))**2))
      PRINT 986,M,RX(M),BETA(M),GAMX(M),WX(M),W(M)
  986 FORMAT(I2,5F15.4)
      TKEQV(M) =(THICK/COSF(XBETA(M)))*(SQRTF(1.+(SINF
     1(XBETA(M))*TANF(YDELTA(M)))**2))
      DWCO(M) = (6.2832/BLNC-TKEQV(M)/RX(M))*COSF(XBETA(M))
      DWFUNC(M) = RX(M)*WX(M)*TANF(XBETA(M))*12.+OMEGA*RX(M)
     1*RX(M)
   51 CONTINUE
      PRINT 880
  880 FORMAT(1H1////////25X9H TABLE   ///17X
     127H DATA FOR CHARACTERISTIC CI///)
C     CHANGE CHAR. NO. FOR EACH COMPUTATION
  882 FORMAT(6H   M = 8X2H 9X1H2 9X1H3 9X1H4 9X1H5//)
      PRINT 883
  883 FORMAT(13X33H LOCATION OF CHARACTERISTIC CURVE//)
      PRINT 884,NS
  884 FORMAT(23H  STARTING NORMAL NO. = ,I2//)
      PRINT 882
      PRINT 885,(GAMMA(M),M=1,5)
  885 FORMAT(10H GAMMA   =,5F10.4)
      PRINT 897,(GML(M),M=1,5)
  897 FORMAT(10H GAM-LAM =,5F10.4)
      PRINT 886,(DNSTAR(M),M=1,5)
  886 FORMAT(10H DNSTAR  =,5F10.4)
```

```
      PRINT 887,(BETA(M),M=1,5)
  887 FORMAT(1CH BETA(P) =,5F10.4)
      PRINT 888,(AR(M),M=1,5)
  888 FORMAT(1CH RADIUS  =,5F10.4///)
      PRINT 889
  889 FORMAT(16X28H LOCATION OF NEW STREAMLINES//)
      PRINT 882
      XDEL(1)=C.
      XDEL(MC)=0.
      PRINT 890,(XDEL(M),M=1,5)
  890 FORMAT(1CH DELTA X =,5F10.4)
      PRINT 891,(ZBETA(M),M=1,5)
  891 FORMAT(1CH BETA(X) =,5F10.4)
      PRINT 888,(RX(M),M=1,5)
      PRINT 892
  892 FORMAT(21X17H VELOCITY PROFILE//)
      PRINT 882
      PRINT 893,(WM(M),M=1,5)
  893 FORMAT(1CH WM(P)   =,5F10.4)
      PRINT 894,(WX(M),M=1,5)
  894 FORMAT(1CH WM(X)   =,5F10.4)
      PRINT 895,(W(M),M=1,5)
  895 FORMAT(1CH REL VEL =,5F10.4)
      PRINT 875,(DWCO(M),M=1,5)
  875 FORMAT(1CH DW COEF =,5F10.4)
      PRINT 874,(DWFUNC(M),M=1,5)
  874 FORMAT(1CH DW FUNC =,5F10.4)
  896 FORMAT(6H   M = 8X2H 69X1H7 9X1H8 9X1H9//)
      PRINT 88C
      PRINT 883
      PRINT 884,NS
      PRINT 896
      PRINT 885,(GAMMA(M),M=6,9)
      PRINT 897,(GML(M),M=6,9)
      PRINT 886,(DNSTAR(M),M=6,9)
      PRINT 887,(BETA(M),M=6,9)
      PRINT 878,(AR(M),M=6,9)
  878 FORMAT(10H RADIUS  =,4F10.4///)
      PRINT 889
      PRINT 896
      PRINT 89C,(XDEL(M),M=6,9)
      PRINT 891,(ZBETA(M),M=6,9)
      PRINT 878,(RX(M),M=6,9)
      PRINT 892
      PRINT 896
      PRINT 893,(WM(M),M=6,9)
      PRINT 894,(WX(M),M=6,9)
      PRINT 895,(W(M),M=6,9)
      PRINT 875,(DWCO(M),M=6,9)
      PRINT 874,(DWFUNC(M),M=6,9)
      PRINT 860
  86C FORMAT(1H1,4H END)
   55 CONTINUE
      END
```

Program ROTOR I

Subroutine PSTAR

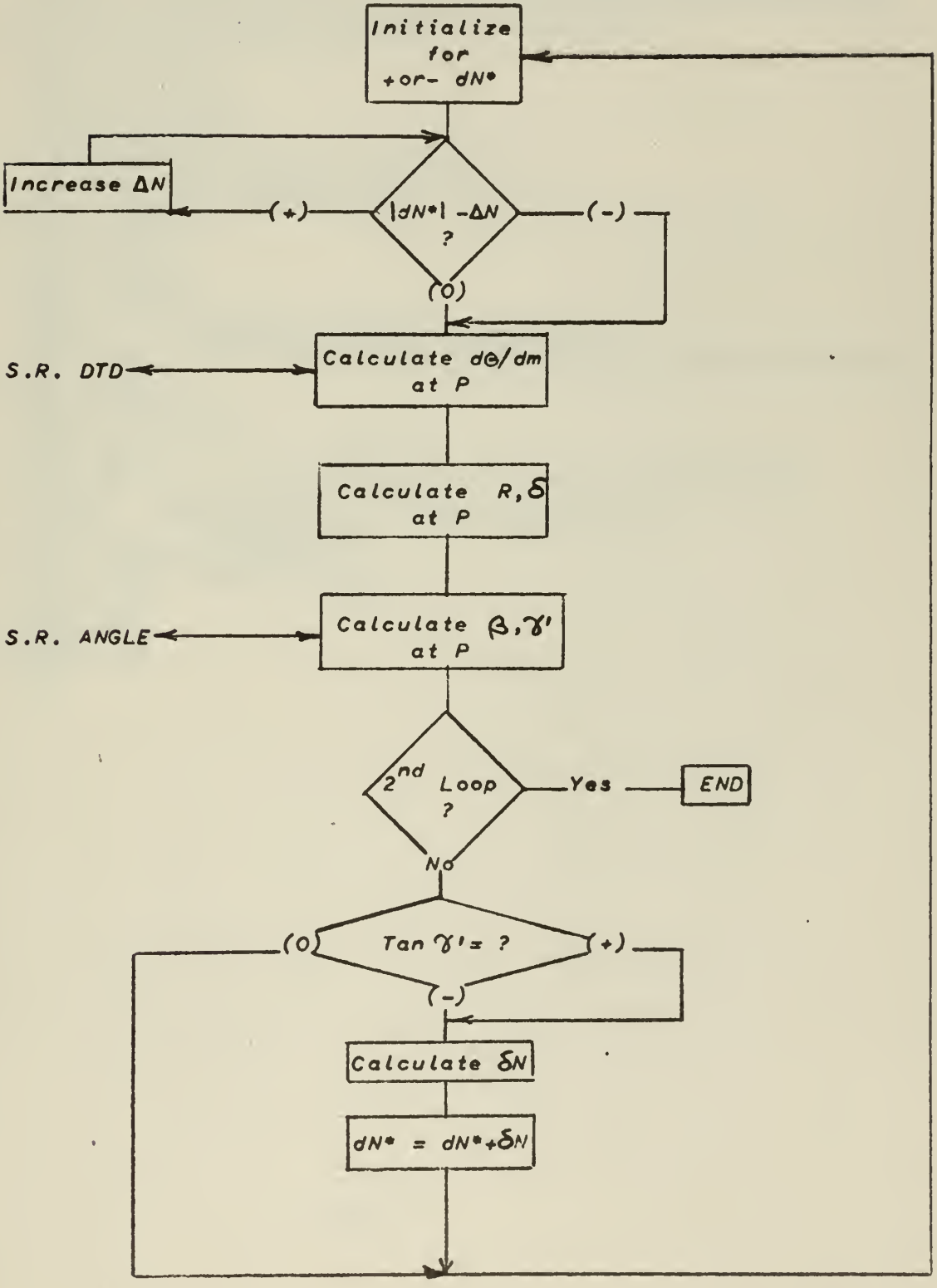

```
      SUBROUTINE PSTAR(NN,JO,B)
      DIMENSION DLAM(9,10),R(9,10),Z(9,10),THETA(9,10) ,
     1ALAM(9,10),ATHETA(9,10),DELTA(9,10),ADELTA(9,10),
     2AR(9),PLAM(9),GAMMA(9),PGAMMA(9),PBETA(9),DELN(9),
     3PDELTA(9),DNSTAR(9),DM(9),D1(9),D2(9),CURV(9,10),
     4PCURV(9),Y1(9),Y2(9),Y3(9),DHEDN(9),DFL(9),WM(9),
     5DWSQ(9),DX(9),AX(9),FX(9),BETA(9),DDELTA(9),XLAM(9),
     6RX(9),WX(9),XGAMMA(9),XBETA(9),GAMX(9),W(9),XDEL(9),
     7ZBETA(9),GML(9),YDELTA(9),DWCO(9),DWFUNC(9),TKEQV(9)
      COMMON M,DELN,ATHETA,NO,DTDM,PBETA,PDELTA,PGAMMA,PLAM,
     1AR,R,DM,DNSTAR,ADELTA,NOGO,ALAM,NS,D1,D2,CURV,PCURV,MO,
     2Y1,Y2,Y3,WM,QDEL,DWSQ,OMEGA,DX,AX,QA,QC,
     3WX,RX,XGAMMA,XBETA,YDELTA
      DO 300 I=1,2
      DEL = DELN(M)
      DO 301 K=1,NN
      NA=NS+JO*(K-1)
      NB = NS+JO*K
      X = (DNSTAR(M)-B*DEL)/DELN(M)
      IF(ABSF(DNSTAR(M))-DEL)302,303,304
304   DEL = DELN(M)*FLOATF(K+1)
      GO TO 301
302   CALL DTD(NB)
      DT1=DTDM
      CALL DTD(NA)
      DT2 = DTDM
      DTDM = DT1-B*(DT2-DT1)*X
      AR(M) = R(M,NB)-B*(R(M,NA)-R(M,NB))*X
      PDELTA(M) = ADELTA(M,NB)-B*(ADELTA(M,NA)-ADELTA(M,NB))*X
      GO TO 305
303   CALL DTD(NB)
      AR(M) = R(M,NB)
      PDELTA(M) = ADELTA(M,NB)
305   CALL ANGLE
      PLAM(M) = ALAM(M,NB)-B*(ALAM(M, NA)-ALAM(M,NB))*X
      IF(I-1) 306,306,300
306   TGAMD = TANF(PGAMMA(M))-TANF(PGAMMA(M-1))
      IF(TGAMD) 307,300,307
307   EN = (DM(M)*TGAMD)/2.
      DNSTAR(M) =DNSTAR(M)+EN
      GO TO 300
301   CONTINUE
      NOGO = I
300   CONTINUE
      END
```

```
      SUBROLTINE DTD(N)
      DIMENSION DLAM(9,10),R(9,10),Z(9,10),THETA(9,10) ,
     1ALAM(9,10),ATHETA(9,10),DELTA(9,10),ADELTA(9,10),
     2AR(9),PLAM(9),GAMMA(9),PGAMMA(9),PBETA(9),DELN(9),
     3PDELTA(9),DNSTAR(9),DM(9),D1(9),D2(9),CURV(9,10),
     4PCURV(9),Y1(9),Y2(9),Y3(9),DHEDN(9),DFL(9),WM(9),
     5DWSQ(9),DX(9),AX(9),FX(9),BETA(9),DDELTA(9),XLAM(9),
     6RX(9),WX(9),XGAMMA(9),XBETA(9),GAMX(9),W(9),XDEL(9),
     7ZBETA(9),GML(9),YDELTA(9),DWCO(9),DWFUNC(9),TKEQV(9)
      COMMON M,DELN,ATHETA,NO,DTDM,PBETA,PDELTA,PGAMMA,PLAM,
     1AR,R,DM,DNSTAR,ADELTA,NOGO,ALAM,NS,D1,D2,CURV,PCURV,MC,
     2Y1,Y2,Y3,WM,QDEL,DWSQ,OMEGA,DX,AX,QA,CC,
     3WX,RX,XGAMMA,XBETA,YDELTA
      DELTA = 12.*DELN(M)
      IF(N-2) 100,100,101
100 DTDM = (-25.*ATHETA(M,N)+48.*ATHETA(M,N+1)-36.*
     1ATHETA(M,N+2)+16.*ATHETA(M,N+3)-3.*ATHETA(M,N+4))/DELTA
      GO TO 104
101 NREM = NC-N
      IF(NREM-1) 102,102,103
102 DTDM = (3.*ATHETA(M,N-4)-16.*ATHETA(M,N-3)+36.*
     1ATHETA(M,N-2)-48.*ATHETA(M,N-1)+25.*ATHETA(M,N)) /DELTA
      GO TO 104
103 DTDM = (ATHETA(M,N-2)-ATHETA(M,N+2) -8.*(ATHETA(M,N-1)
     1-ATHETA(M,N+1)))/DELTA
104 CONTINUE
      END
```

```
      SUBROUTINE ANGLE
      DIMENSION DLAM(9,10),R(9,10),Z(9,10),THETA(9,10) ,
     1ALAM(9,10),ATHETA(9,10),DELTA(9,10),ADELTA(9,10),
     2AR(9),PLAM(9),GAMMA(9),PGAMMA(9),PBETA(9),DELN(9),
     3PDELTA(9),DNSTAR(9),DM(9),D1(9),D2(9),CURV(9,10),
     4PCURV(9),Y1(9),Y2(9),Y3(9),DHEDN(9),DFL(9),WM(9),
     5DWSQ(9),DX(9),AX(9),FX(9),BETA(9),DDELTA(9),XLAM(9),
     6RX(9),WX(9),XGAMMA(9),XBETA(9),GAMX(9),W(9),XDEL(9),
     7ZBETA(9),GML(9),YDELTA(9),DWCO(9),DWFUNC(9),TKEQV(9)
      COMMON M,DELN,ATHETA,NO,DTDM,PBETA,PDELTA,PGAMMA,PLAM,
     1AR,R,DM,DNSTAR,ADELTA,NOGO,ALAM,NS,D1,D2,CURV,PCURV,MO,
     2Y1,Y2,Y3,WM,QDEL,DWSQ,OMEGA,DX,AX,QA,QC,
     3WX,RX,XGAMMA,XBETA,YDELTA
      TBETA = AR(M)*DTDM
      PBETA(M) = ATANF(TBETA)
      TGAMMA=(SINF(PBETA(M))**2)* TANF(PDELTA(M))
      PGAMMA(M) = ATANF(TGAMMA)
      END
```

Subroutine COY

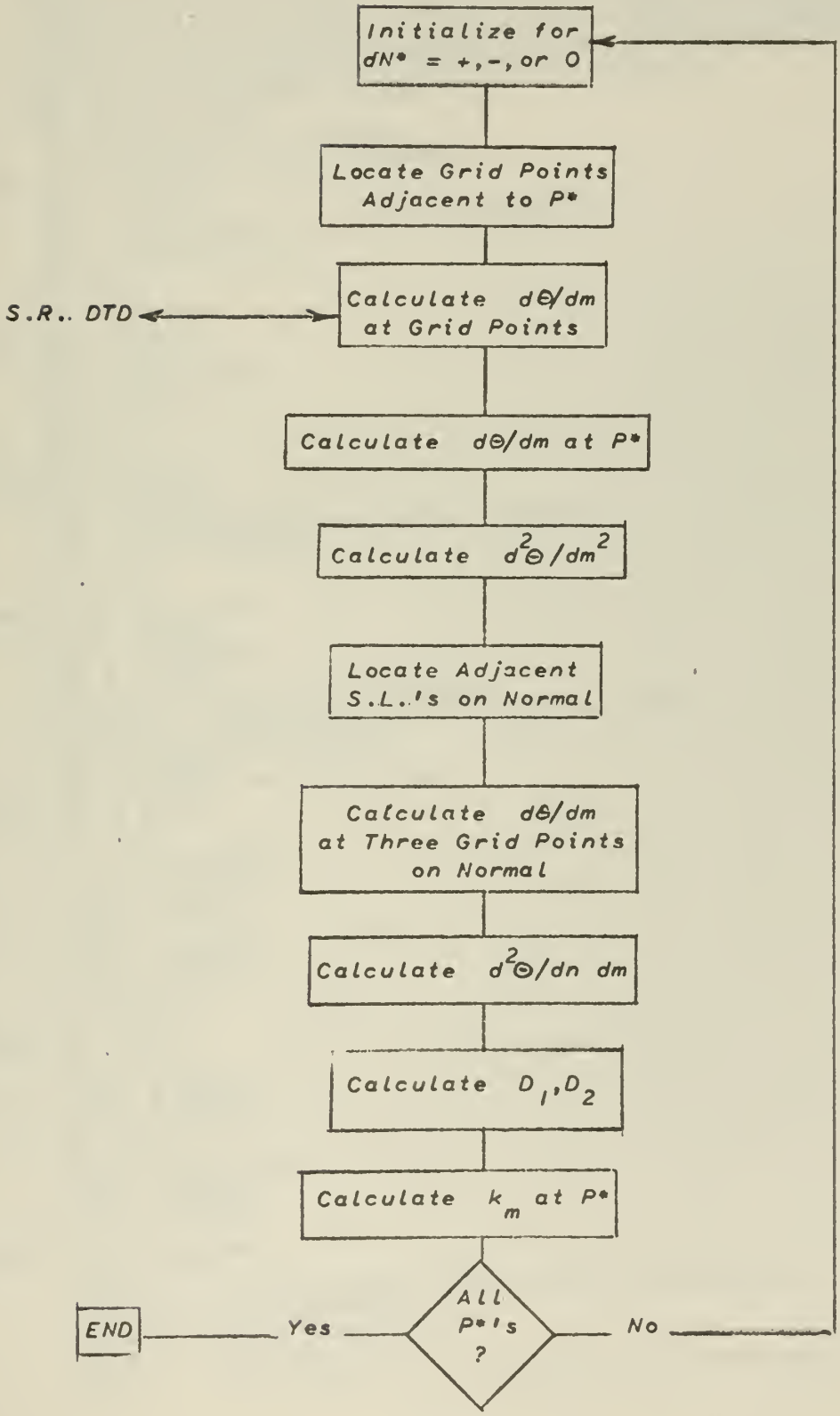

```
      SUBROUTINE COY
      DIMENSION DLAM(9,10),R(9,10),Z(9,10),THETA(9,10) ,
     1ALAM(9,10),ATHETA(9,10),DELTA(9,10),ADELTA(9,10),
     2AR(9),PLAM(9),GAMMA(9),PGAMMA(9),PBETA(9),DELN(9),
     3PDELTA(9),DNSTAR(9),DM(9),D1(9),D2(9),CURV(9,10),
     4PCURV(9),Y1(9),Y2(9),Y3(9),DHEDN(9),DFL(9),WM(9),
     5DWSQ(9),DX(9),AX(9),FX(9),BETA(9),DDELTA(9),XLAM(9),
     6RX(9),WX(9),XGAMMA(9),XBETA(9),GAMX(9),W(9),XDEL(9),
     7ZBETA(9),GML(9),YDELTA(9),DWCO(9),DWFUNC(9),TKEQV(9)
      COMMON M,DELN,ATHETA,NC,DTDM,PBETA,PDELTA,PGAMMA,PLAM,
     1AR,R,DM,DNSTAR,ADELTA,NOGO,ALAM,NS,D1,D2,CURV,PCURV,MO,
     2Y1,Y2,Y3,WM,QDEL,DWSQ,OMEGA,DX,AX,QA,CC,
     3WX,RX,XGAMMA,XBETA,YDELTA
      DO 402 M=1,MO
      NX = DNSTAR(M)/DELN(M)
      IF(DNSTAR(M)) 401,402,403
401   NA = NS+NX
      NB = NA-1
      XA = -DNSTAR(M)+FLOATF(NX)*DELN(M)
      XB = XA-DELN(M)
      JO = -1
      B = 1.
      GO TO 404
402   NA = NS+1
      NB = NS-1
      XA = DELN(M)
      XB = -XA
      JO = -1
      B = 1.
      GO TO 404
403   NB = NS+NX
      NA = NB+1
      XB = -DNSTAR(M)+FLOATF(NX)*DELN(M)
      XA = DELN(M)-XB
      JO = 1
      B = -1.
404   CALL DTD(NA)
      DA = DTDM
      CALL DTD(NB)
      DB = DTDM
      DC = TANF(PBETA(M))/AR(M)
      D2TDM2 = (XA*XA*(DB-DC)-XB*XB*(DA-DC))/
     1(XA*XA*XB-XB*XB*XA)
      NN = NS+NX
      IF(MO-2-M) 405,406,406
405   ZA = DM(M)
      MZ = M
      M = M-1
      ZB = ZA-DM(M)
      CALL DTD(NN)
      DNA = DTDM
      M = M-1
      CALL DTD(NN)
      DNB = DTDM
      M = MZ
      GO TO 407
406   MZ = M
      M = M+1
      ZA = DM(M)
      CALL DTD(NN)
      DNA = DTDM
      M = M+1
      ZB = ZA+DM(M)
      CALL DTD(NN)
      DNB = DTDM
      M = MZ
407   CALL DTD(NN)
      DNO = DTDM
      D2TDNM = (ZB*ZB*(DNA-DNO)-ZA*ZA*(DNB-DNO))/
     1(ZB*ZB*ZA-ZA*ZA*ZB)
      ALFA = PDELTA(M)-PLAM(M)
      D1(M) = COSF(ALFA)
      D2(M) = (2.*TANF(PBETA(M))*D1(M))/(AR(M)*COSF(PDELTA(M)))
```

```
     1+AR(M)*(TANF(PDELTA(M))*D2TDM2 + D2TDNM)
      IF(M-1) 408,408,409
  408 PCURV(1) = CURV(1,NS)
  954 GO TO 950
C--REPLACE WITH (GOTO 400)
  409 AM= FLOATF(M-1)/FLOATF(MO-1)
      CURV(M,NN) =CURV(1,NN)+(CURV(MO,NN)-CURV(1,NN))*AM
      CURV(M,NN+JO) = CURV(1,NN+JO)+(CURV(MO,NN+JO)-CURV(1,
     1NN+JO))*AM
      X = DNSTAR(M)/DELN(M)-FLOATF(NX*JO)
      PCURV(M) = CURV(M,NN)-B*(CURV(M,NN+JO)-CURV(M,NN))*X
  950 CONTINUE
      PRINT 953,M,NX,D2TDM2,D2TDNM,D1(M),D2(M),PCURV(M)
  953 FORMAT(I2,I5,5F15.4//)
  400 CONTINUE
      END
```

Subroutine RELVEL

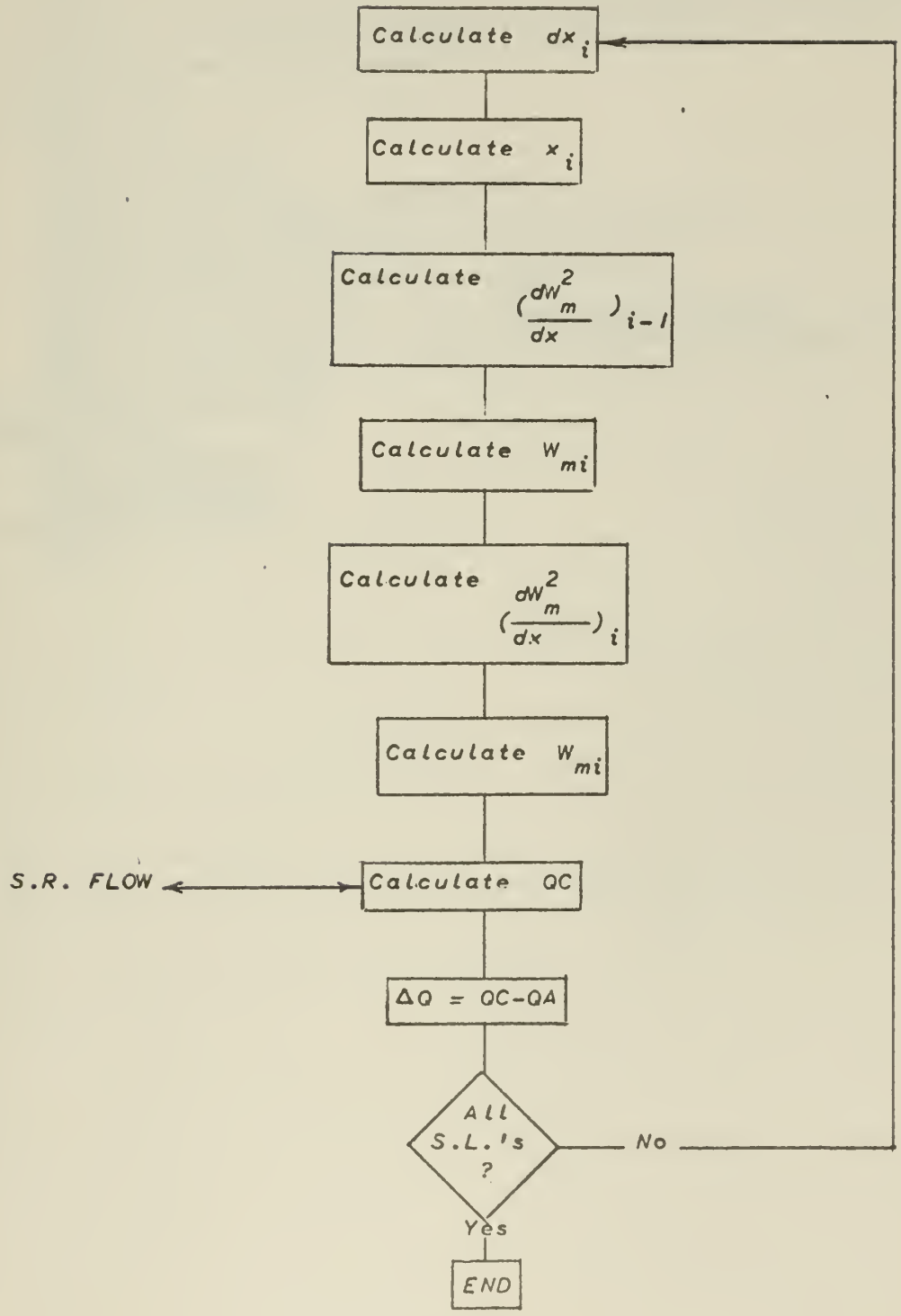

```
      SUBROUTINE RELVEL
      DIMENSION DLAM(9,10),R(9,10),Z(9,10),THETA(9,10) ,
     1ALAM(9,10),ATHETA(9,10),DELTA(9,10),ADELTA(9,10),
     2AR(9),PLAM(9),GAMMA(9),PGAMMA(9),PBETA(9),DELN(9),
     3PDELTA(9),DNSTAR(9),DM(9),D1(9),D2(9),CURV(9,10),
     4PCURV(9),Y1(9),Y2(9),Y3(9),DHEDN(9),DFL(9),WM(9),
     5DWSQ(9),DX(9),AX(9),FX(9),BETA(9),DDELTA(9),XLAM(9),
     6RX(9),WX(9),XGAMMA(9),XBETA(9),GAMX(9),W(9),XDEL(9),
     7ZBETA(9),GML(9),YDELTA(9),DWCC(9),DWFUNC(9),TKEQV(9)
      COMMON M,DELN,ATHETA,NO,DTDM,PBETA,PDELTA,PGAMMA,PLAM,
     1AR,R,DM,DNSTAR,ADELTA,NOGO,ALAM,NS,D1,D2,CURV,PCURV,MC,
     2Y1,Y2,Y3,WM,QDEL,DWSQ,OMEGA,DX,AX,QA,QC,
     3WX,RX,XGAMMA,XBETA,YDELTA
      PRINT 975
975   FORMAT(10X,1HM,10X,2HWM)
      AX(1) =0.
      PRINT 973,M,WM(1)
      DO 500 M=2,MO
      DX(M) =DM(M)/COSF(PGAMMA(M-1))
      AX(M) = AX(M-1)+DX(M)
      DWSQ(M-1) = Y3(M-1)-(WM(M-1)**2)*Y1(M-1)
     1-WM(M-1)*OMEGA*Y2(M-1)
      WSQ = WM(M-1)**2 +DWSQ(M-1)*DX(M)/12.
      WM(M) = SQRTF(WSQ)
      DWSQ(M) = Y3(M)-WSQ*Y1(M)-WM(M)*OMEGA*Y2(M)
      WSQ = WM(M-1)**2 +((DWSQ(M-1)+DWSQ(M))/2.)*DX(M)/12.
      WM(M) = SQRTF(WSQ)
      PRINT 973,M,WM(M)
973   FORMAT(I10,F15.4)
500   CONTINUE
      CALL FLOW(MO,0.)
      QDEL = QC-QA
      PRINT 974,QDEL
974   FORMAT(/8HQC-QA =  ,F10.4)
      END
```

Subroutine FLOW

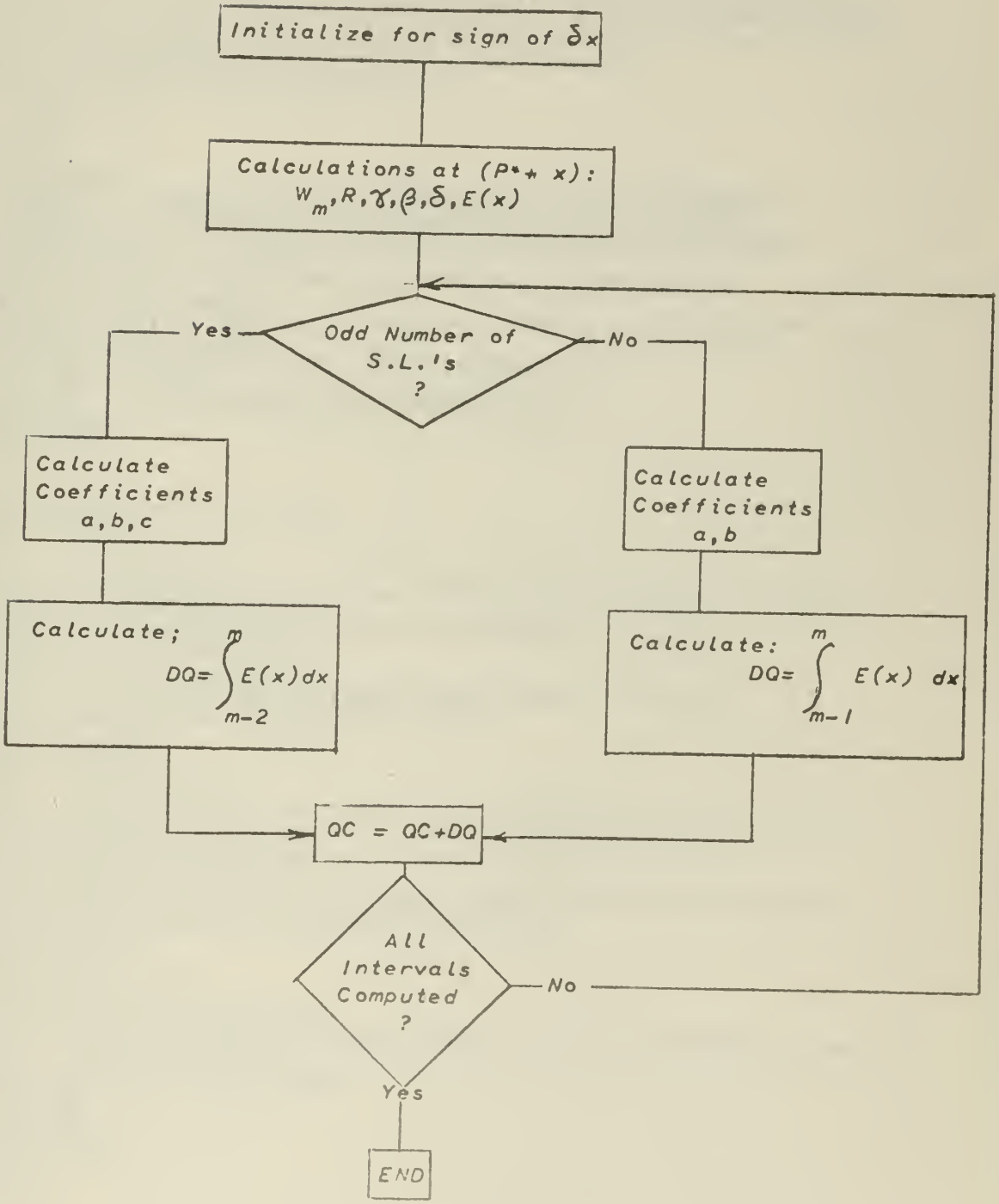

```
      SUBROLTINE FLOW(MM,DELTAX)
      DIMENSION DLAM(9,10),R(9,10),Z(9,10),THETA(9,10) ,
     1ALAM(9,10),ATHETA(9,10),DELTA(9,10),ADELTA(9,10),
     2AR(9),PLAM(9),GAMMA(9),PGAMMA(9),PBETA(9),DELN(9),
     3PDELTA(9),DNSTAR(9),CM(9),D1(9),D2(9),CURV(9,10),
     4PCURV(9),Y1(9),Y2(9),Y3(9),DHEDN(9),DFL(9),WM(9),
     5DWSQ(9),DX(9),AX(9),FX(9),BETA(9),DDELTA(9),XLAM(9),
     6RX(9),WX(9),XGAMMA(9),XBETA(9),GAMX(9),W(9),XDEL(9),
     7ZBETA(9),GML(9),YDELTA(9),DWCO(9),DWFUNC(9),TKEQV(9)
      COMMON M,DELN,ATHETA,NO,DTDM,PBETA,PDELTA,PGAMMA,PLAM,
     1AR,R,CM,DNSTAR,ADELTA,NOGO,ALAM,NS,D1,D2,CURV,PCURV,MO,
     2Y1,Y2,Y3,WM,QDEL,DWSQ,OMEGA,DX,AX,QA,QC,
     3WX,RX,XGAMMA,XBETA,YDELTA
      IF(DELTAX) 620,620,630
620   JD=0
      GO TO 640
630   JD=1
640   CONTINUE
      RX(MM) = AR(MM)+DELTAX*COSF(PGAMMA(MM)+PLAM(MM))
      WX(MM) = WM(MM)+(DELTAX*DWSQ(MM))/(24.*WM(MM))
      XGAMMA(MM) = PGAMMA(MM)+DELTAX*(PGAMMA(MM)-PGAMMA
     1(MM-1))/DX(MM+JD)
      XBETA(MM) = PBETA(MM)+DELTAX*(PBETA(MM)-PBETA
     1(MM-1))/DX(MM+JD)
      YDELTA(MM) = PDELTA(MM)+DELTAX*(PDELTA(MM)-PDELTA
     1(MM-1))/DX(MM+JD)
      FX(MM) = RX(MM)*WX(MM)*COSF(XGAMMA(MM))
      DO 600 M=1,MM-1
      FX(M) = AR(M)*WM(M)*COSF(PGAMMA(M))
600   CONTINUE
      QC = C.
      I = 1
606   IQ = I+2
      IF(IQ-MM) 601,607,602
607   AA = FX(I)
      X1 = DX(I+1)
      X2 = X1+DX(I+2)
      BB = (X2*X2*FX(I+1)- X1*X1 *FX(I+2)-AA*(X2**2-X1**2))
     1/(X1*X2*X2-X2*X1*X1)
      CC =(X2*(FX(I+1)-FX(I))-X1*(FX(I+2)-FX(I)))/
     1(X1*X1*X2-X2*X2*X1)
      XAX = AX(I+2)+DELTAX
      DQ = (AA*(XAX-AX(I))+BB*(XAX**2-AX(I) **2)/2.
     1+CC*(XAX**3-AX(I)**3)/3.)/144.
      GO TO 603
601   AA = FX(I)
      X1 = DX(I+1)
      X2 = X1+DX(I+2)
      BB = (X2*X2*FX(I+1)- X1*X1 *FX(I+2)-AA*(X2**2-X1**2))
     1/(X1*X2*X2-X2*X1*X1)
      CC =(X2*(FX(I+1)-FX(I))-X1*(FX(I+2)-FX(I)))/
     1(X1*X1*X2-X2*X2*X1)
      DQ =(AA*(AX(I+2)-AX(I))+BB* (AX(I+2)**2-AX(I)**2)/2.
     1+CC*(AX(I+2)**3-AX(I)**3)/3.)/144.
      GO TO 603
602   A=FX(I)
      XY = DX(I+1)
      XX = DX(I+1)+DELTAX
      B=(FX(I+1)-FX(I))/XY
      DQ= (A*XX+B*((AX(I+1)+DELTAX)**2-(AX(I))**2)/2.)/144.
603   QC = QC+LQ*6.28318
      IF(IQ-MM) 604,605,605
604   I=I+2
      GO TO 606
605   CONTINUE
      END
      END
```

Program ROTOR 2

Main Program

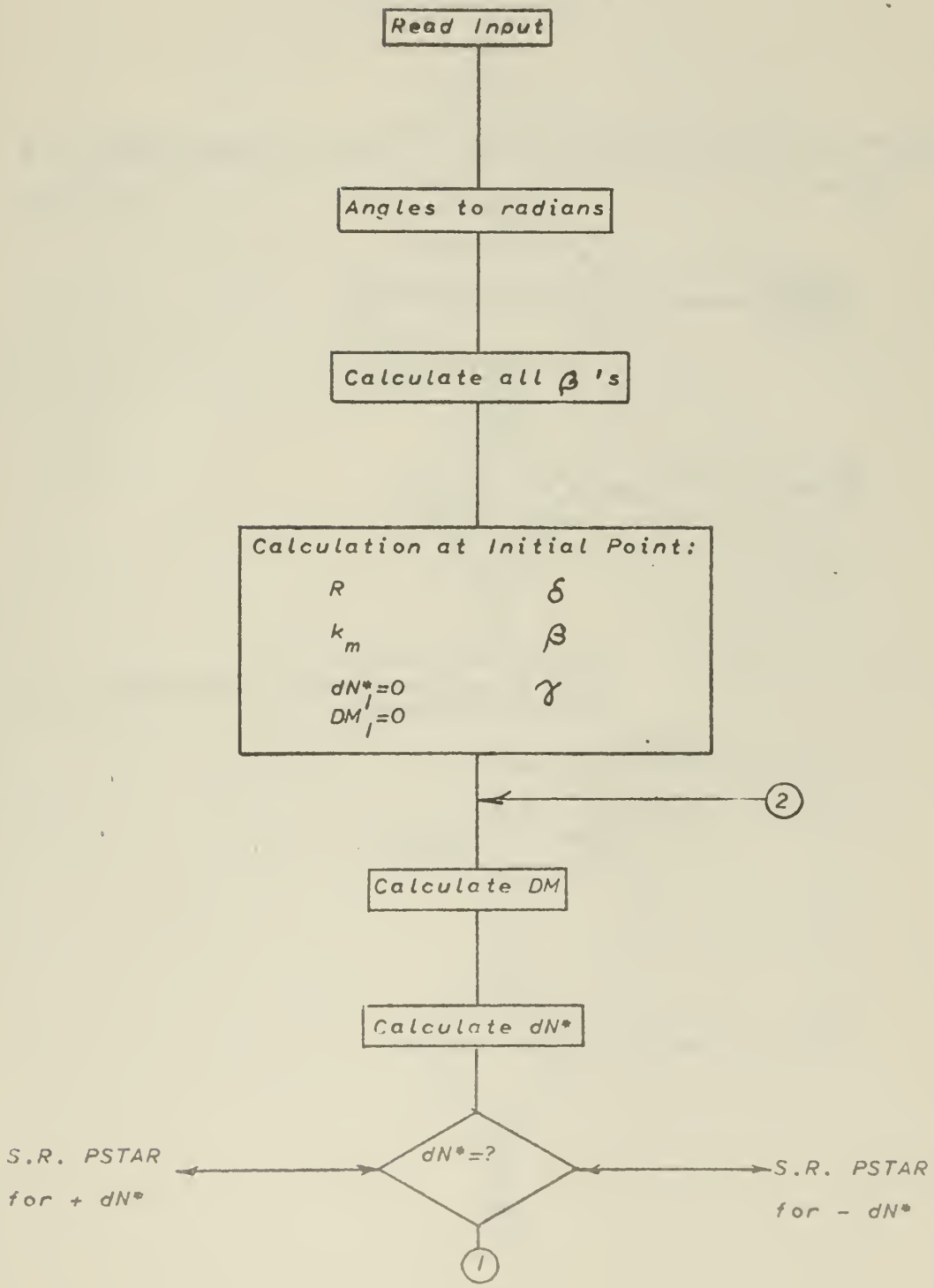

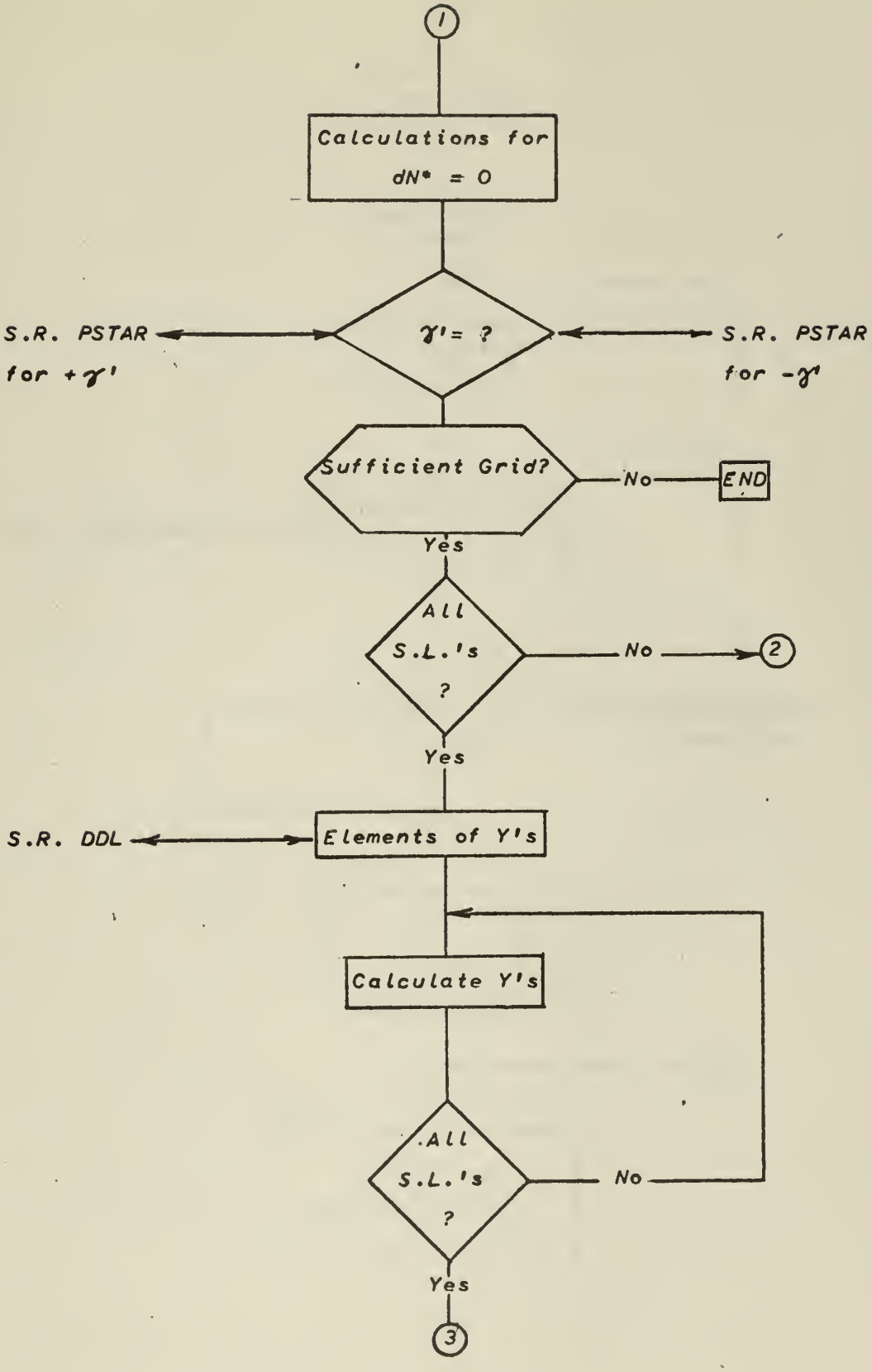
1
Calculations for dN* = 0
γ'= ?
S.R. PSTAR for +γ'
S.R. PSTAR for -γ'
Sufficient Grid?
No
END
Yes
All S.L.'s ?
No
2
Yes
S.R. DDL
Elements of Y's
Calculate Y's
All S.L.'s ?
No
Yes
3

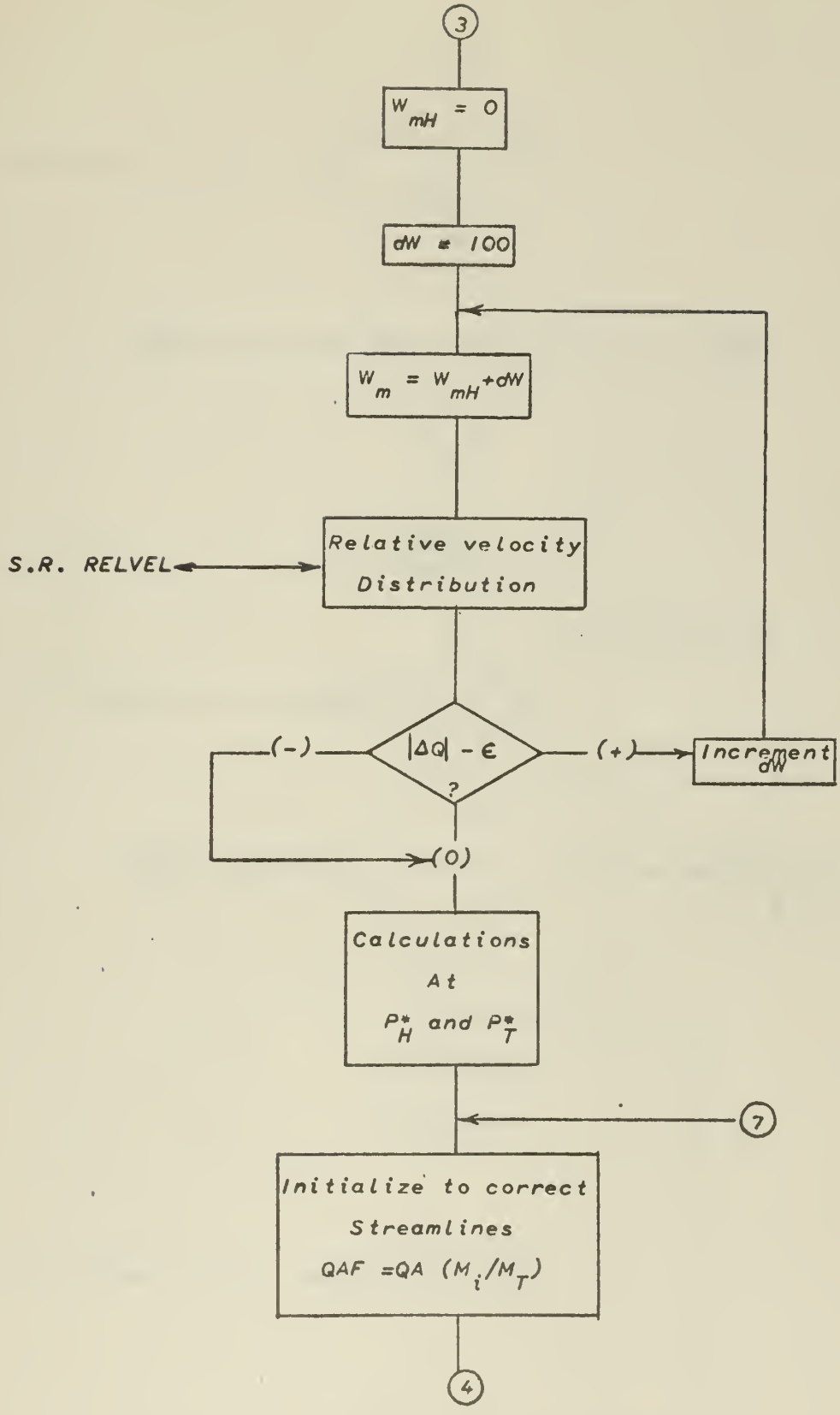
3
$W_{mH} = 0$
$dW = 100$
$W_m = W_{mH} + dW$
S.R. RELVEL
Relative velocity Distribution
$|\Delta Q| - \epsilon$?
(-)
(+)
Increment dW
(0)
Calculations At P_H^* and P_T^*
7
Initialize to correct Streamlines
$QAF = QA\ (M_i/M_T)$
4

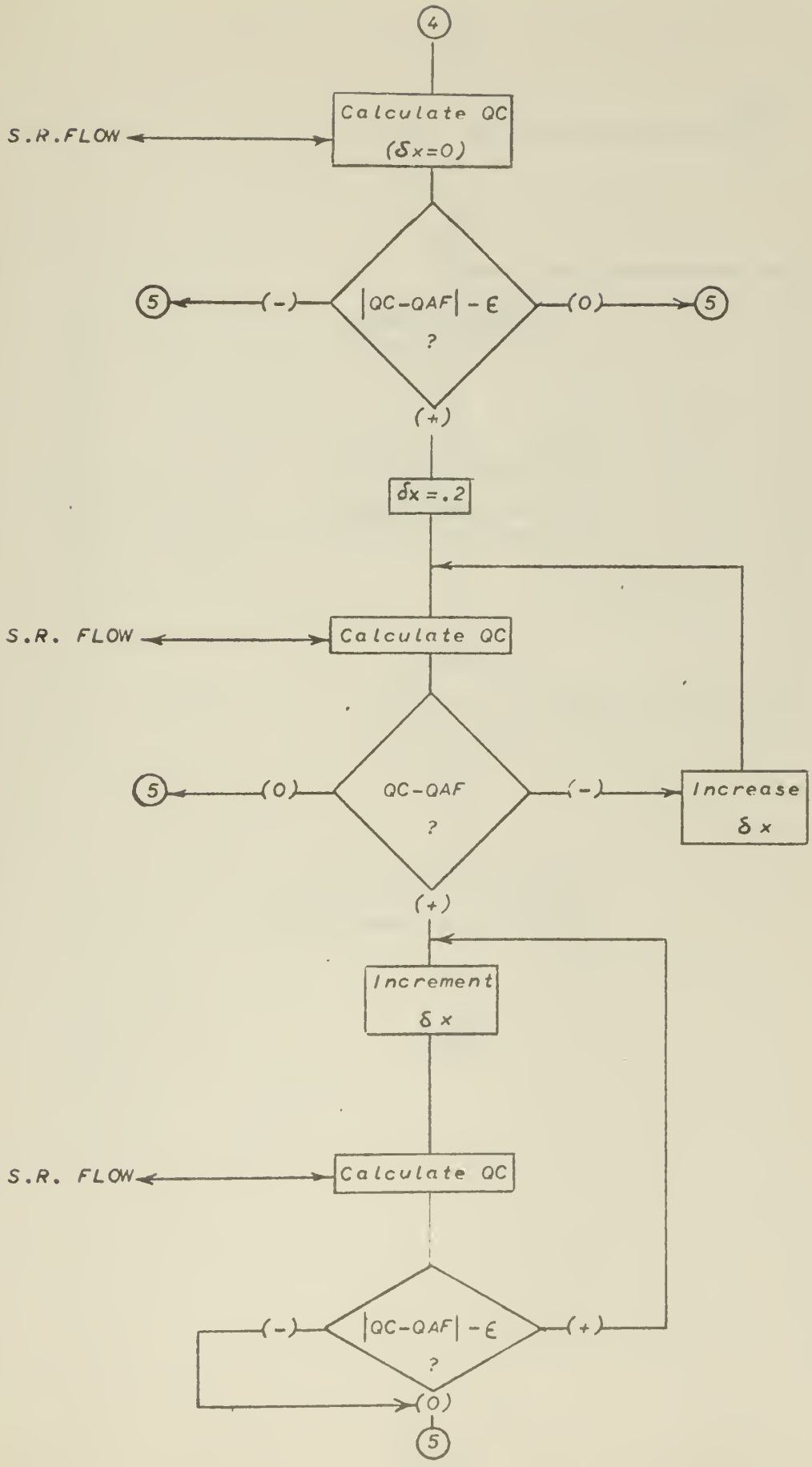
4
Calculate QC
(δx=0)
S.R.FLOW
|QC-QAF| - ε
?
(-)
(0)
5
5
(+)
δx = .2
Calculate QC
S.R. FLOW
QC-QAF
?
(0)
5
(-)
Increase
δx
(+)
Increment
δx
Calculate QC
S.R. FLOW
|QC-QAF| - ε
?
(-)
(+)
(0)
5

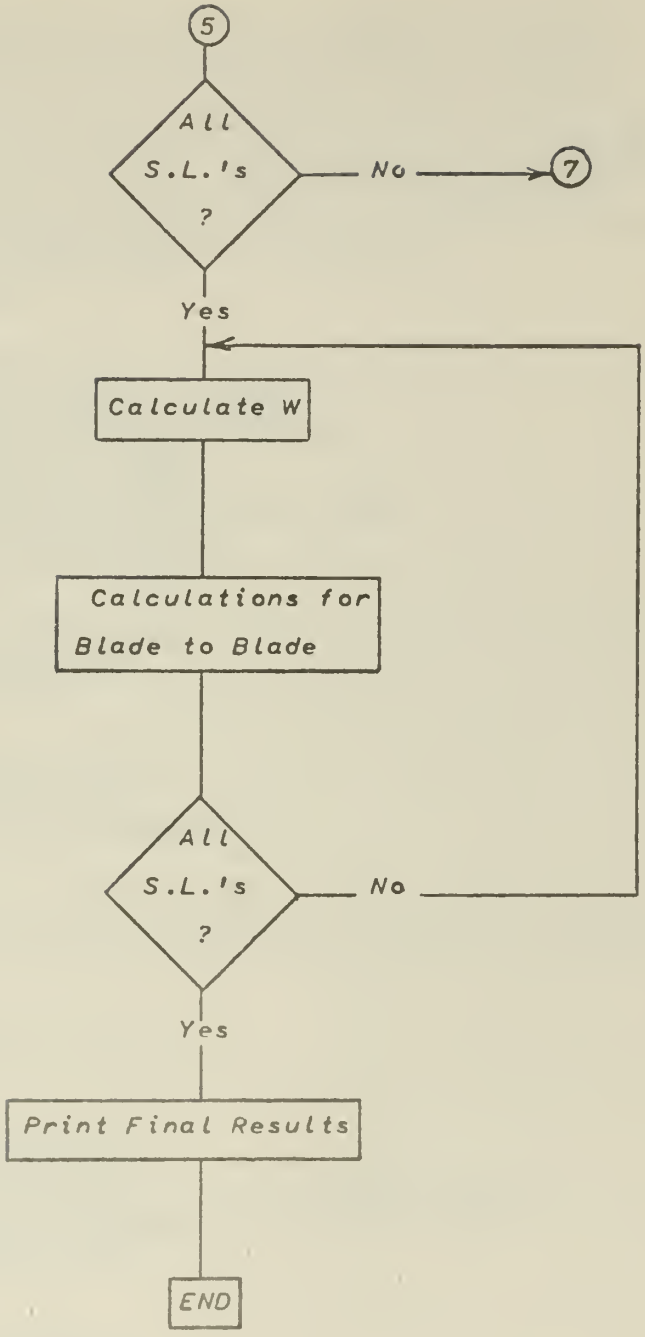
5
All S.L.'s ?
No
7
Yes
Calculate W
Calculations for Blade to Blade
All S.L.'s ?
No
Yes
Print Final Results
END

```
      PROGRAM ROTOR 2
      DIMENSION DLAM(9,10),R(9,10),Z(9,10),ABETA(9,10),
     1ALAM(9,10),BETA(9,10),DELTA(9,10),ADELTA(9,10),
     2AR(9),PLAM(9),GAMMA(9),PGAMMA(9),PBETA(9),DELN(9),
     3PDELTA(9),DNSTAR(9),DM(9),D1(9),D2(9),CURV(9,10),
     4PCURV(9),Y1(9),Y2(9),Y3(9),DHEDN(9),DFL(9),WM(9),
     5DWSQ(9),DX(9),AX(9),FX(9),APBETA(9),DDELTA(9),XLAM(9),
     6RX(9),WX(9),XGAMMA(9),XBETA(9),GAMX(9),W(9),XDEL(9),
     7ZBETA(9),GML(9),YDELTA(9),DWCO(9),DWFUNC(9),TKEQV(9)
      COMMON M,DELN,ABETA,NC,PBETA,PDELTA,PGAMMA,PLAM,
     1AR,R,DM,DNSTAR,ADELTA,NOGO,ALAM,NS,D1,D2,CURV,PCURV,MO,
     2Y1,Y2,Y3,WM,CDEL,DWSQ,OMEGA,CX,AX,QA,CC,
     3WX,RX,XGAMMA,XBETA,YDELTA
      READ 10,MC,NC,NS
   11 FORMAT(6F10.0)
   10 FORMAT(3I10)
      READ 11,(DELN(M),M=1,MO)
      READ 11,((R(M,N),N=1,NO),M=1,MO)
      READ 11,((Z(M,N),N=1,NO),M=1,MO)
      READ 11,((DLAM(M,N),N=1,NO),M=1,MO)
      READ 11,(BETA(1,N),N=1,NO)
      READ 11,(BETA(9,N),N=1,NO)
      READ 11,((DELTA(M,N),N=1,NO),M=1,MO)
      READ 11, (CURV(1,N),N=1,NO)
      READ 11, (CURV(9,N),N=1,NO)
      READ 90,OMEGA,QA
   90 FORMAT(2F15.0)
      READ 11,(DHEDN(M),M=1,MO)
      READ 11,(DFL(M),M=1,MO)
      READ 90,THICK,BLNO
      DO 12 M=1,MO
      DO 12 N=1,NO
      C = 3.14159/180.
      ABETA(M,N) = BETA(M,N)*C
      ALAM(M,N) = DLAM(M,N)*C
      ADELTA (M,N) = DELTA(M,N)*C
   12 CONTINUE
      DO 29 M=2,MO-1
      AM = FLOATF(M-1)/FLOATF(MO-1)
      DO 29 N=1,NO
      ABETA(M,N) = ABETA(1,N)+(ABETA(9,N)-ABETA(1,N))*AM
   29 CONTINUE
      DO 997 M=1,MO
      DO 997 N=1,NC
      BETA(M,N) = ABETA(M,N)/C
  997 CONTINUE
      M = 1
      AR(M) = R(M,NS)
      PCURV(M) = CURV(M,NS)
      PDELTA(M) = ADELTA(M,NS)
      PBETA(M) = ABETA(M,NS)
      TGAMMA=(SINF(PBETA(M))**2)* TANF(PDELTA(M))
      PGAMMA(M) = ATANF(TGAMMA)
      GAMMA(M) = PGAMMA(M)/C
      DNSTAR(1) =0.
      DM(1) = 0.
      PLAM(M) =ALAM(M,NS)
      APBETA(M) = PBETA(M)/C
      DDELTA(M) = PDELTA(M)/C
      XLAM(M) = PLAM(M)/C
      GML(M) = GAMMA(M)-XLAM(M)
      DO 16 M=2,MO
      NOGO = 0
      NP = DNSTAR(M-1)/DELN(M-1)
      NE = NS+NP
      IF(PLAM(M-1)-.7854) 17,17,18
   17 ADM = (R(M,NE)-R(M-1,NE))/COSF(PLAM(M-1))
      DM(M) = ABSF(ADM)
      GO TO 19
   18 ADM = (Z(M,NE)-Z(M-1,NE))/SINF(PLAM(M-1))
      DM(M) = ABSF(ADM)
   19 DNSTAR(M) = DNSTAR(M-1)+DM(M)*TANF(PGAMMA(M-1))
      IF(DNSTAR(M)) 20,21,22
```

```
   20 CALL PSTAR(NS,-1,-1.)
      GO TO 23
   22 CALL PSTAR(NC-NS,1,1.)
      GO TO 23
   21 PBETA(M) = ABETA(M,NS)
      PLAM(M) = ALAM(M,NS)
      PCURV(M) = CURV(M,NS)
      PDELTA(M) = ADELTA(M,NS)
      AR(M) = R(M,NS)
      TGAMMA=(SINF(PBETA(M))**2)* TANF(PDELTA(M))
      PGAMMA(M) = ATANF(TGAMMA)
      IF(PGAMMA(M)) 24,23,25
   24 CALL PSTAR(NS,-1,-1.)
      GO TO 23
   25 CALL PSTAR(NC-NS ,1,1.)
   23  CONTINUE
      IF(1-NOGO) 26,26,28
   26 PRINT 27,M
   27 FORMAT(27HINSUFFICIENT GRID WIDTH  M=,I2)
      GO TO 55
   28 GAMMA(M) = PGAMMA(M)/C
      APBETA(M) = PBETA(M)/C
      DDELTA(M) = PDELTA(M)/C
      XLAM(M) = PLAM(M)/C
      GML(M) = GAMMA(M)-XLAM(M)
   16 CONTINUE
      CALL CDL
      CONTINUE
      DO 31 M=1,MC
      Y1(M) = COSF(PGAMMA(M))*(2.*PCURV(M)*(COSF(PBETA(M)))**2
     1+SINF(2.*PBETA(M))*D2(M))*12.
      Y2(M) = 2.*COSF(PGAMMA(M))*SINF(2.*PBETA(M))*D1(M)
     1/COSF(PDELTA(M))
      Y3(M) =  (DHEDN(M)-OMEGA*DFL(M))*COSF(PLAM(M))*2.*
     1COSF(PGAMMA(M))*( COSF(PBETA(M)))**2
   31 CONTINUE
      EE = .001
      WM(1) = 0.
      I = 1
   32 WDEL = 100.*(-.1**(I-1))
      WM(1) = WM(1)+WDEL
      CALL RELVEL
      IF(ABSF(QDEL)-EE ) 38,38,33
   33 IF(QDEL) 32,38,34
   34 I = I+1
   35 WDEL = 100.*(-.1**(I-1))
      WM(1) = WM(1)+WDEL
      CALL RELVEL
      IF(ABSF(QDEL)-EE) 38,38,36
   36 IF(QDEL) 37,38,35
   37 I = I+1
      GO TO 32
   38 CONTINUE
      WX(1) = WM(1)
      WX(MC) = WM(MC)
      RX(1) = AR(1)
      RX(MC) = AR(MC)
      XBETA(1) = PBETA(1)
      XBETA(MC) = PBETA(MC)
      XGAMMA(1) = PGAMMA(1)
      XGAMMA(MC) = PGAMMA(MC)
      YDELTA(1) = PDELTA(1)
      YDELTA(MC) = PDELTA(MC)
      MC1=MC-1
      DO 50 K=2,MC1
      KK = MC+1-K
      F = FLOATF(MC-K)/FLOATF(MC-1)
      QAF = QA*F
      EE = .001
      CALL FLOW(KK,0.)
      IF(ABSF(QC-QAF)-EE) 50,50,40
   40 XDEL(KK) = .2
      CDD = XDEL(KK)
```

```
   41 CALL FLOW(KK,DDD)
      IF(QC-QAF) 42,50,43
   42 XDEL(KK) = XDEL(KK)+.1
      DDD = XDEL(KK)
C... DRIVES QC GREATER THAN QA TO START
      GO TO 41
   43 J = 1
   44 XDEL(KK) = XDEL(KK)-.1*(-.1**(J-1))
      DDD = XDEL(KK)
      CALL FLOW(KK,DDD)
      IF(ABSF(QC-QAF)-EE) 50,50,45
   45 IF(QC-QAF) 46,50,44
   46 J = J+1
   47 XDEL(KK) = XDEL(KK)-.1*(-.1**(J-1))
      DDD=XDEL(KK)
      CALL FLOW(KK,DDD)
      IF(ABSF(QC-QAF)-EE) 50,50,48
   48 IF(QC-QAF) 47,50,49
   49 J = J+1
      GO TO 44
   50 CONTINUE
      DO 51 M=1,MO
      ZBETA(M) = XBETA(M)/C
      GAMX(M) =·PGAMMA(M)/C
      W(M) = WX(M)*SQRTF(1.+(TANF(XBETA(M))**2))
      TKEQV(M) =(THICK/COSF(XBETA(M)))*(SQRTF(1.+(SINF
     1(XBETA(M))*TANF(YDELTA(M)))**2))
      DWCO(M) = (6.2832/BLNO-TKEQV(M)/RX(M))*COSF(XBETA(M))
      DWFUNC(M) = RX(M)*WX(M)*TANF(XBETA(M))*12.+OMEGA*RX(M)
     1*RX(M)
   51 CONTINUE
      PRINT 880
  880 FORMAT(1H1////////25X9H TABLE   ///17X
     127H DATA FOR CHARACTERISTIC C9///)
C     CHANGE CHAR. NO. FOR EACH COMPUTATION
  882 FORMAT(6H  M = 8X2H 19X1H2 9X1H3 9X1H4 9X1H5//)
      PRINT 883
  883 FORMAT(13X33H LOCATION OF CHARACTERISTIC CURVE//)
      PRINT 884,NS
  884 FORMAT(23H  STARTING NORMAL NO. = ,I2//)
      PRINT 882
      PRINT 886,(CNSTAR(M),M=1,5)
  886 FORMAT(1CH CNSTAR  =,5F1C.4)
      PRINT 897,(GML(M),M=1,5)
  897 FORMAT(1CH GAM-LAM =,5F10.4)
      PRINT 885,(GAMMA(M),M=1,5)
  885 FORMAT(1CH GAMMA   =,5F1C.4)
      PRINT 887,(APBETA(M),M=1,5)
  887 FORMAT(1CH BETA(P) =,5F10.4)
      PRINT 888,(AR(M),M=1,5)
  888 FORMAT(1CH RADIUS  =,5F1C.4///)
      PRINT 889
  889 FORMAT(16X28H LOCATION OF NEW STREAMLINES//)
      PRINT 882
      XDEL(1)=C.
      XDEL(MO)=0.
      PRINT 890,(XDEL(M),M=1,5)
  890 FORMAT(1CH DELTA X =,5F10.4)
      PRINT 891,(ZBETA(M),M=1,5)
  891 FORMAT(1CH BETA(X) =,5F10.4)
      PRINT 888,(RX(M),M=1,5)
      PRINT 892
  892 FORMAT(21X17H VELOCITY PROFILE//)
      PRINT 882
      PRINT 893,(WM(M),M=1,5)
  893 FORMAT(1CH WM(P)   =,5F10.4)
      PRINT 894,(WX(M),M=1,5)
  894 FORMAT(1CH WM(X)   =,5F10.4)
      PRINT 895,(W(M),M=1,5)
  895 FORMAT(1CH REL VEL =,5F1C.4)
      PRINT 875,(DWCO(M),M=1,5)
  875 FORMAT(1CH DW COEF =,5F1C.4)
      PRINT 874,(DWFUNC(M),M=1,5)
```

```
874 FORMAT(10H DW FUNC =,5F10.0)
896 FORMAT(6H   M = 8X2H 69X1H7 9X1H8 9X1H9//)
    PRINT 88C
    PRINT 883
    PRINT 884,NS
    PRINT 896
    PRINT 886,(CNSTAR(M),M=6,9)
    PRINT 897,(GML(M),M=6,9)
    PRINT 885,(GAMMA(M),M=6,9)
    PRINT 887,(APBETA(M),M=6,9)
    PRINT 878,(AR(M),M=6,9)
878 FORMAT(10H RADIUS   =,4F10.4///)
    PRINT 889
    PRINT 896
    PRINT 890,(XDEL(M),M=6,9)
    PRINT 891,(ZBETA(M),M=6,9)
    PRINT 878,(RX(M),M=6,9)
    PRINT 892
    PRINT 896
    PRINT 893,(WM(M),M=6,9)
    PRINT 894,(WX(M),M=6,9)
    PRINT 895,(W(M),M=6,9)
    PRINT 875,(DWCC(M),M=6,9)
    PRINT 874,(DWFUNC(M),M=6,9)
    PRINT 86C
860 FORMAT(1H1,4H END)
 55 CONTINUE
    END
```

Program ROTOR 2

Subroutine PSTAR

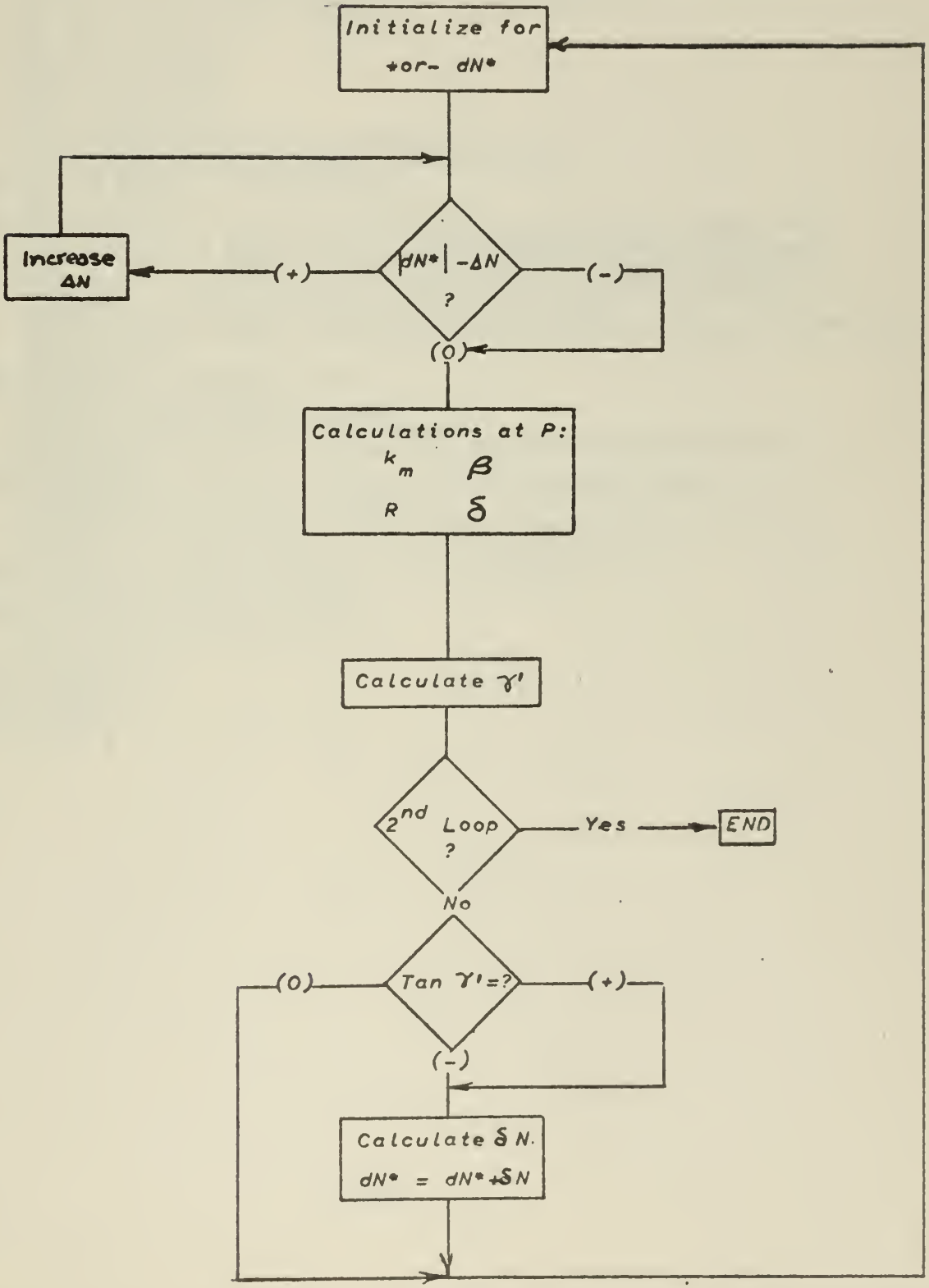

```
      SUBROUTINE PSTAR(NN,JC,B)
      DIMENSION CLAM(9,10),R(9,10),Z(9,10),ABETA(9,10),
     1ALAM(9,10),BETA(9,10),DELTA(9,10),ADELTA(9,10),
     2AR(9),PLAM(9),GAMMA(9),PGAMMA(9),PBETA(9),DELN(9),
     3PDELTA(9),DNSTAR(9),DM(9),D1(9),D2(9),CURV(9,10),
     4PCURV(9),Y1(9),Y2(9),Y3(9),DHEDN(9),DFL(9),WM(9),
     5DWSQ(9),DX(9),AX(9),FX(9),APBETA(9),DDELTA(9),XLAM(9),
     6RX(9),WX(9),XGAMMA(9),XBETA(9),GAMX(9),W(9),XDEL(9),
     7ZBETA(9),GML(9),YDELTA(9),DWCO(9),DWFUNC(9),TKEQV(9)
      COMMON M,DELN,ABETA,NC,PBETA,PDELTA,PGAMMA,PLAM,
     1AR,R,DM,DNSTAR,ADELTA,NOGO,ALAM,NS,D1,D2,CURV,PCURV,MC,
     2Y1,Y2,Y3,WM,DDEL,DWSQ,OMEGA,DX,AX,QA,QC,
     3WX,RX,XGAMMA,XBETA,YDELTA
      DO 30C I=1,2
      DEL = DELN(M)
      DO 301 K=1,NN
      NA=NS+JC*(K-1)
      NB = NS+JC*K
      X = (DNSTAR(M)-B*DEL)/DELN(M)
      IF(ABSF(DNSTAR(M))-DEL)302,303,304
304   DEL = DELN(M)*FLOATF(K+1)
      GO TO 3C1
302   AM = FLOATF(M-1)/FLOATF(MC-1)
      CURV(M,NA) = CURV(1,NA)+(CURV(MC,NA)-CURV(1,NA))*AM
      CURV(M,NB) = CURV(1,NB)+(CURV(MC,NB)-CURV(1,NB))*AM
      PCURV(M) = CURV(M,NB)-B*(CURV(M,NA)-CURV(M,NA))*X
      PBETA(M) = ABETA(M,NB)-B*(ABETA(M,NA)-ABETA(M,NB))*X
      AR(M) = R(M,NB)-B*(R(M,NA)-R(M,NB))*X
      PDELTA(M) = ADELTA(M,NB)-B*(ADELTA(M,NA)-ADELTA(M,NB))*X
      GO TO 305
303   PBETA(M) = ABETA(M,NB)
      AR(M) = R(M,NB)
      PDELTA(M) = ADELTA(M,NB)
      AM = FLOATF(M-1)/FLOATF(MC-1)
      PCURV(M) = CURV(1,NB)+(CURV(MC,NB)-CURV(1,NB))*AM
305   CONTINUE
      TGAMMA=(SINF(PBETA(M))**2)* TANF(PDELTA(M))
      PGAMMA(M) = ATANF(TGAMMA)
      PLAM(M) = ALAM(M,NB)-B*(ALAM(M,NA)-ALAM(M,NB))*X
      IF(I-1) 306,306,300
306   TGAMD = TANF(PGAMMA(M))-TANF(PGAMMA(M-1))
      IF(TGAMD) 3C7,300,3C7
3C7   EN = (DM(M)*TGAMD)/2.
      DNSTAR(M) =DNSTAR(M)+EN
      GO TO 300
301   CONTINUE
      NOGO = 1
300   CONTINUE
      END
```

Subroutine DDL

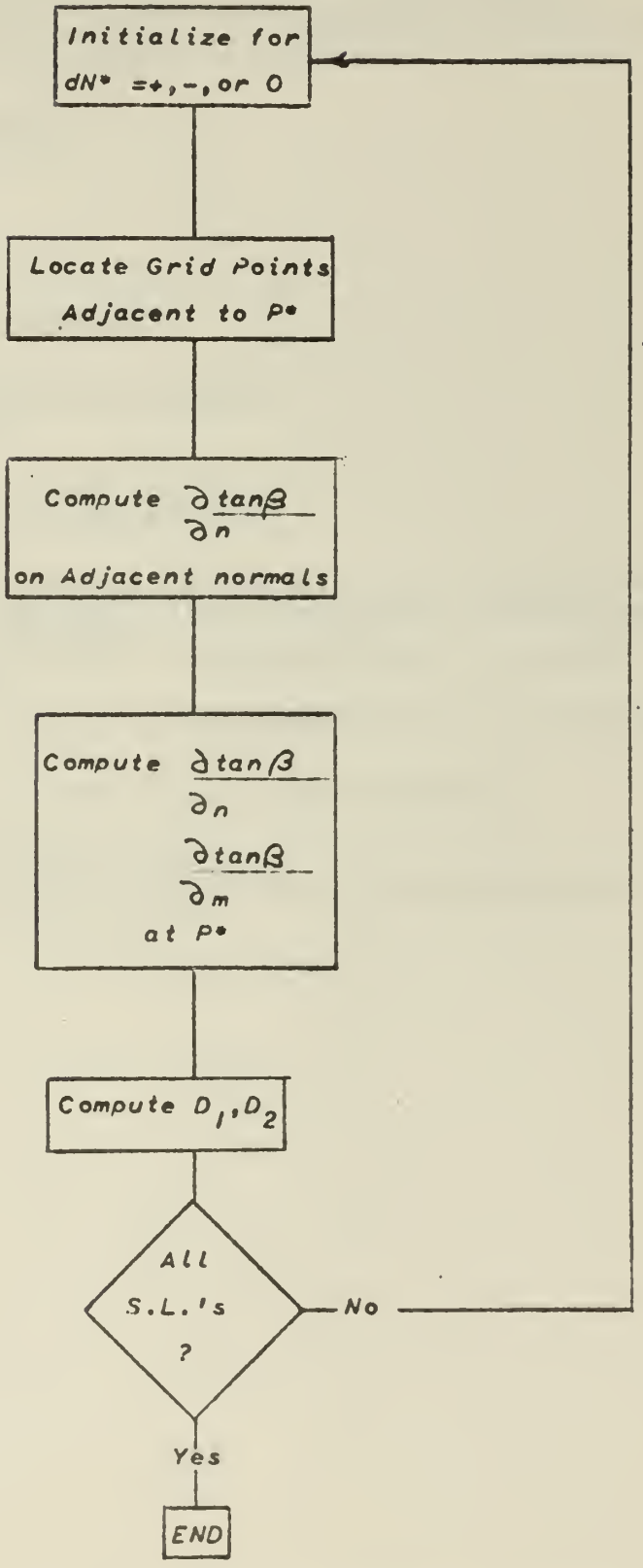

```
      SUBROUTINE CDL
      DIMENSION DLAM(9,10),R(9,10),Z(9,10),ABETA(9,10),
     1ALAM(9,10),BETA(9,10),DELTA(9,10),ADELTA(9,10),
     2AR(9),PLAM(9),GAMMA(9),PGAMMA(9),PBETA(9),CELN(9),
     3PDELTA(9),DNSTAR(9),DM(9),D1(9),D2(9),CURV(9,10),
     4PCURV(9),Y1(9),Y2(9),Y3(9),DHEDN(9),DFL(9),WM(9),
     5DWSQ(9),DX(9),AX(9),FX(9),APBETA(9),DDELTA(9),XLAM(9),
     6RX(9),WX(9),XGAMMA(9),XBETA(9),GAMX(9),W(9),XDEL(9),
     7ZBETA(9),GML(9),YDELTA(9),DWCC(9),DWFUNC(9),TKEQV(9)
      COMMON M,DELN,ABETA,NC,PBETA,PDELTA,PGAMMA,PLAM,
     1AR,R,DM,DNSTAR,ADELTA,NCCC,ALAM,NS,D1,D2,CURV,PCURV,MC,
     2Y1,Y2,Y3,WM,QDEL,DWSQ,OMEGA,DX,AX,QA,QC,
     3WX,RX,XGAMMA,XBETA,YDELTA
      DO 400 M=1,MO
      NX = DNSTAR(M)/DELN(M)
      IF(M-MC) 401,402,400
401   MM=M+1
      MX=MM
      BB=1.
      GO TO 403
402   MM=M-1
      MX=M
      BB=-1.
403   IF(DNSTAR(M)) 404,408,405
404   NA=NS+NX
      NB=NA-1
      X = -DNSTAR(M)+FLOATF(NX)*DELN(M)
      DEL = 1.-X/DELN(M)
      GO TO 406
405   NB=NS+NX
      NA=NB+1
      X = DNSTAR(M)-FLOATF(NX)*DELN(M)
      DEL = X/DELN(M)
406   IF(X) 407,408,407
407   ADN = (TANF(ABETA(MM,NA))-TANF(ABETA(M,NA)))/DM(MX)*BB
      BDN = (TANF(ABETA(MM,NB))-TANF(ABETA(M,NB)))/DM(MX)*BB
      DTBN = BDN+(ADN-BDN)*DEL
      DTBM = (TANF(ABETA(M,NA))-TANF(ABETA(M,NB)))/DELN(M)
      GO TO 409
408   NC=NS+NX
      DTBN = (TANF(ABETA(MM,NC))-TANF(ABETA(M,NC)))/DM(MX)*BB
      NA=NS+NX+1
      NB=NS+NX-1
      DTBM = (TANF(ABETA(M,NA))-TANF(ABETA(M,NB)))/
     1(DELN(M)*2.)
409   CONTINUE
      D1(M) = COSF(PDELTA(M)-PLAM(M))
      D2(M) = TANF(PDELTA(M))*DTBM+DTBN+(D1(M)*TANF(PBETA
     1(M)))/(AR(M)*COSF(PDELTA(M)))
400   CONTINUE
      END
```

Subroutine RELVEL

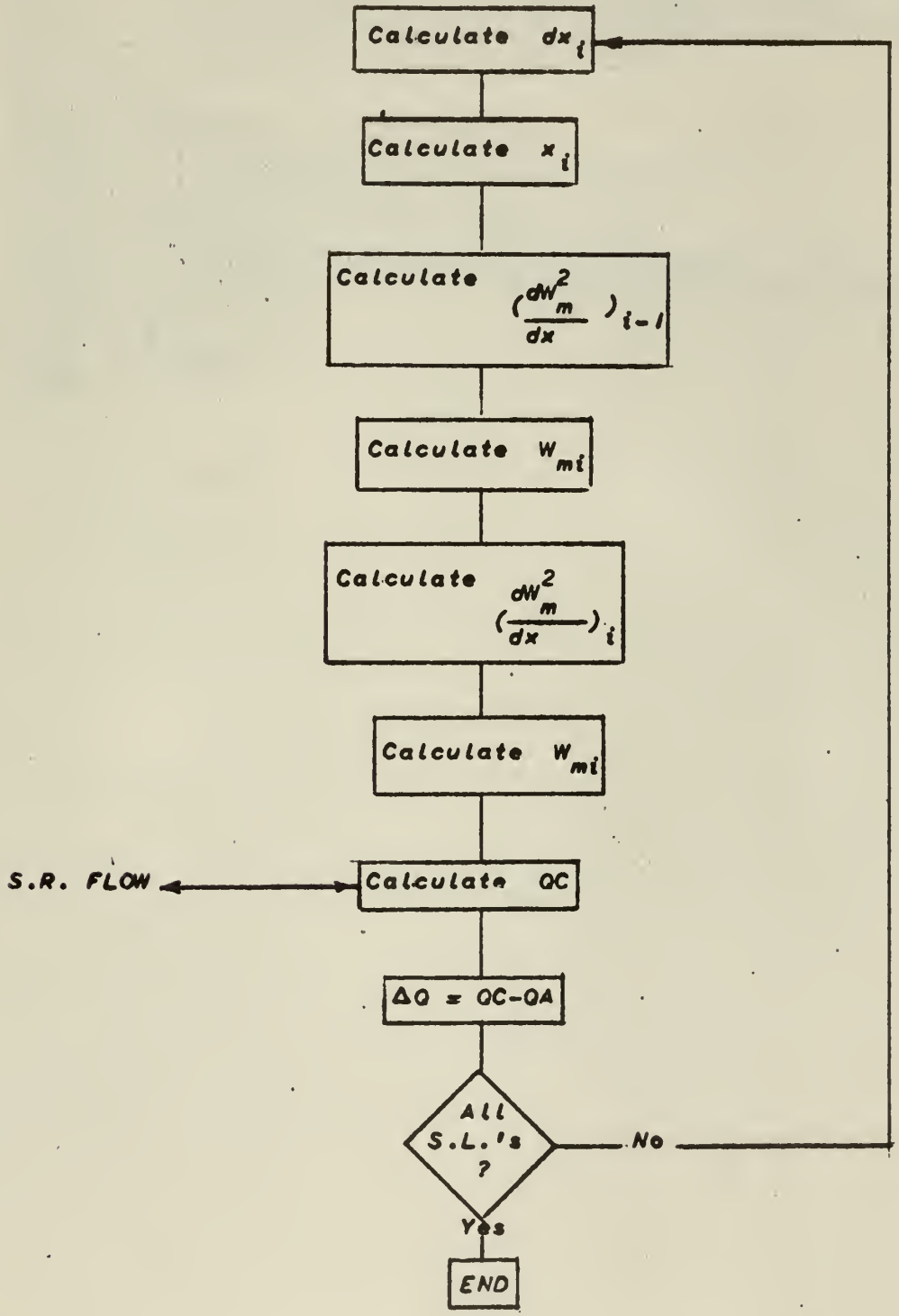

```
      SUBROUTINE RELVEL
      DIMENSION DLAM(9,10),R(9,10),Z(9,10),ABETA(9,10),
     1ALAM(9,10),BETA(9,10),DELTA(9,10),ADELTA(9,10),
     2AR(9),PLAM(9),GAMMA(9),PGAMMA(9),PBETA(9),DELN(9),
     3PDELTA(9),DNSTAR(9),DM(9),D1(9),D2(9),CURV(9,10),
     4PCURV(9),Y1(9),Y2(9),Y3(9),DHEDN(9),DFL(9),WM(9),
     5DWSQ(9),DX(9),AX(9),FX(9),APBETA(9),DDELTA(9),XLAM(9),
     6RX(9),WX(9),XGAMMA(9),XBETA(9),GAMX(9),W(9),XDEL(9),
     7ZBETA(9),GML(9),YDELTA(9),DWCO(9),DWFUNC(9),TKEQV(9)
      COMMON M,DELN,ABETA,NC,PBETA,PDELTA,PGAMMA,PLAM,
     1AR,R,DM,DNSTAR,ADELTA,NOGO,ALAM,NS,D1,D2,CURV,PCURV,MC,
     2Y1,Y2,Y3,WM,QDEL,DWSQ,OMEGA,DX,AX,QA,QC,
     3WX,RX,XGAMMA,XBETA,YDELTA
      AX(1) =0.
      DO 500 M=2,MC
      DX(M) =DM(M)/COSF(PGAMMA(M-1))
      AX(M) = AX(M-1)+DX(M)
      DWSQ(M-1) = Y3(M-1)-(WM(M-1)**2)*Y1(M-1)
     1-WM(M-1)*OMEGA*Y2(M-1)
      WSQ = WM(M-1)**2 +DWSQ(M-1)*DX(M)/12.
      WM(M) = SQRTF(WSQ)
      DWSQ(M) = Y3(M)-WSQ*Y1(M)-WM(M)*OMEGA*Y2(M)
      WSQ = WM(M-1)**2 +((DWSQ(M-1)+DWSQ(M))/2.)*DX(M)/12.
      WM(M) = SQRTF(WSQ)
500   CONTINUE
      CALL FLOW(MC,0.)
      QDEL = QC-QA
      END
```

Subroutine FLOW

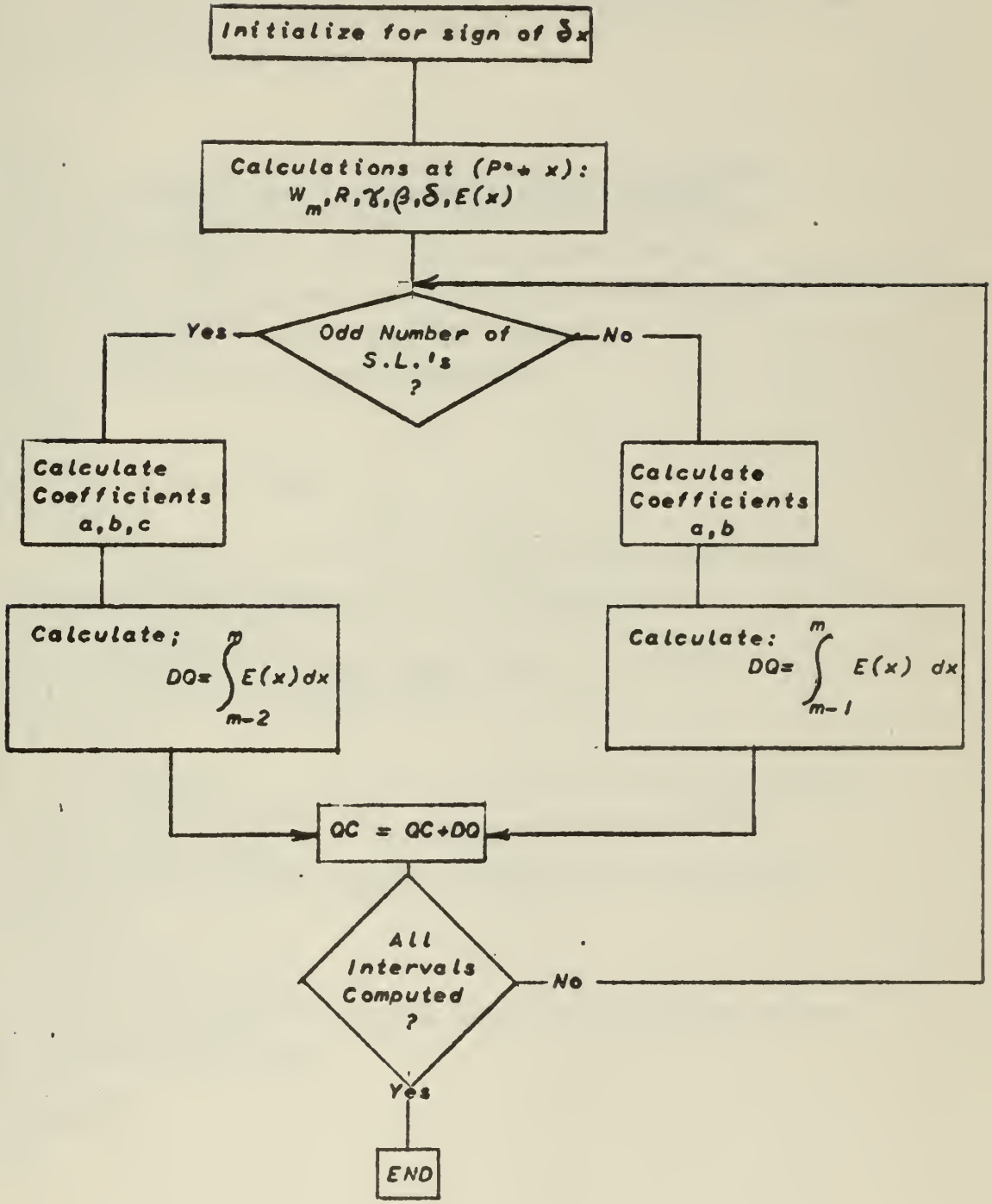

```
      SUBROUTINE FLOW(MM,DELTAX)
      DIMENSION DLAM(9,10),R(9,10),Z(9,10),ABETA(9,10),
     1ALAM(9,10),BETA(9,10),DELTA(9,10),ADELTA(9,10),
     2AR(9),PLAM(9),GAMMA(9),PGAMMA(9),PBETA(9),DELN(9),
     3PDELTA(9),DNSTAR(9),DM(9),D1(9),D2(9),CURV(9,10),
     4PCURV(9),Y1(9),Y2(9),Y3(9),DHDN(9),DEL(9),WM(9),
     5DWSQ(9),DX(9),AX(9),FX(9),APBETA(9),DDELTA(9),XLAM(9),
     6RX(9),WX(9),XGAMMA(9),XBETA(9),GAMX(9),W(9),XDEL(9),
     7ZBETA(9),GML(9),YDELTA(9),DWCC(9),DWFUNC(9),TKEQV(9)
      COMMON M,DELN,ABETA,AC,PBETA,PDELTA,PGAMMA,PLAM,
     1AR,R,DM,DNSTAR,ADELTA,NOGO,ALAM,NS,D1,D2,CURV,PCURV,MC,
     2Y1,Y2,Y3,WM,QDEL,DWSQ,OMEGA,DX,AX,QA,QC,
     3WX,RX,XGAMMA,XBETA,YDELTA
      IF(DELTAX) 620,620,630
620   JD=0
      GO TO 640
630   JD=1
640   CONTINUE
      RX(MM)   = AR(MM)+DELTAX*COSF(PGAMMA(MM)-PLAM(MM))
      WX(MM) = WM(MM)+(DELTAX*DWSQ(MM))/(2.*WM(MM))
      XGAMMA(MM) = PGAMMA(MM)+DELTAX*(PGAMMA(MM)-PGAMMA
     1(MM-1))/DX(MM+JD)
      XBETA(MM) = PBETA(MM)+DELTAX*(PBETA(MM)-PBETA
     1(MM-1))/DX(MM+JD)
      YDELTA(MM) = PDELTA(MM)+DELTAX*(PDELTA(MM)-PDELTA
     1(MM-1))/DX(MM+JD)
      FX(MM) = RX(MM)*WX(MM)*COSF(XGAMMA(MM))
      DO 600 M=1,MM-1
      FX(M) = AR(M)*WM(M)*COSF(PGAMMA(M))
600   CONTINUE
      QC = 0.
      I = 1
606   IQ = I+2
      IF(IQ-MM) 601,607,602
607   AA = FX(I)
      X1 = DX(I+1)
      X2 = X1+DX(I+2)
      BB = (X2*X2*FX(I+1)- X1*X1 *FX(I+2)-AA*(X2**2-X1**2))
     1/(X1*X2*X2-X2*X1*X1)
      CC =(X2*(FX(I+1)-FX(I))-X1*(FX(I+2)-FX(I)))/
     1(X1*X1*X2-X2*X2*X1)
      XAX = AX(I+2)+DELTAX
      DQ = (AA*(XAX-AX(I))+BB*(XAX**2-AX(I) **2)/2.
     1+CC*(XAX**3-AX(I)**3)/3.)/144.
      GO TO 603
601   AA = FX(I)
      X1 = DX(I+1)
      X2 = X1+DX(I+2)
      BB = (X2*X2*FX(I+1)- X1*X1 *FX(I+2)-AA*(X2**2-X1**2))
     1/(X1*X2*X2-X2*X1*X1)
      CC =(X2*(FX(I+1)-FX(I))-X1*(FX(I+2)-FX(I)))/
     1(X1*X1*X2-X2*X2*X1)
      DQ =(AA*(AX(I+2)-AX(I))+BB* (AX(I+2)**2-AX(I)**2)/2.
     1+CC*(AX(I+2)**3-AX(I)**3)/3.)/144.
      GO TO 603
602   A=FX(I)
      XY = DX(I+1)
      XX = DX(I+1)+DELTAX
      B=(FX(I+1)-FX(I))/XY
      DQ= (A*XX+B*((AX(I+1)+DELTAX)**2-(AX(I))**2)/2.)/144.
603   QC = QC+DQ*6.28318
      IF(IQ-MM) 604,605,605
604   I=I+2
      GO TO 606
605   CONTINUE
      END
      END
```

PROGRAM BLADE

VARIABLE NAMES

Name	Equivalent to	Units
DELN	ΔN	in.
DWCO	DW_{coef}	
DWFUNC	DW_{func}	
DDM	$d(DW_{func})/dm$	
W	W	ft./sec.
WDEL	ΔW	ft./sec.
WSUC	W_s	ft./sec.
WPRESS	W_p	ft./sec.

INDEX NAMES

MO = Number of streamlines

NMAX = Maximum number of data points

NN = Number of data point on a streamline

Program BLADE

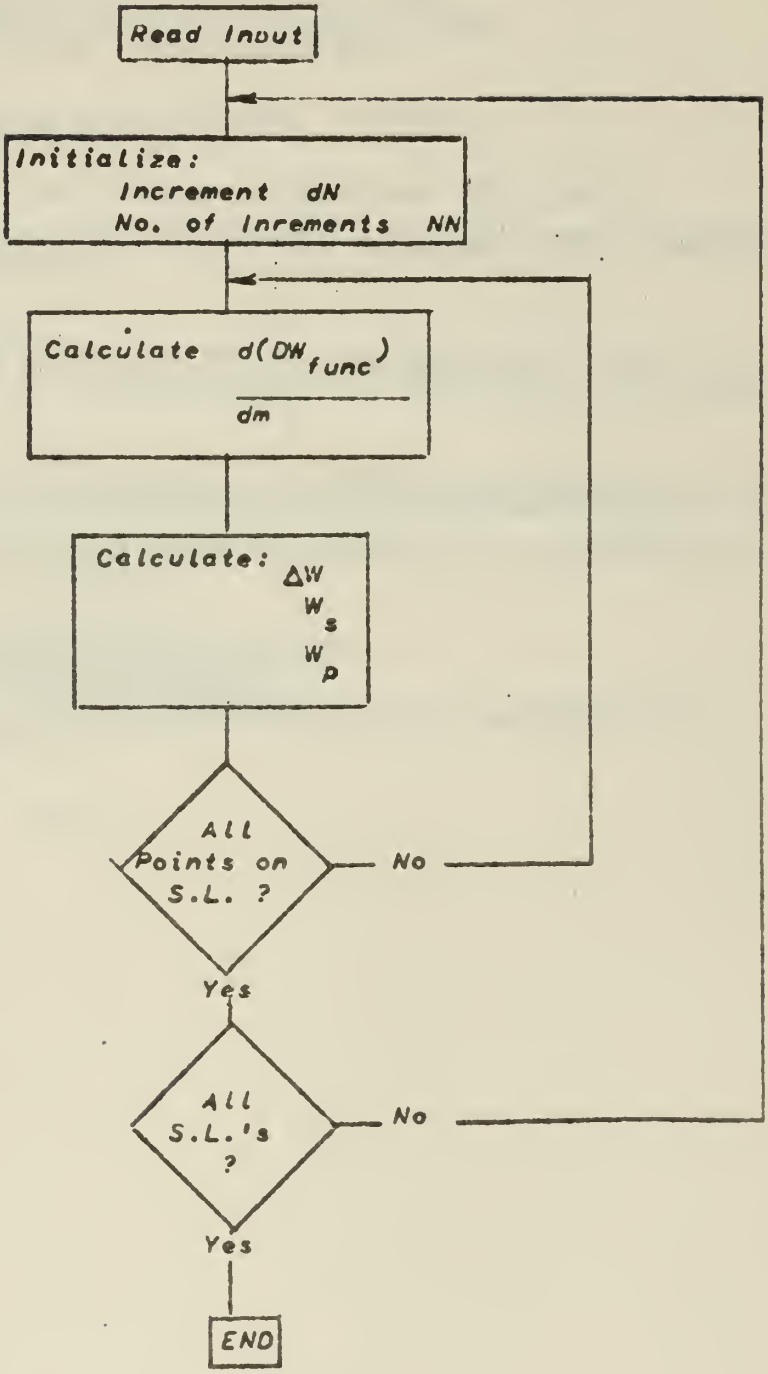

```
      PROGRAM BLADE
      DIMENSION DWCO(10,30),DWFUNC(10,30),W(10,30),NN(10),
     1WDEL(10,30),WSUC(10,30),WPRESS(10,30),DELN(10),DDM(30)
      READ 10,MO,NMAX
   10 FORMAT(6I10)
      READ 10,(NN(M),M=1,MO)
      READ 20,(DELN(M),M=1,MO)
   20 FORMAT(6F10.0)
      READ 20,((DWCO(M,N),N=1,NMAX),M=1,MO)
       READ 20,((DWFUNC(M,N),N=1,NMAX),M=1,MO)
      READ 20,((W(M,N),N=1,NMAX),M=1,MO)
      DO 30 M=1,MO
      PRINT 40
   40 FORMAT(1H1////////25X9H TABLE   ///21X
     118H VELOCITY PROFILE ///)
      PRINT 50,M
   50 FORMAT(16X,26H MERIDIONAL STREAMLINE NO.,I2///)
      PRINT 60
   60 FORMAT(4H   M1CX1HW14X2HDW8X9HW SUCTION4X1CHW PRESSURE//)
      DELTA = 12.*DELN(M)
      NM = NN(M)
      DO 30 N=1,NM
       IF(N-2)41,41,42
   41 DDM(N) = (-25.*DWFUNC(M,N)+48.*DWFUNC(M,N+1)-36.*
     1DWFUNC(M,N+2)+16.*DWFUNC(M,N+3)-3.*DWFUNC(M,N+4))/DELTA
      GO TO 45
   42 NREM = NM-N
      IF(NREM-1)43,43,44
   43 DDM(N) = (3.*DWFUNC(M,N-4)-16.*DWFUNC(M,N-3)+36.*
     1DWFUNC(M,N-2)-48.*DWFUNC(M,N-1)+25.*DWFUNC(M,N))/DELTA
      GO TO 45
   44 DDM(N) = (DWFUNC(M,N-2)-DWFUNC(M,N+2)-8.*(DWFUNC(M,N-1)
     1-DWFUNC(M,N+1)))/DELTA
   45 CONTINUE
      X = DELN(M)*FLOATF(N-1)
      WDEL(M,N) = DWCO(M,N)*DDM(N)/24.
      WSUC(M,N) = W(M,N)+WDEL(M,N)
      WPRESS(M,N) = W(M,N)-WDEL(M,N)
      PRINT 100,X,W(M,N),WDEL(M,N),WSUC(M,N),WPRESS(M,N)
  100 FORMAT(F6.2,4F14.4)
   30 CONTINUE
      PRINT 70
   70 FORMAT(1H1,5H  END)
      END
      END
```